

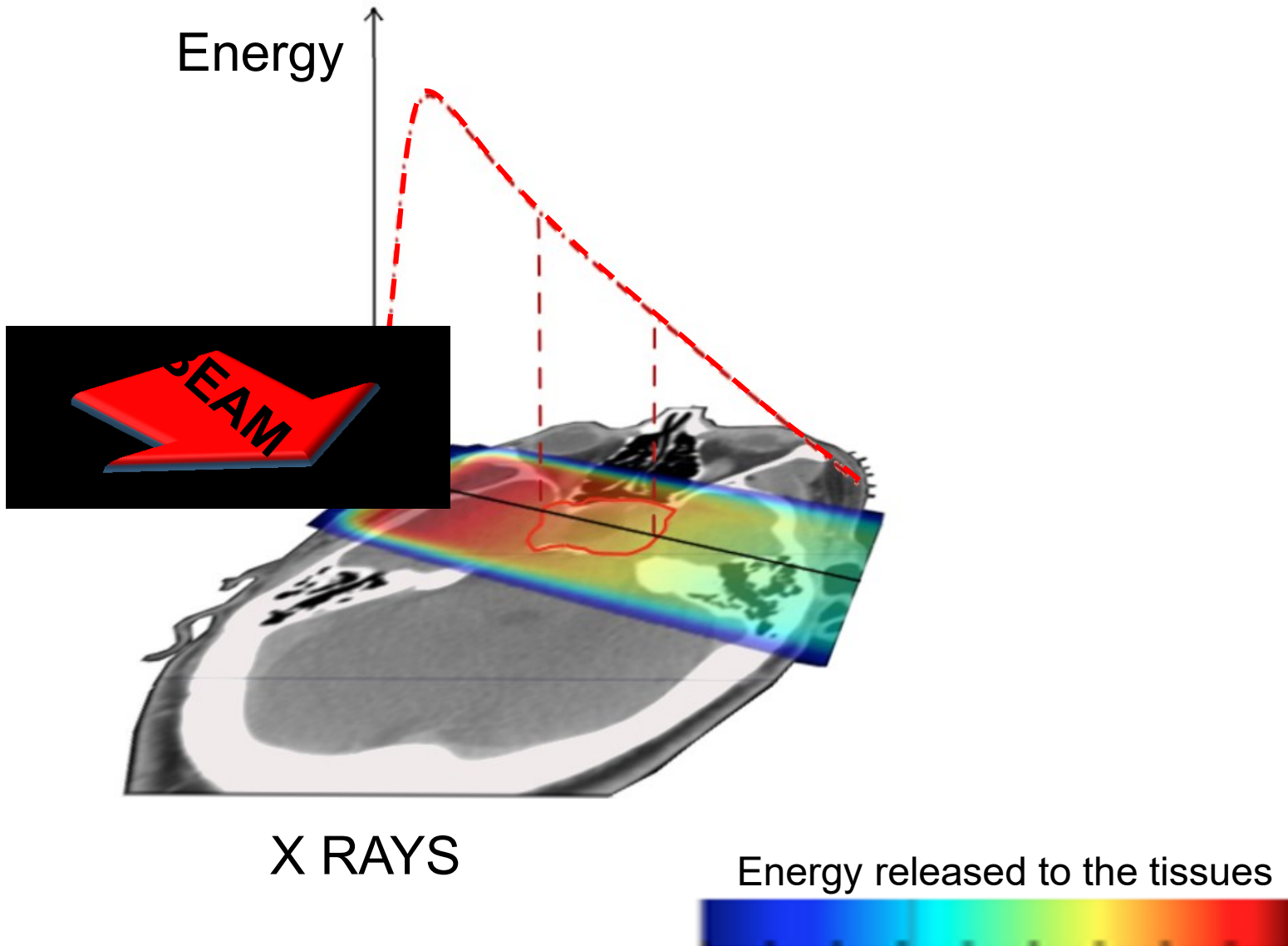


Fast Silicon Detectors for beam monitoring in proton therapy: preliminary results

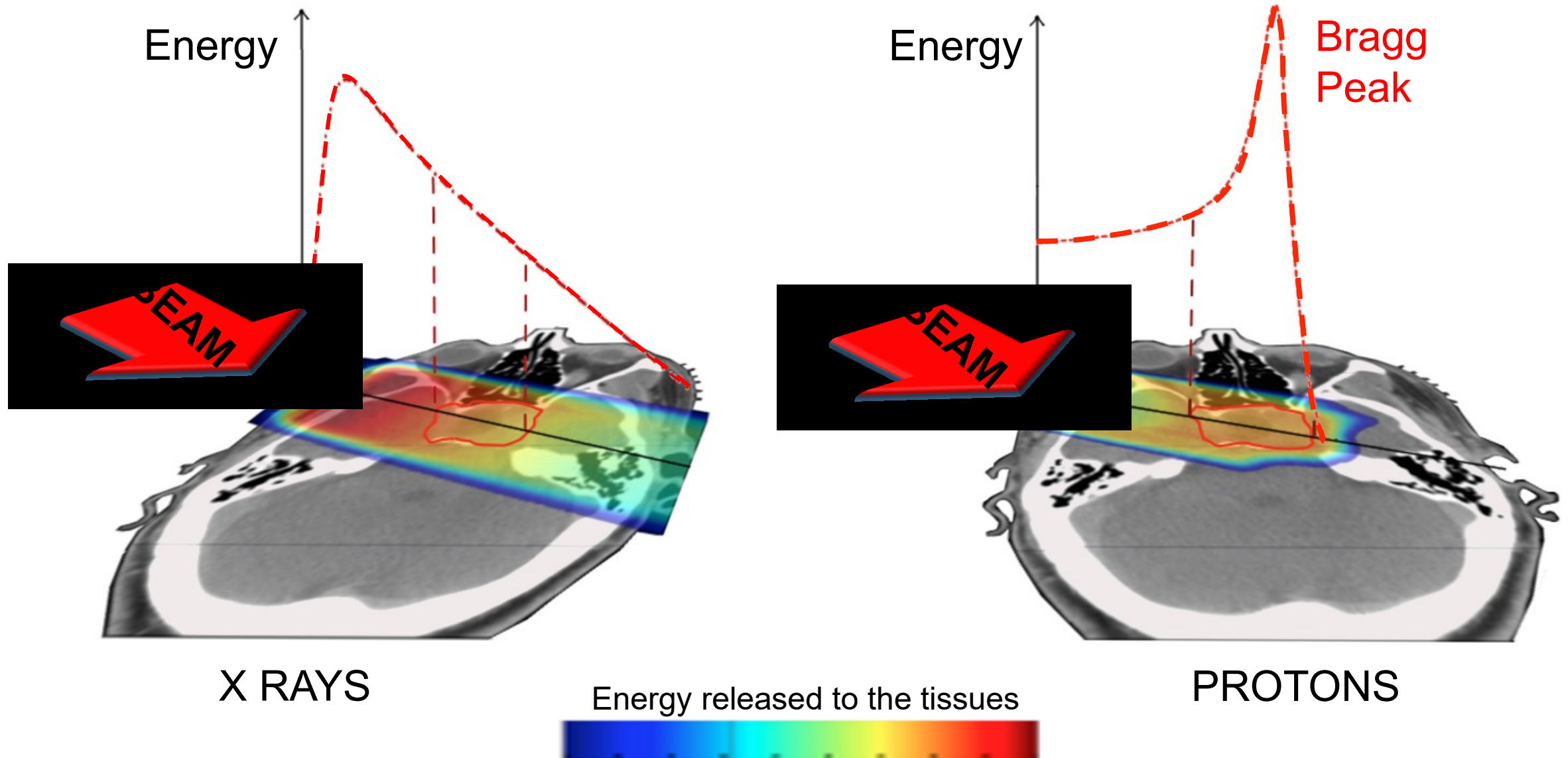
A Vignati¹, Z Ahmadi Ganjeh², A Attili¹, M Boscardin^{3,4}, N Cartiglia¹, GF Dalla Betta⁴, M Donetti⁵, F Fausti^{1,6}, M Ferrero¹, F Ficarella^{3,4}, S Giordanengo¹, O Hammad Ali^{1,7}, M Mandurrino¹, L Manganaro^{1,7}, G Mazza¹, V Monaco^{1,7}, G Paternoster^{3,4}, R Sacchi^{1,7}, Z Shakarami^{1,7}, V Sola¹, A Staiano¹, R Cirio^{1,7}

1 – National Institute for Nuclear Physics (INFN) – Torino (Italy), 2 – Faculty of Physics, University of Yazd, Iran, 3 – Fondazione Bruno Kessler (FBK), Trento (Italy), 4 – National Institute for Nuclear Physics (INFN), TIFPA, Trento (Italy), 5 – Fondazione CNAO, Pavia (Italy), 6 – Politecnico di Torino (Italy), 7 – Università degli Studi di Torino (Italy).

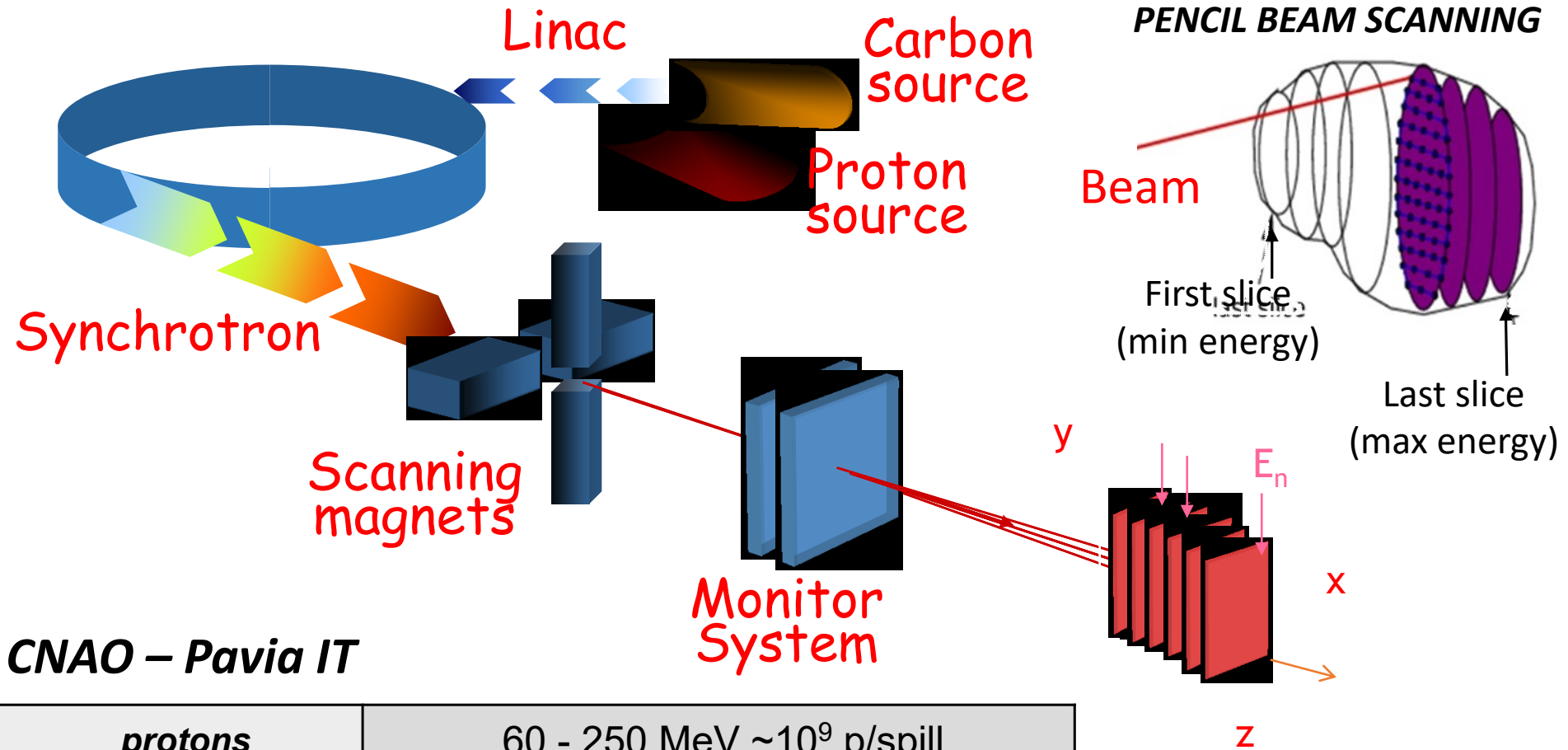
Introduction – Charged Particle Therapy



Introduction – Charged Particle



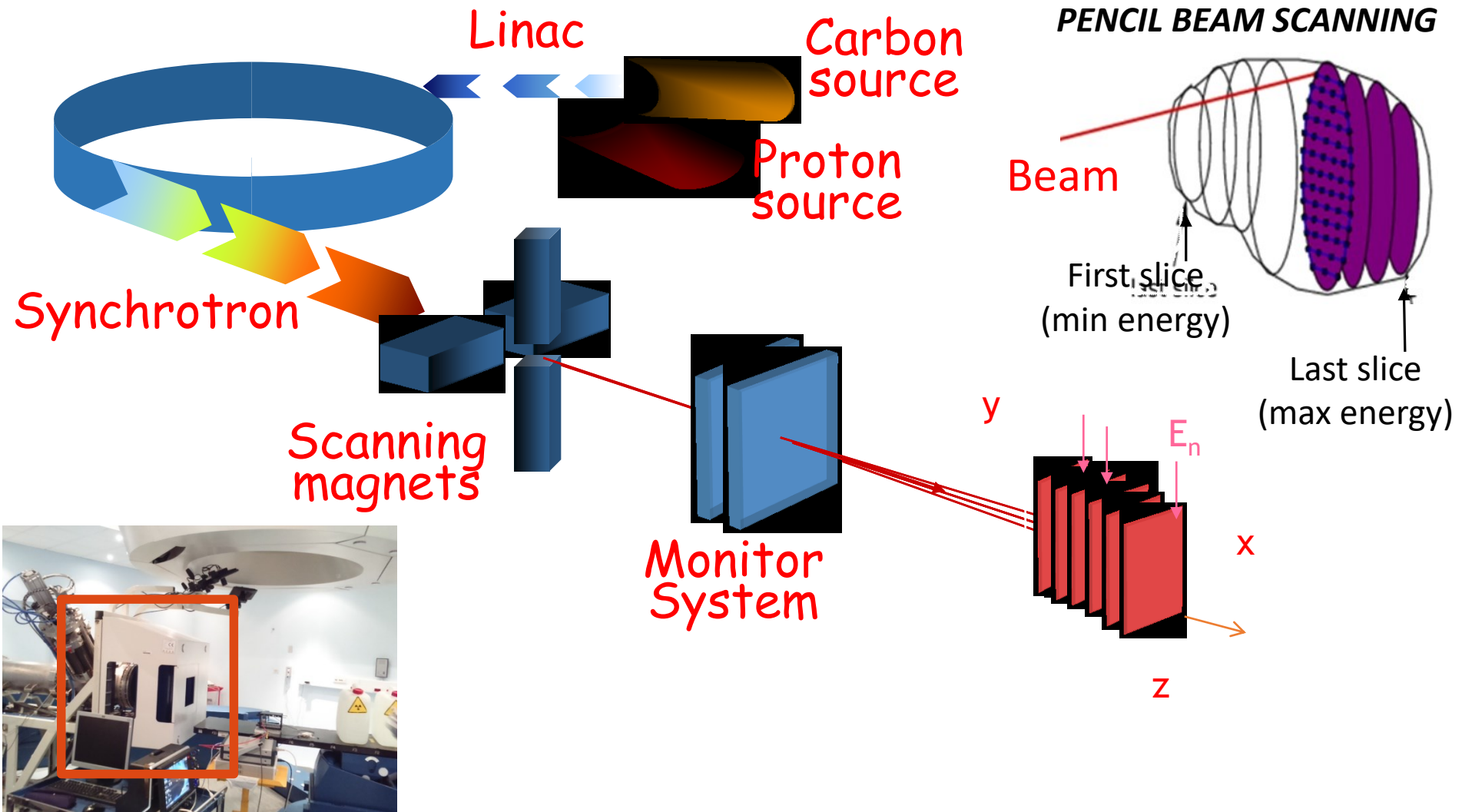
Introduction – Charged Particle Therapy



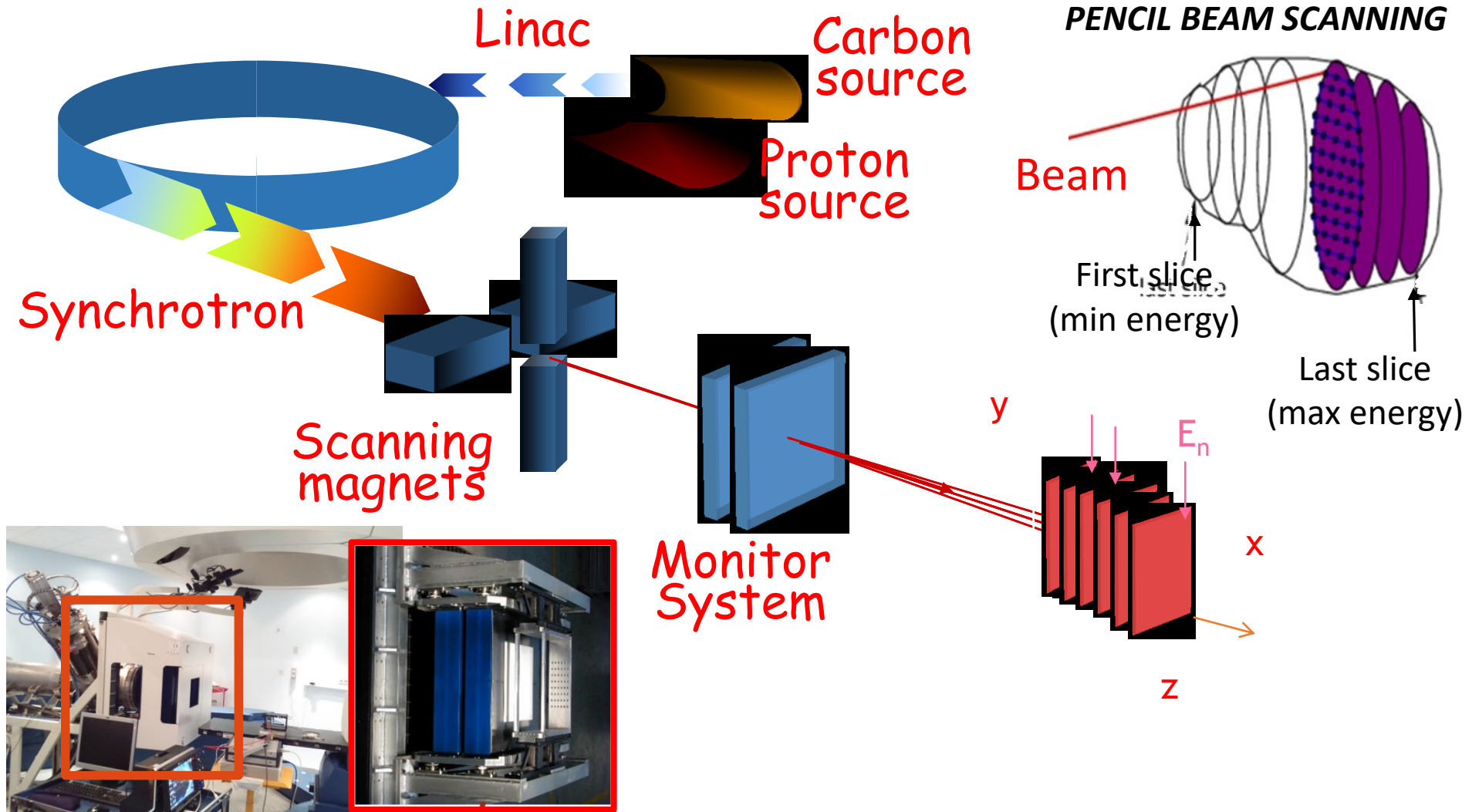
CNAO – Pavia IT

<i>protons</i>	60 - 250 MeV $\sim 10^9$ p/spill
C^{6+}	120 - 400 MeV/u $\sim 10^8$ p/spill
<i>Range in water</i>	3 - 27 cm

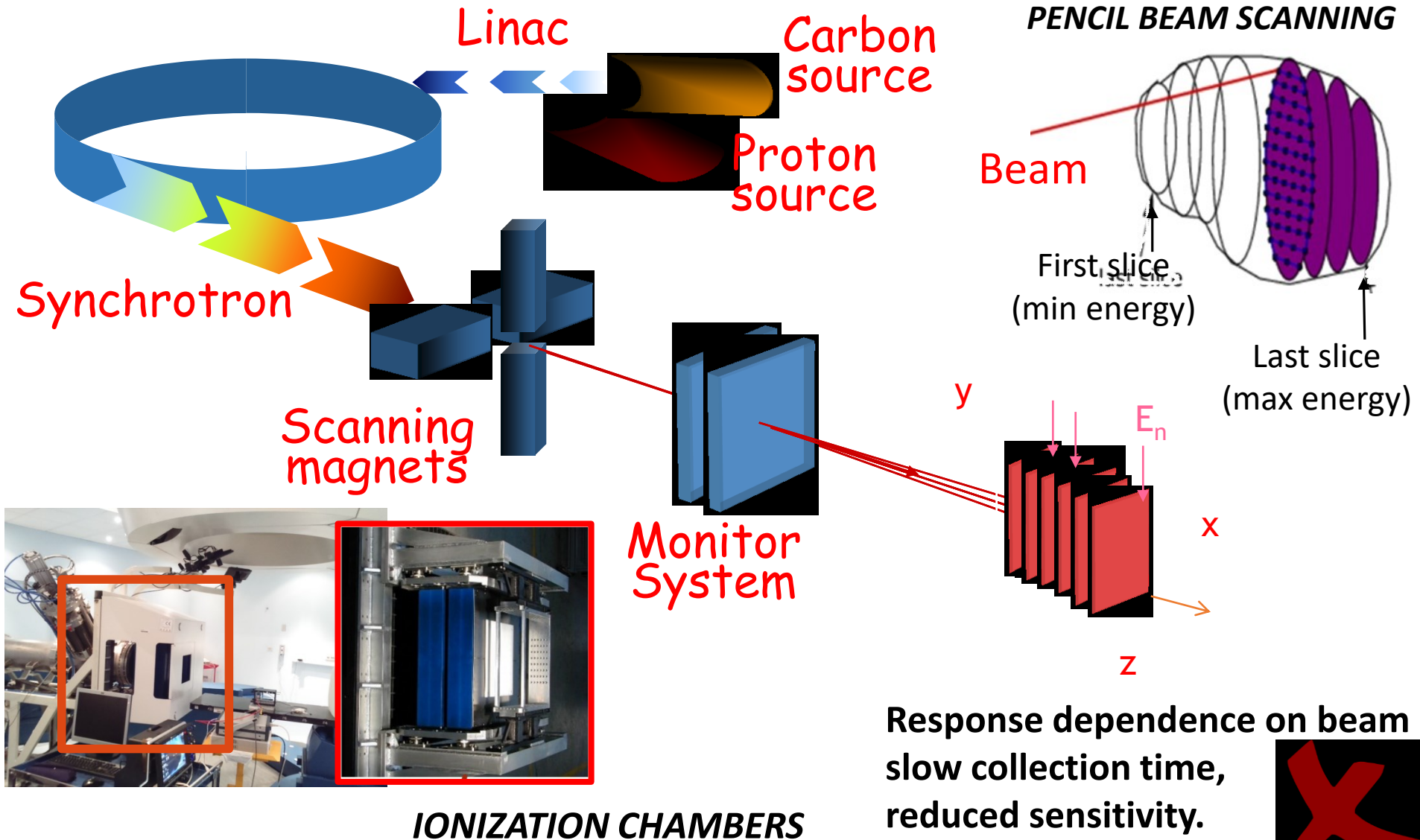
Introduction – Charged Particle Therapy



Introduction – Charged Particle Therapy



Introduction – Charged Particle Therapy



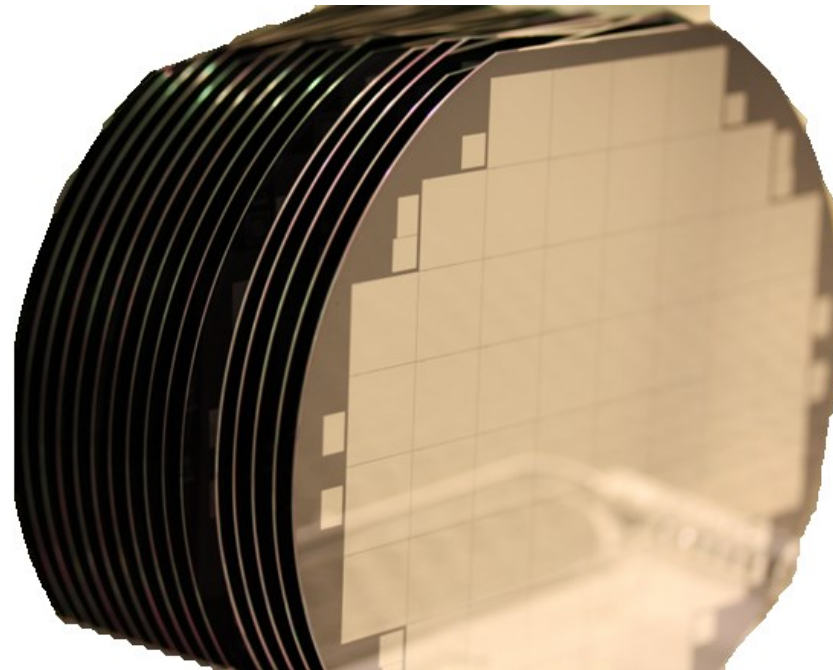
Motivation: beam monitoring in PT

Solid state detectors



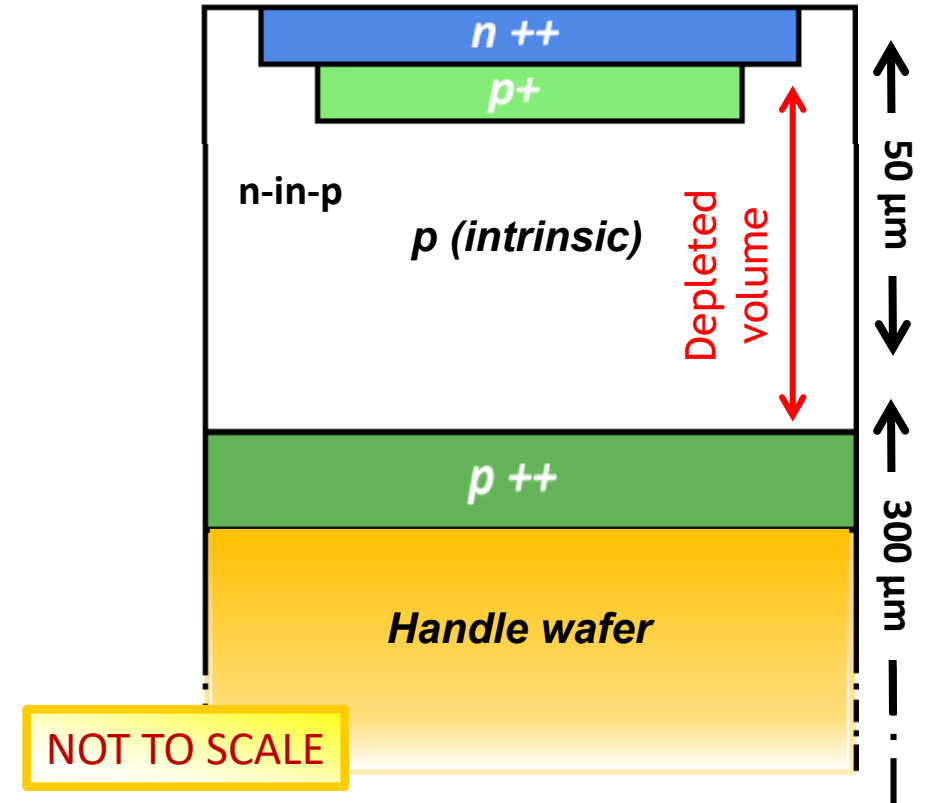
Fast response time,
time resolution,
large granularity.

Radiation damage
Pile-up effects,
High readout complexity.



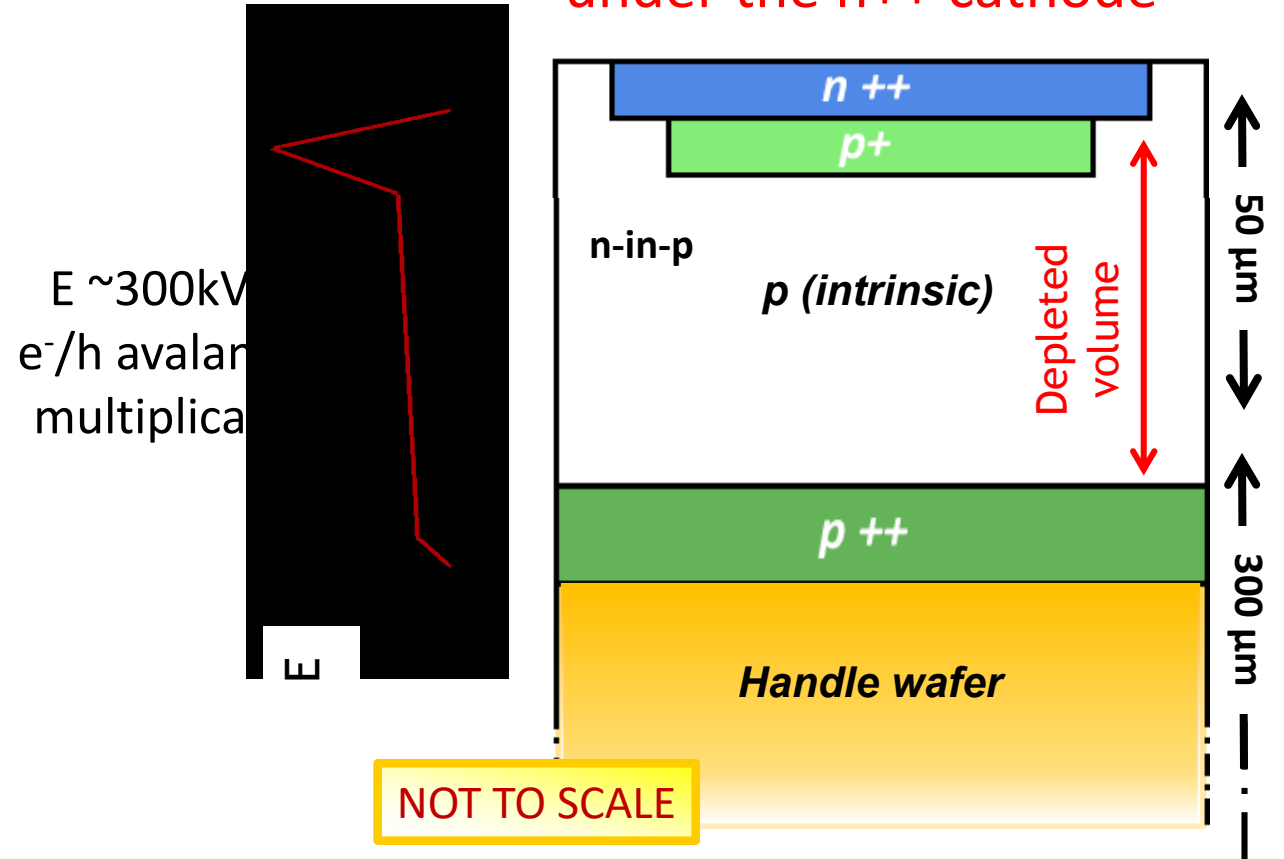
Ultra Fast Silicon Detector (UFSD)

Thin p^+ gain layer implanted under the n^{++} cathode



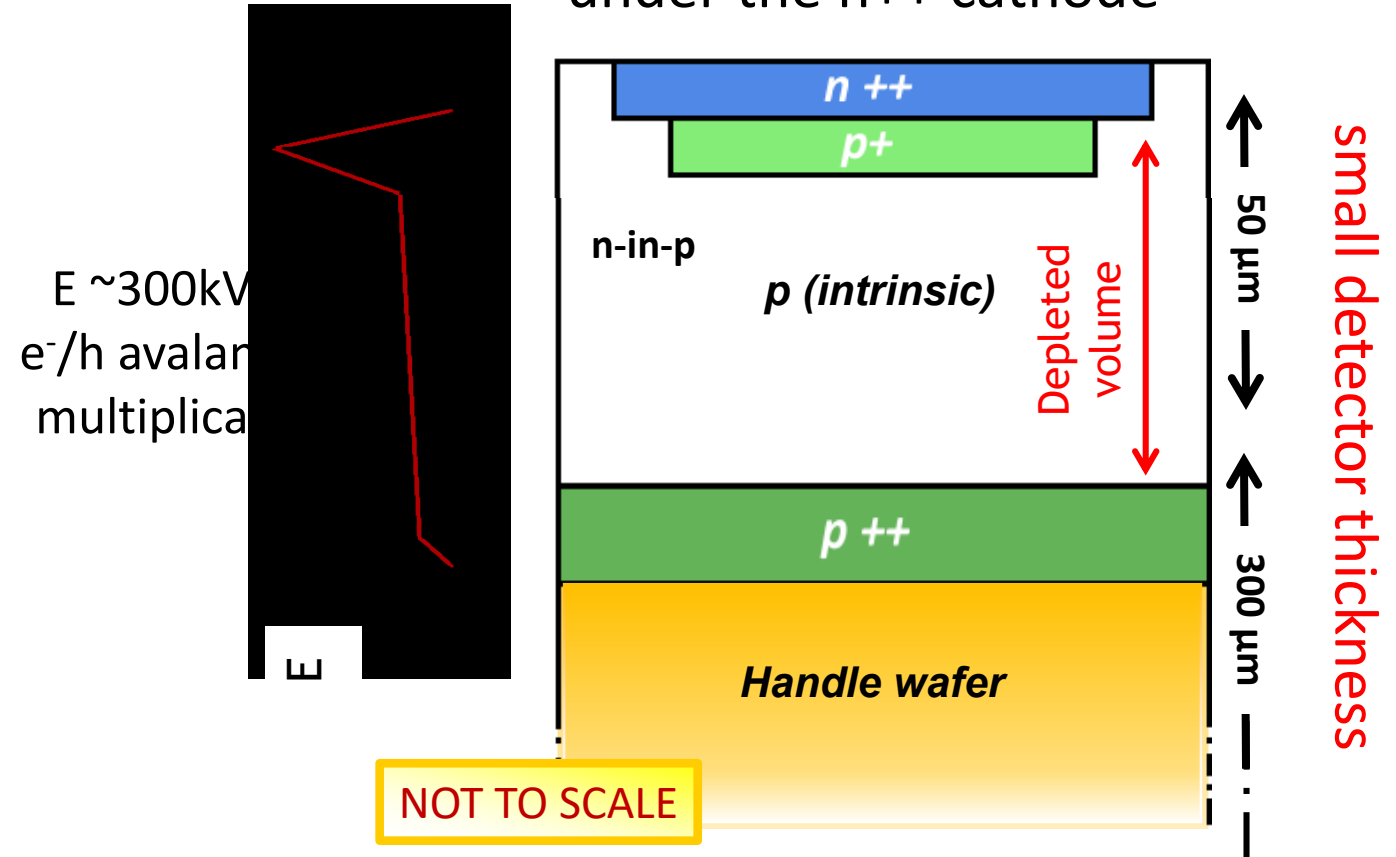
Ultra Fast Silicon Detector (UFSD)

Thin p^+ gain layer implanted under the n^{++} cathode

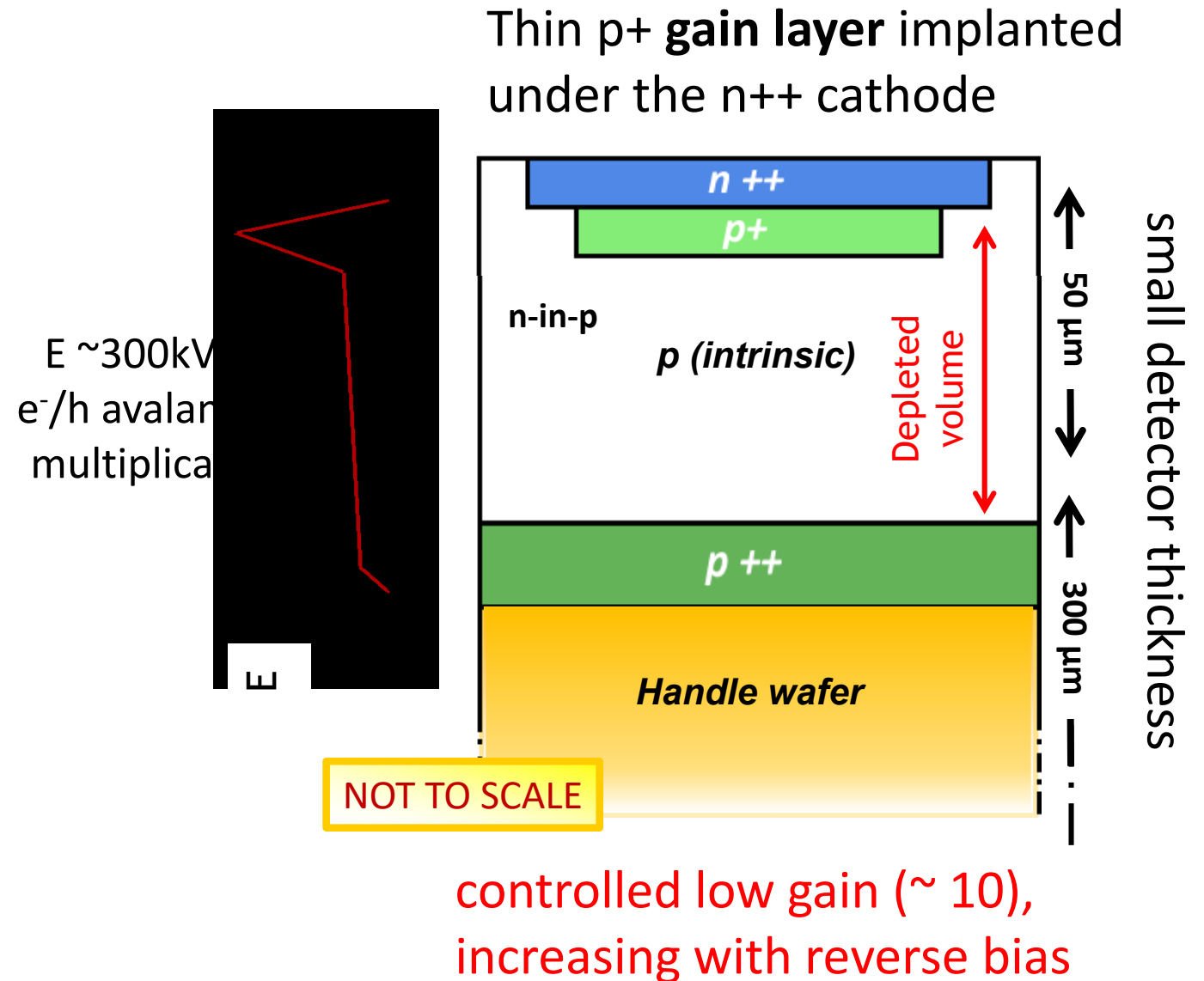


Ultra Fast Silicon Detector (UFSD)

Thin p^+ **gain layer** implanted under the n^{++} cathode



Ultra Fast Silicon Detector (UFSD)



Ultra Fast Silicon Detector (UFSD)

Small signal duration (1 ns)

→ **particle counting**

Excellent time resolution (tens of ps)

→ beam **energy measurement**

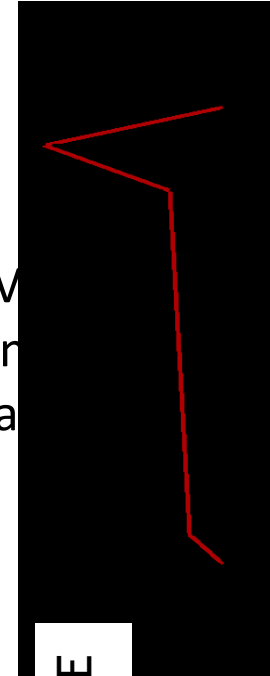


single particle detection capability

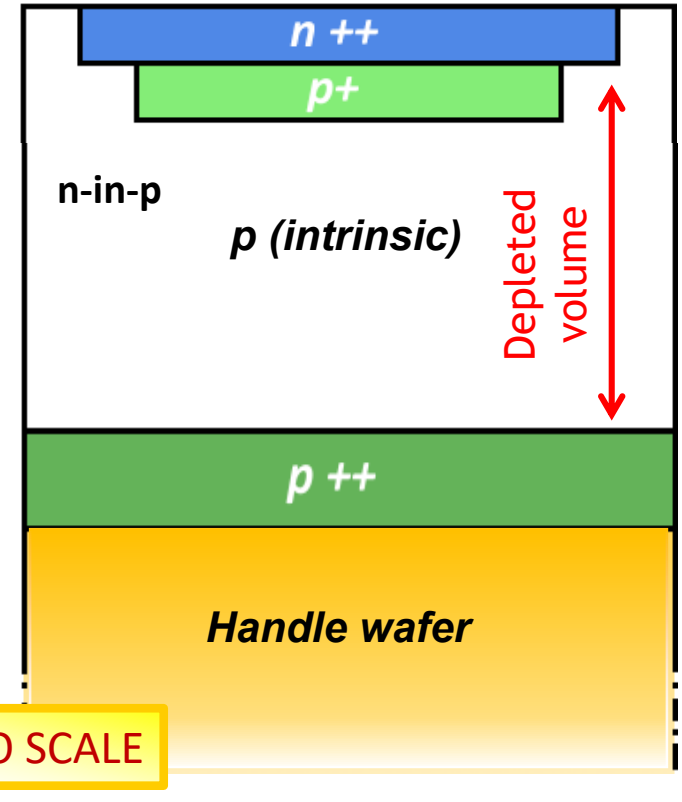


energy measurement from time of Flight (ToF).

$E \sim 300\text{kV}$
 e^-/h avalanche
multiplication



Thin p^+ gain layer implanted under the n^{++} cathode

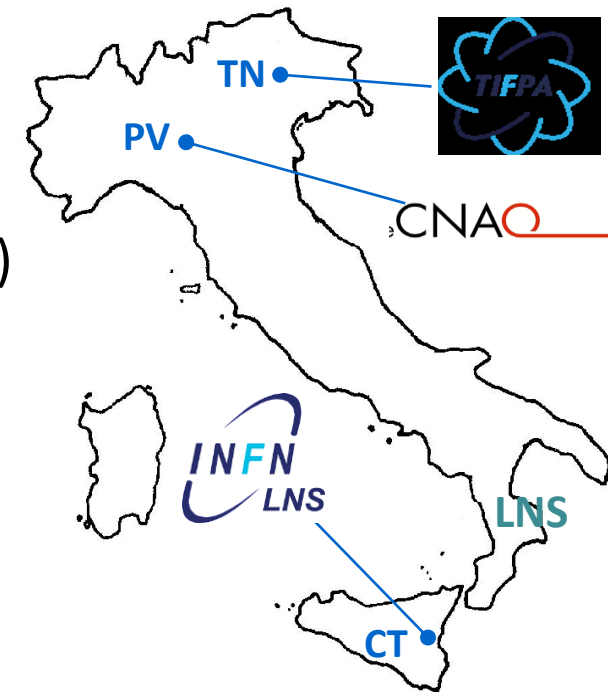


small detector thickness

controlled low gain (~ 10),
increasing with reverse bias

Two prototypes of UFSD for radiobiological applications @ three irradiation facilities:

1. to **directly count** individual protons:
 - area $3 \times 3 \text{ cm}^2$;
 - up to fluence rate of 10^8 p/s cm^2 (with error $< 1\%$ - clinical requirement)
 - segmented in strips \rightarrow beam projections in two orthogonal directions;
2. to **measure the beam energy** with time-of-flight techniques, using a telescope of two UFSD sensors:
 - error $< 1 \text{ mm}$ range in water.



For additional details <http://www.tifpa.infn.it/projects/move-it/>

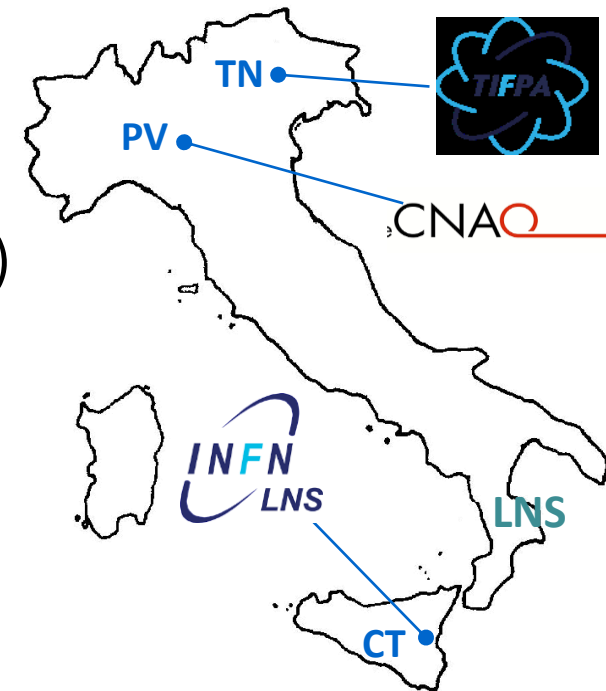
Modeling and **Ve**rification for
Ion beam **T**reatment planning



Implementation of advanced radiobiological models in
ion TPS, experimental verification in-vitro and in-vivo.

Two prototypes of UFSD for radiobiological applications @ three irradiation facilities:

1. to **directly count** individual protons:
 - area $3 \times 3 \text{ cm}^2$;
 - up to fluence rate of 10^8 p/s cm^2 (with error $< 1\%$ - clinical requirement)
 - segmented in strips \rightarrow beam projections in two orthogonal directions;
2. to **measure the beam energy** with time-of-flight techniques, using a telescope of two UFSD sensors:
 - error $< 1 \text{ mm}$ range in water.



For additional details <http://www.tifpa.infn.it/projects/move-it/>

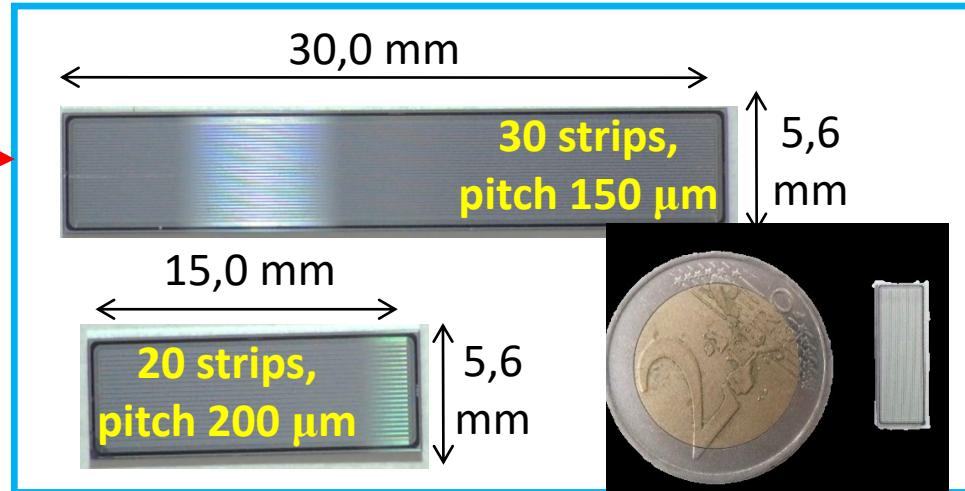
Particle Counting



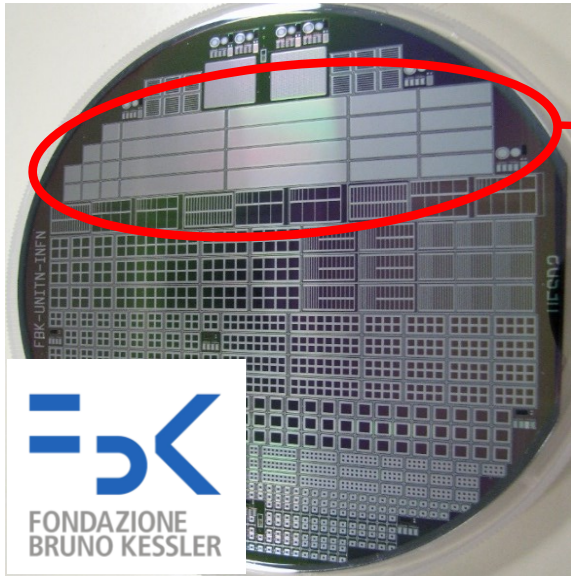
Test of 50 μm UFSD prototypes @ CNAO (protons)



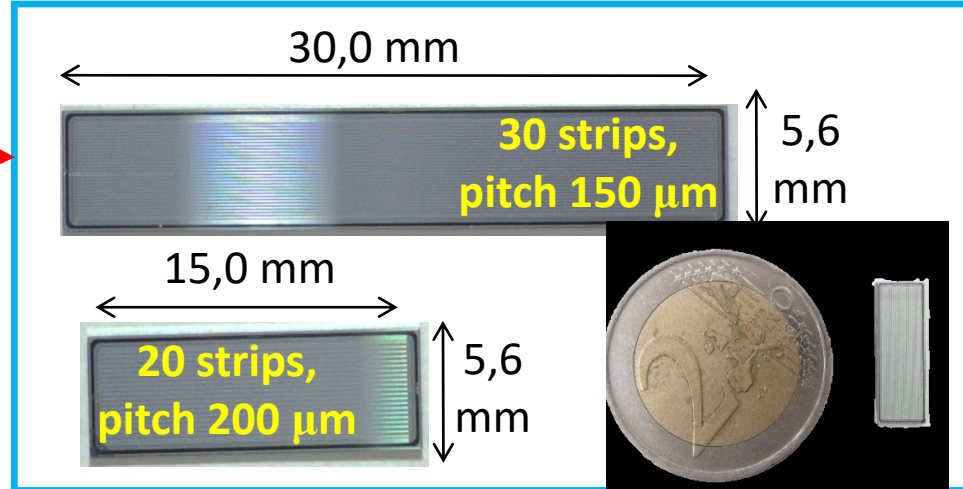
18 silicon-on-silicon wafers
different **doping strategies**
for the gain layer to improve
radiation resistance.



Test of 50 μm UFSD prototypes @ CNAO (protons)

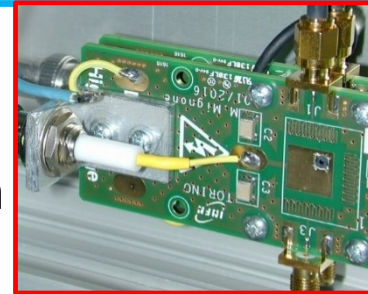


18 silicon-on-silicon wafers
different **doping strategies**
for the gain layer to improve
radiation resistance.



Readout

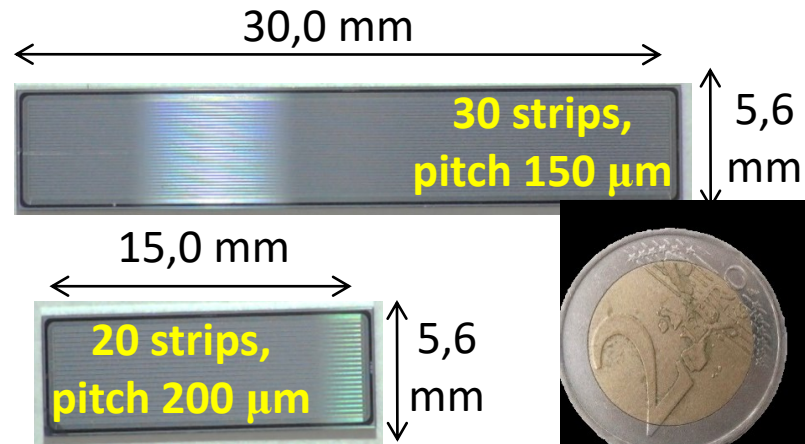
- Passive FE boards aligned to the beam
- CIVIDEC broadband 40 dB amplifiers
- CAEN digitizer (5 Gs/s)



Test of 50 μm UFSD prototypes @ CNAO (protons)

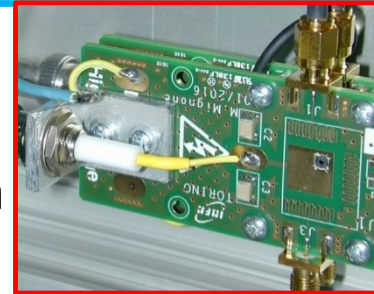


18 silicon-on-silicon wafers
different **doping strategies**
for the gain layer to improve
radiation resistance.



Readout

- Passive FE boards aligned to the beam
- CIVIDEC broadband 40 dB amplifiers
- CAEN digitizer (5 Gs/s)

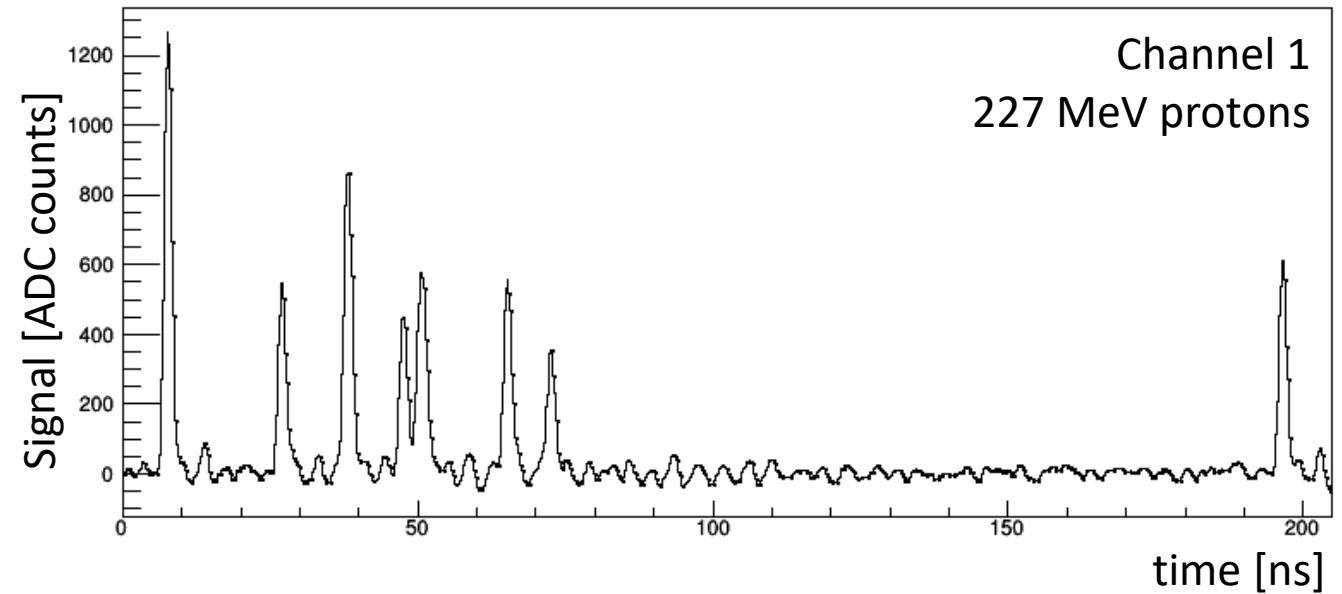


CNAO Technical Proton Beam

- **Beam FWHM** $\sim 10\text{mm}$
- **Max flux** $\sim 10^9$ p/s delivered in spills
- **Beam flux range:** 20% - 100% of max flux.
- **Beam energy range:** 62 – 227 MeV (5 – 2 MIPs)

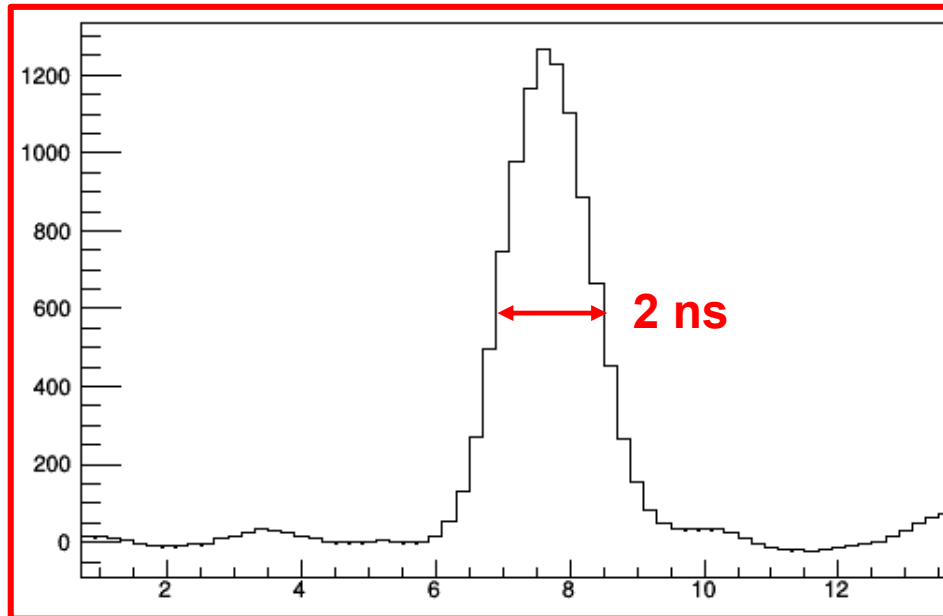
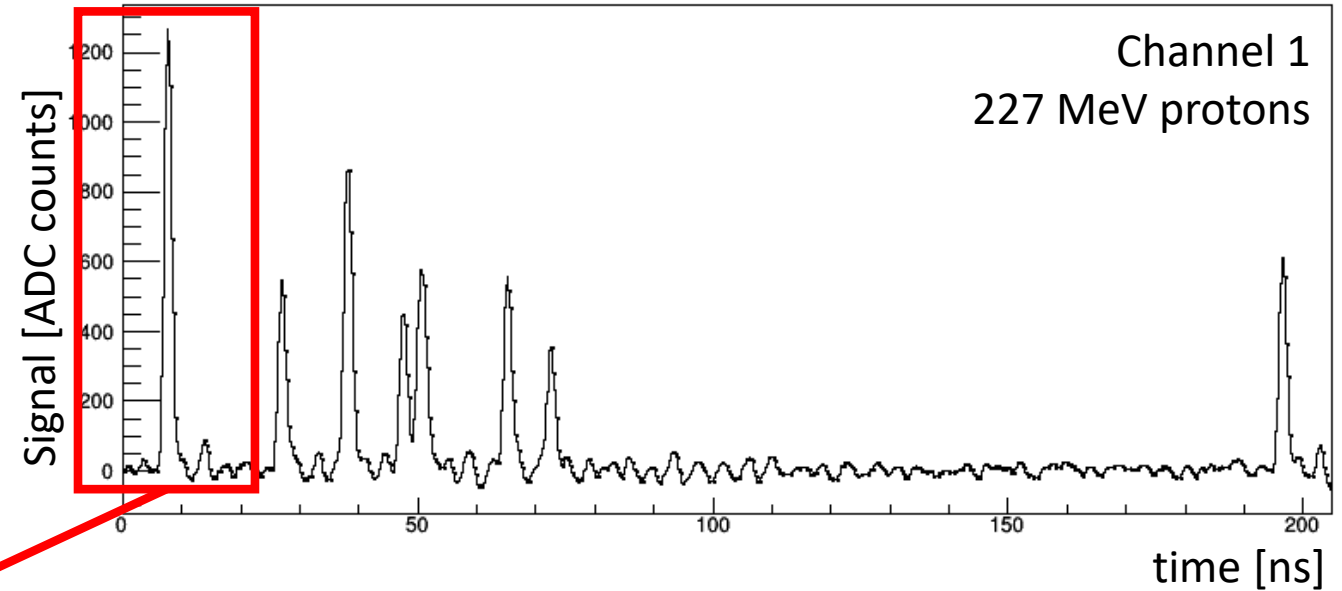
Signal waveform acquired on a clinical proton beam

- Peaks corresponding to **individual protons** can be easily distinguished;
- large amplitude fluctuations;



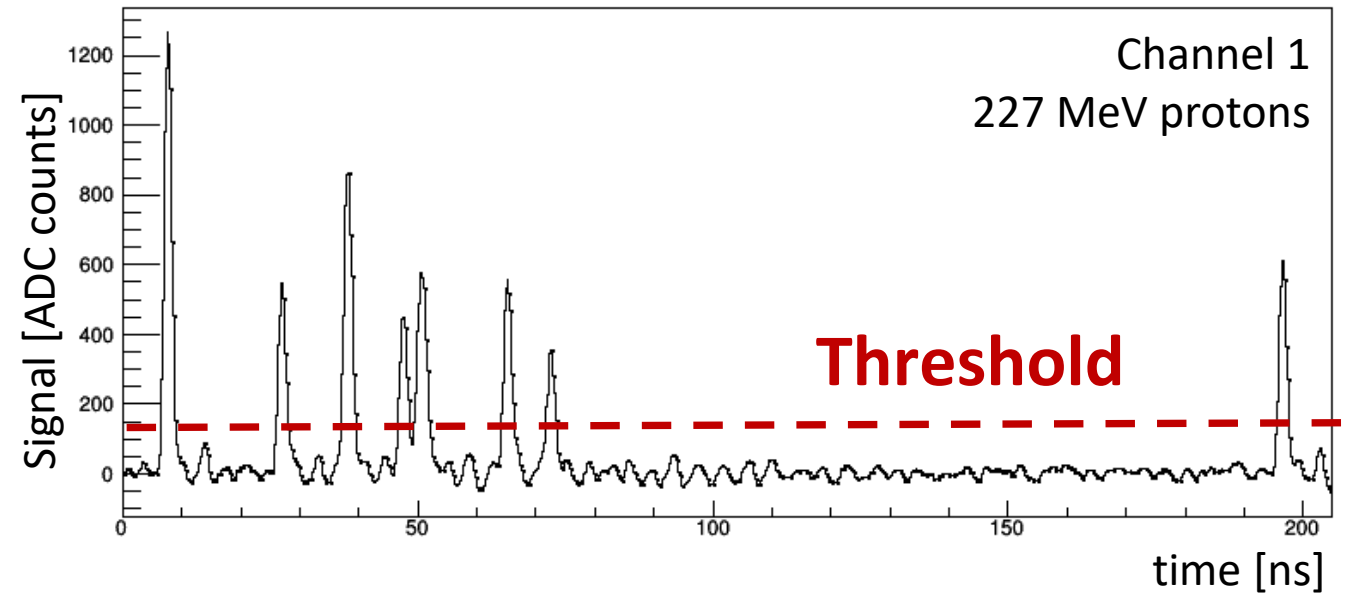
Signal waveform acquired on a clinical proton beam

- Peaks corresponding to **individual protons** can be easily distinguished;
- large amplitude fluctuations;
- short peak duration;



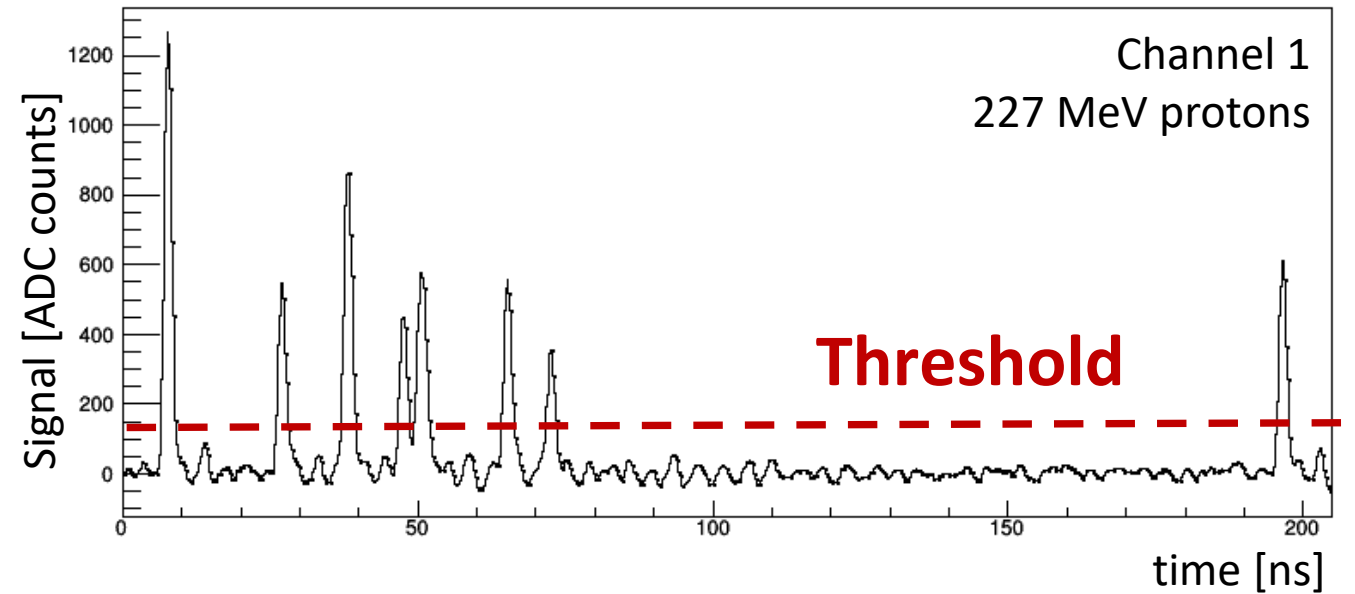
Signal waveform acquired on a clinical proton beam

- Peaks corresponding to **individual protons** can be easily distinguished;
- large amplitude fluctuations;
- short peak duration;
- fixed threshold can be applied to **count the pulses**;



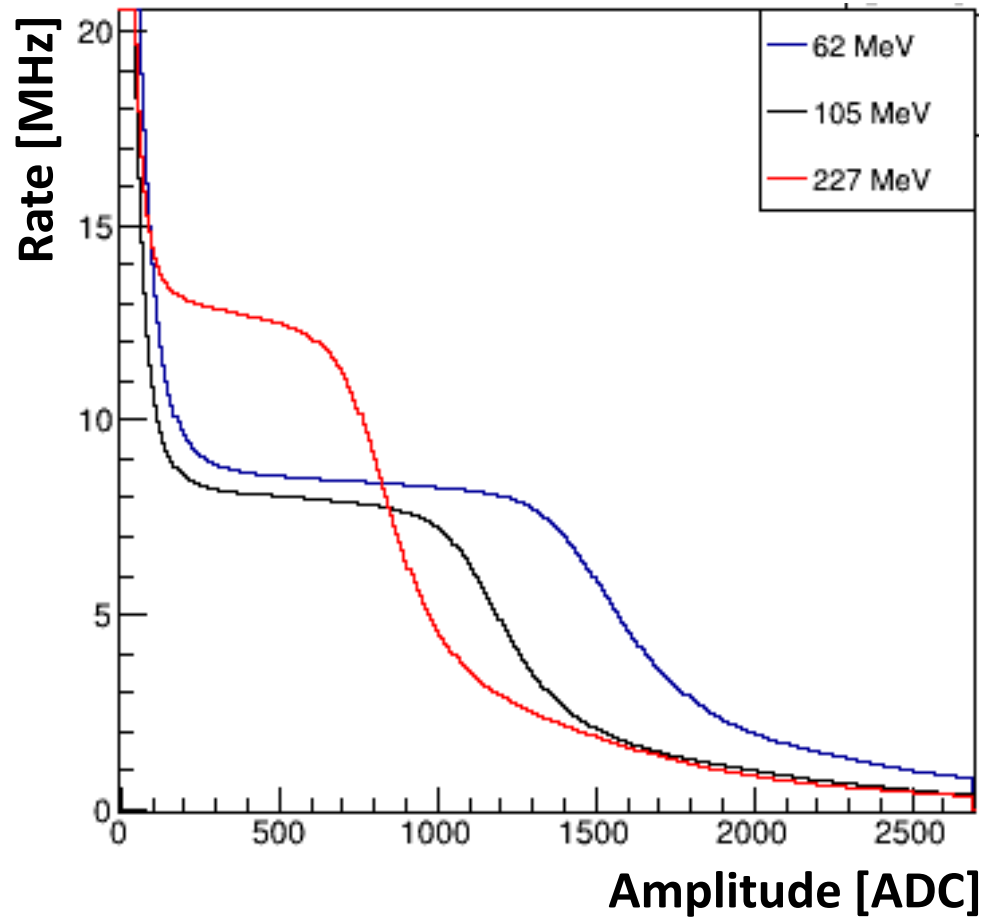
Signal waveform acquired on a clinical proton beam

- Peaks corresponding to **individual protons** can be easily distinguished;
- large amplitude fluctuations;
- short peak duration;
- fixed threshold can be applied to **count the pulses**;



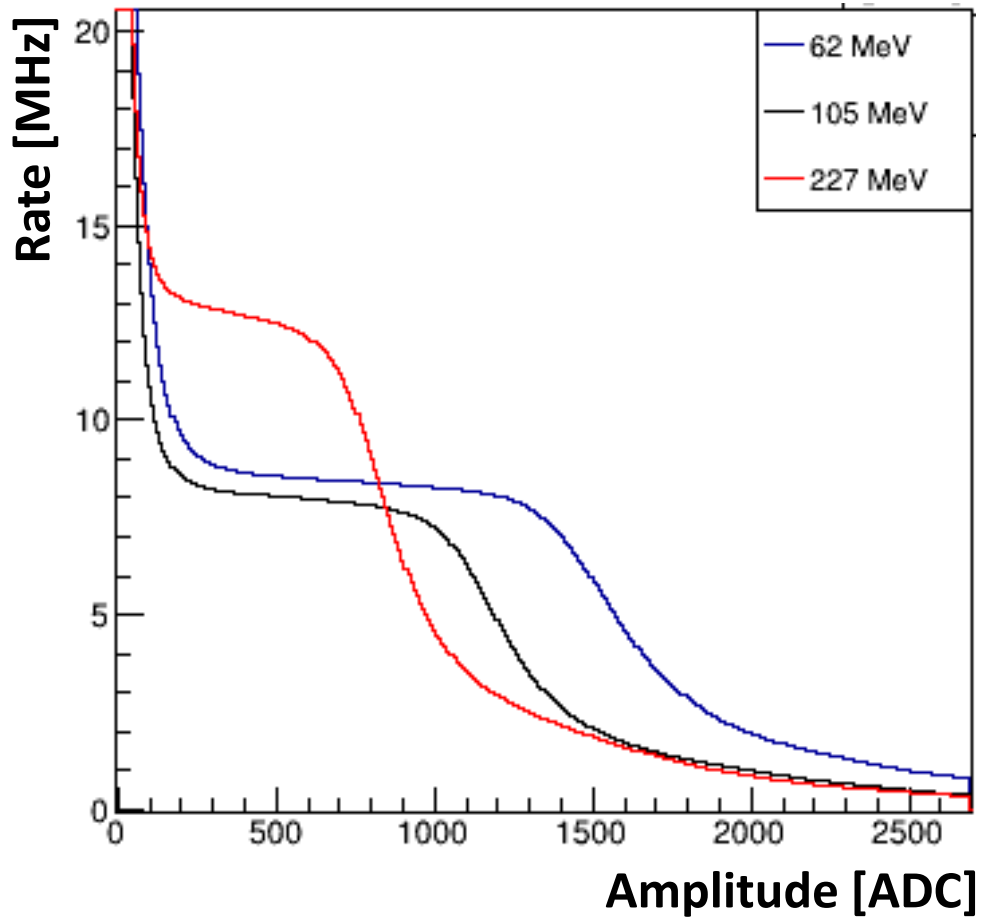
Count protons

Signal distribution

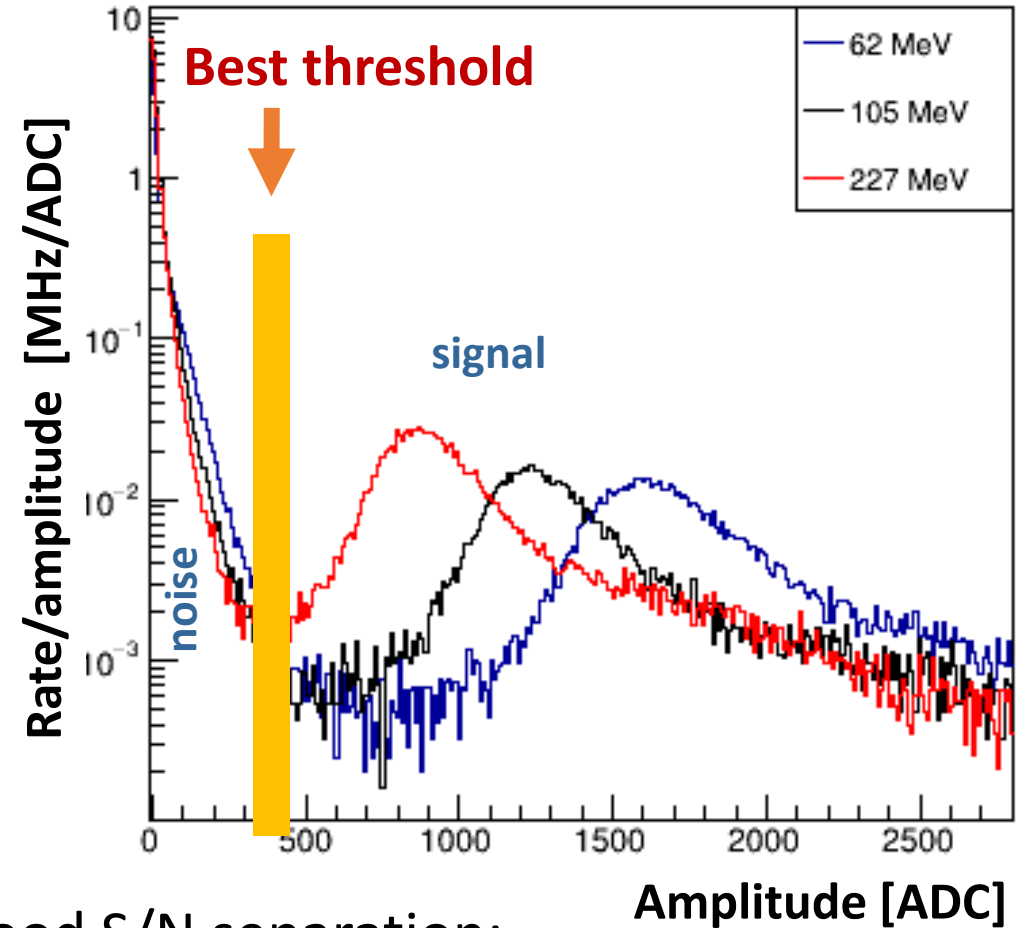


Increasing threshold

Signal distribution



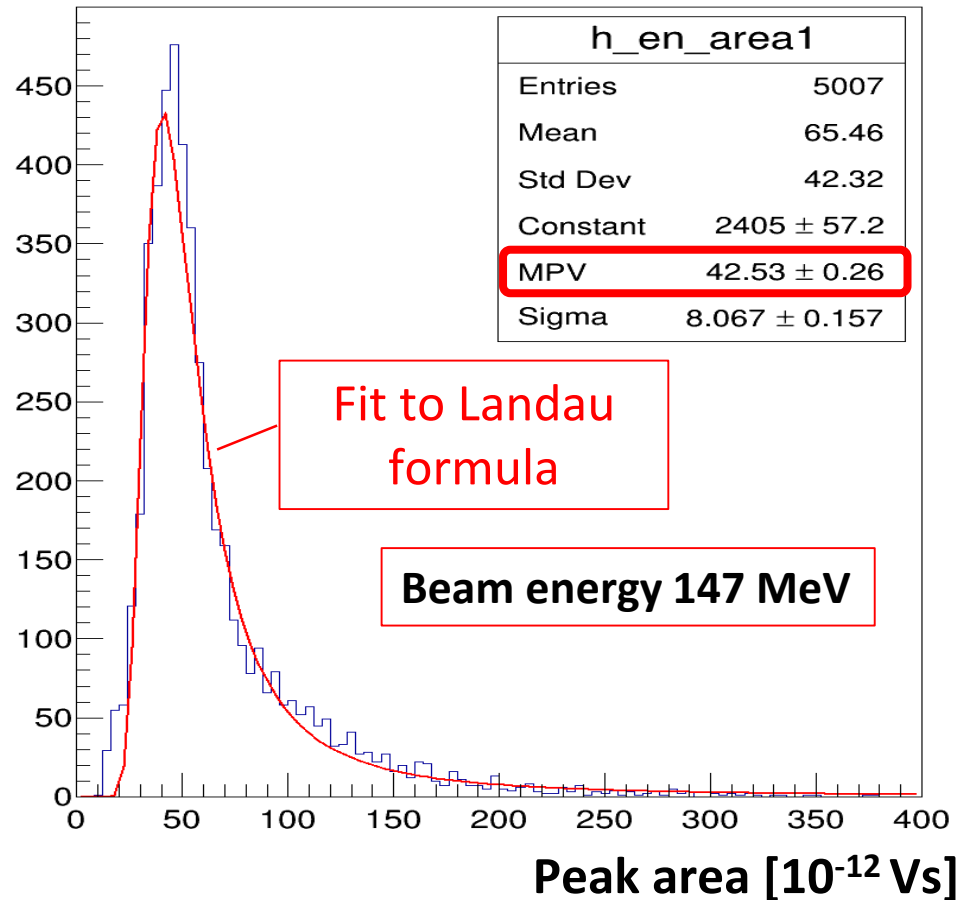
Increasing threshold



- Good S/N separation;
- Larger S/N at lower beam energies;
- Best threshold is beam energy dependent.

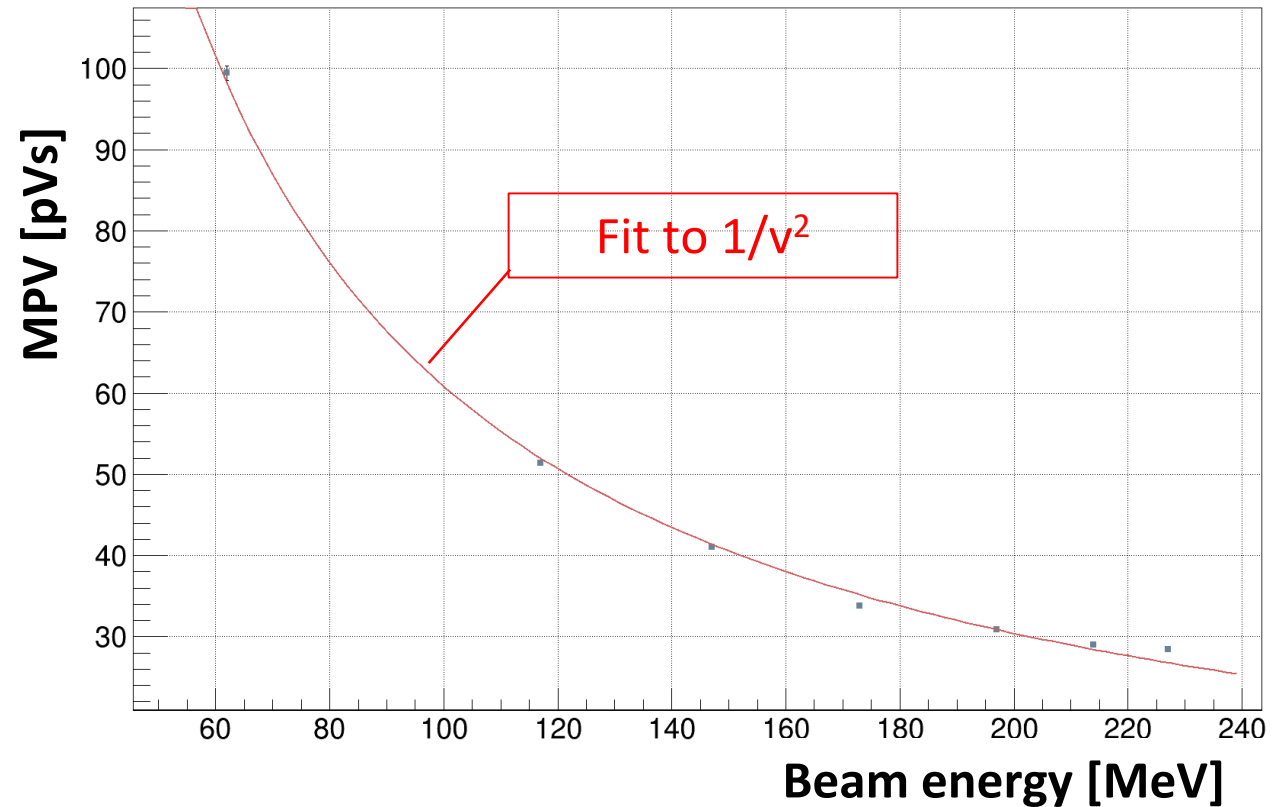
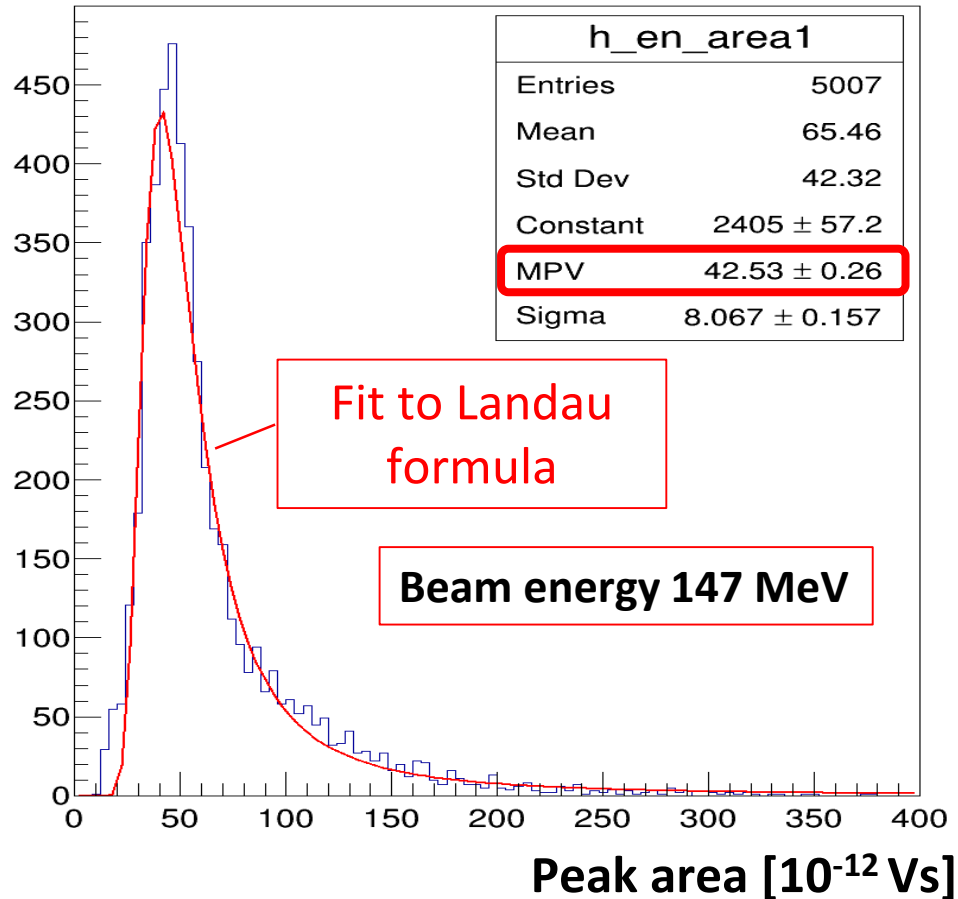
Peak Area and Landau distribution

- Area of peaks proportional to collected charge;
- well described by Landau formula

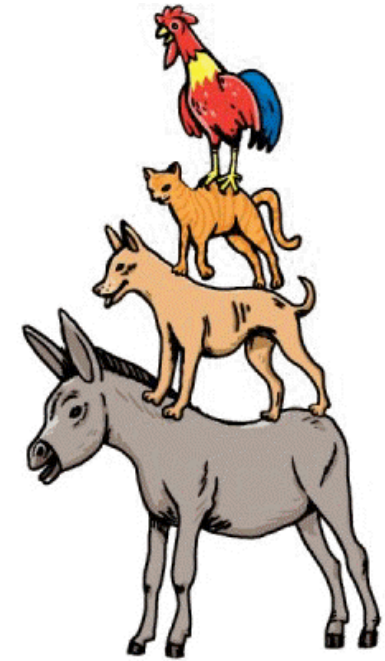


Peak Area and Landau distribution

- Area of peaks proportional to collected charge;
- well described by Landau formula
- Landau's MPV dependence on beam energy well described by Bethe-Bloch $1/v^2$ dependence

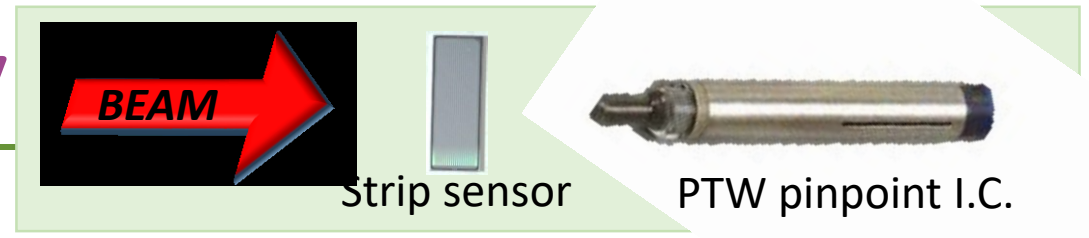


Particle Counting

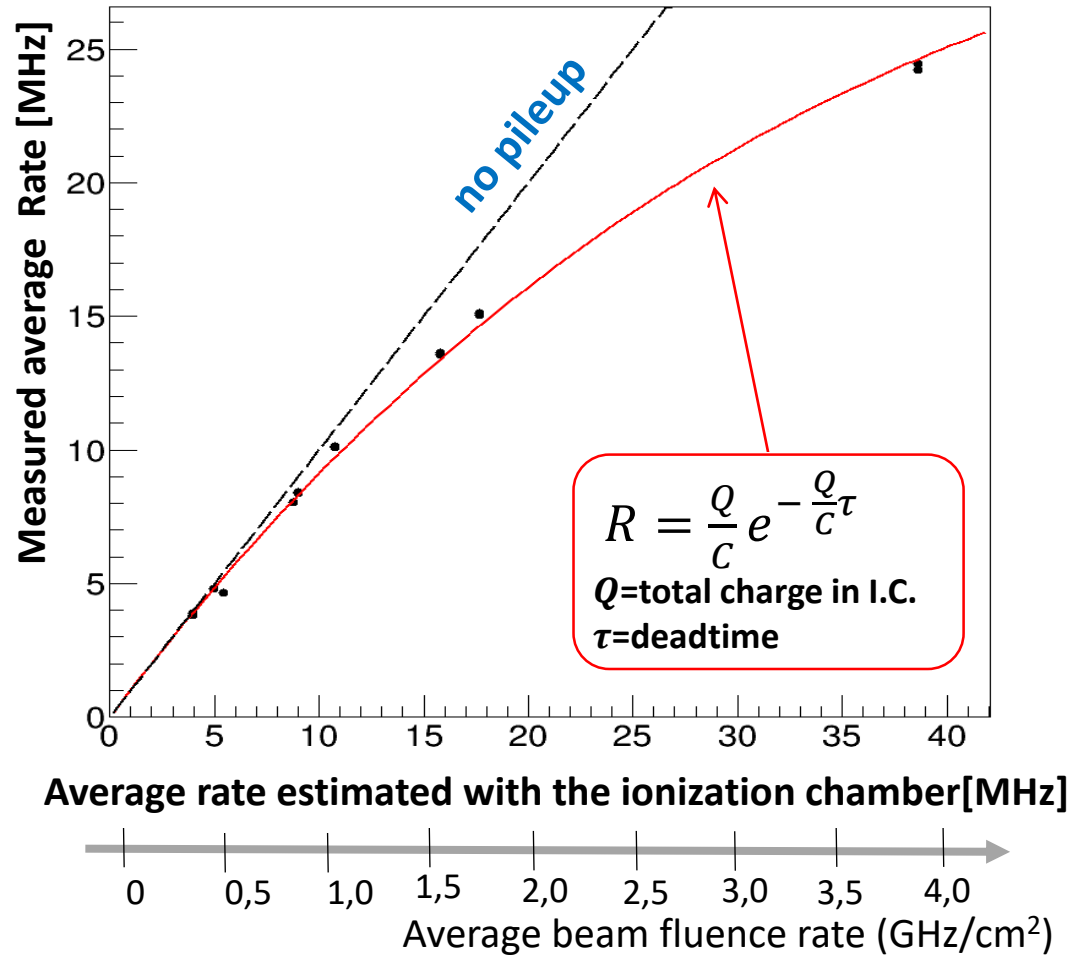


Pile-up inefficiency

Concern: pile-up inefficiency

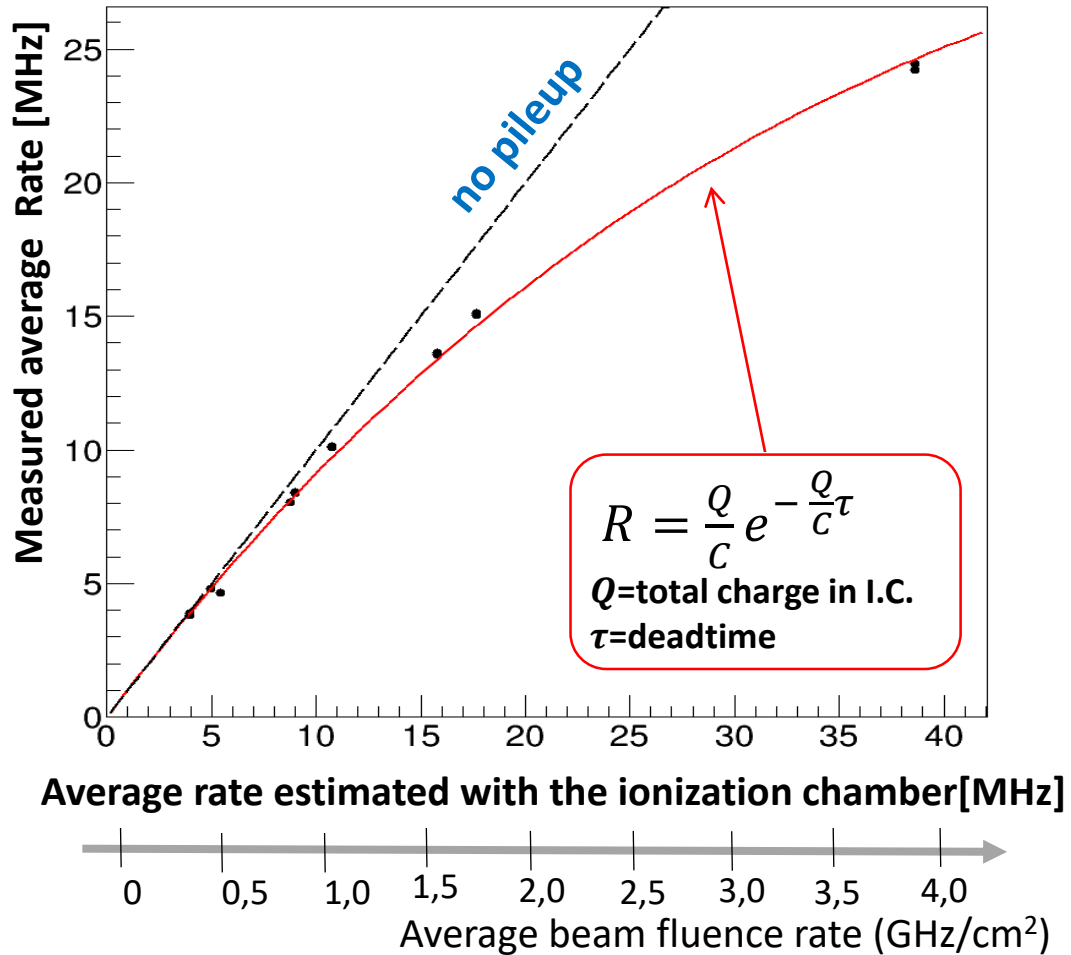


Measured vs. estimated rate, using a PTW pinpoint I.C. and a varied beam flux (20 – 50 – 100% of max)



Concern: pile-up inefficiency

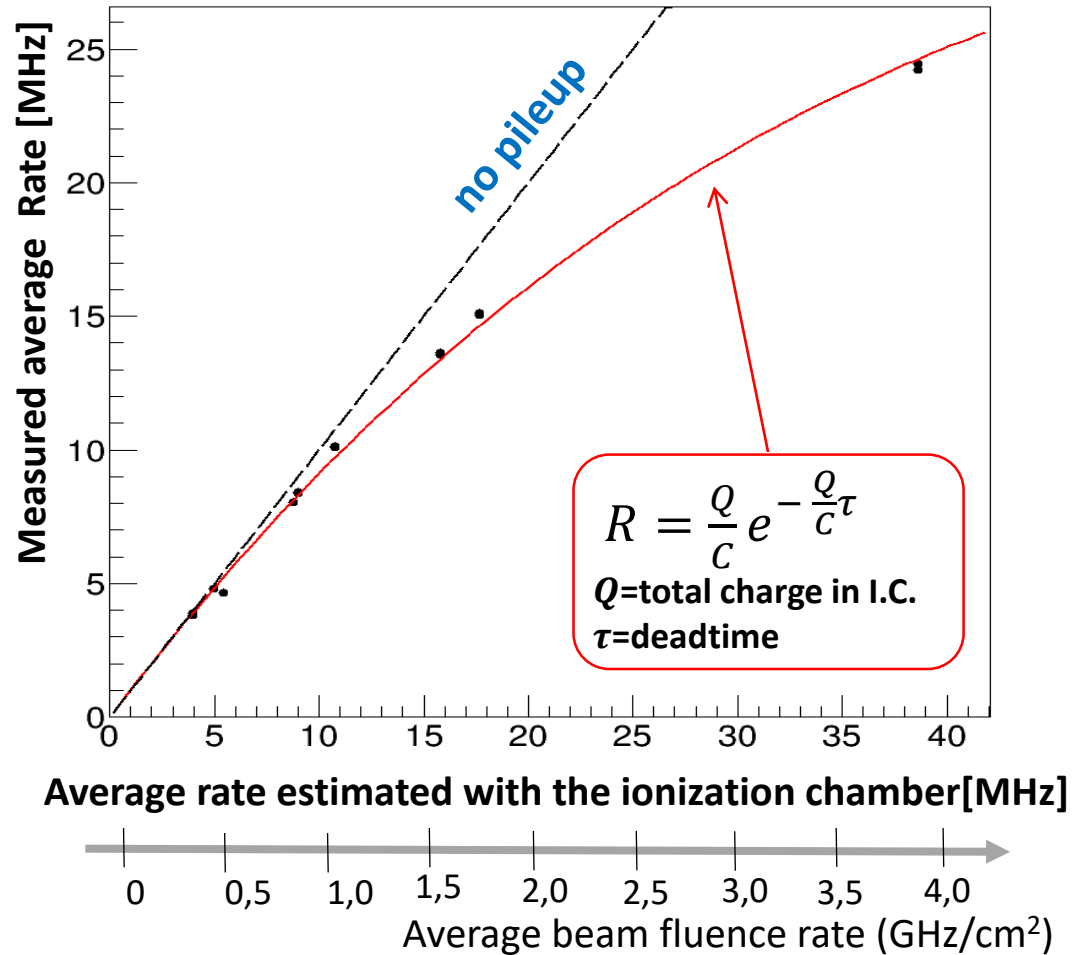
Measured vs. estimated rate, using a PTW pinpoint I.C. and a varied beam flux (20 – 50 – 100% of max)



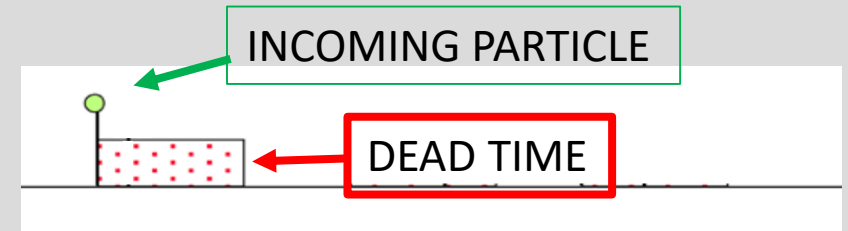
- Large inefficiency observed (up to 25% at largest clinical fluxes) → Correction required
- Data well described by paralyzable pileup model

Concern: pile-up inefficiency

Measured vs. estimated rate, using a PTW pinpoint I.C. and a varied beam flux (20 – 50 – 100% of max)

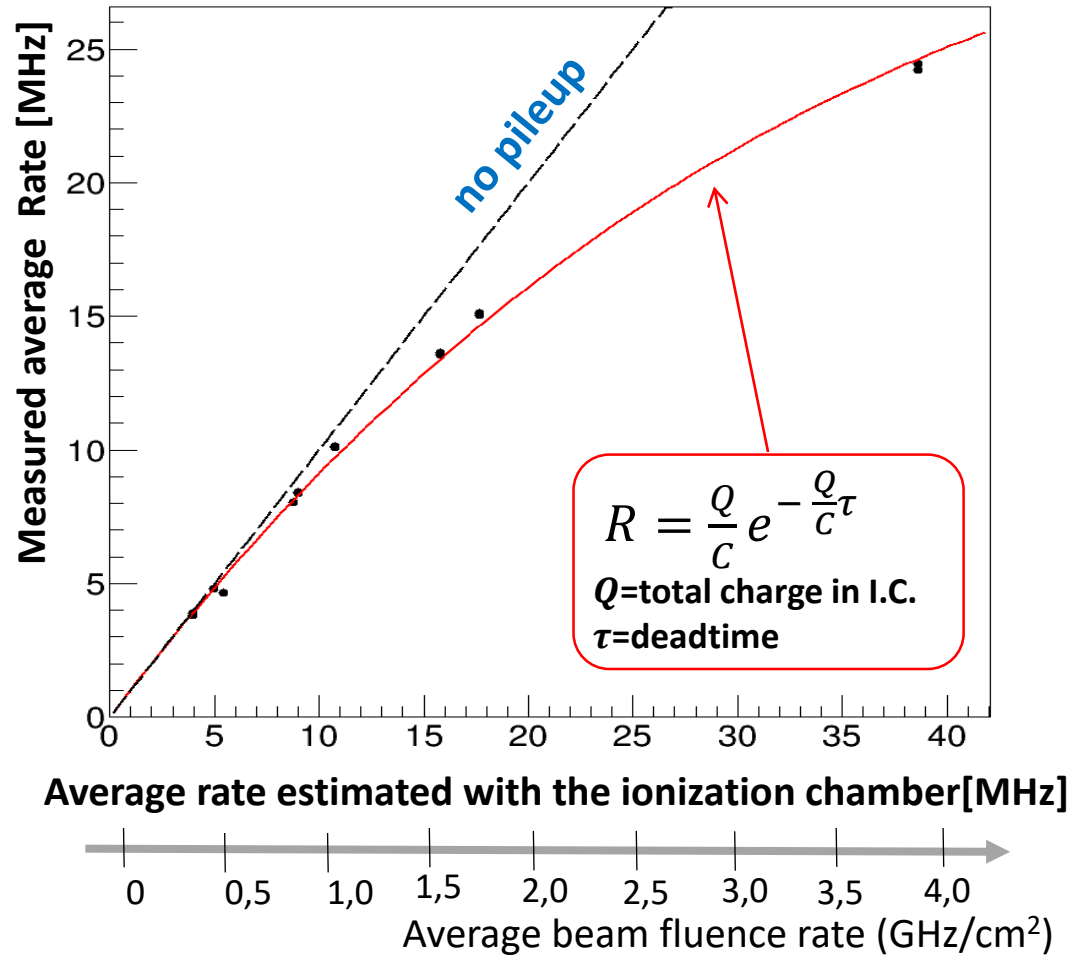


- Large inefficiency observed (up to 25% at largest clinical fluxes) → Correction required
- Data well described by paralyzable pileup model

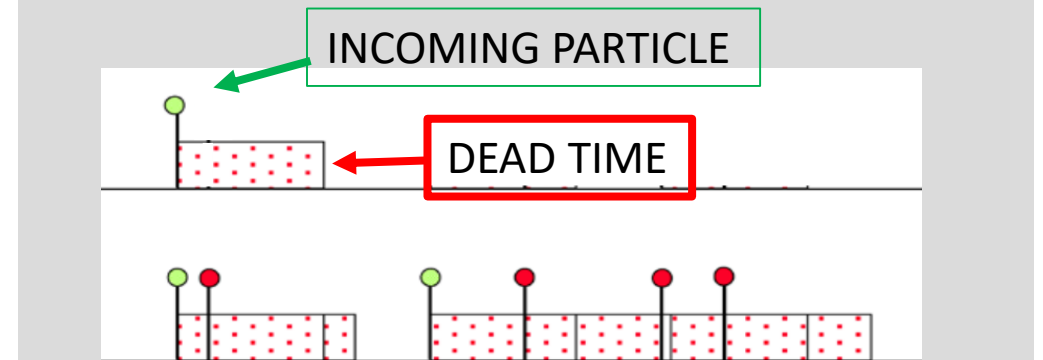


Concern: pile-up inefficiency

Measured vs. estimated rate, using a PTW pinpoint I.C. and a varied beam flux (20 – 50 – 100% of max)

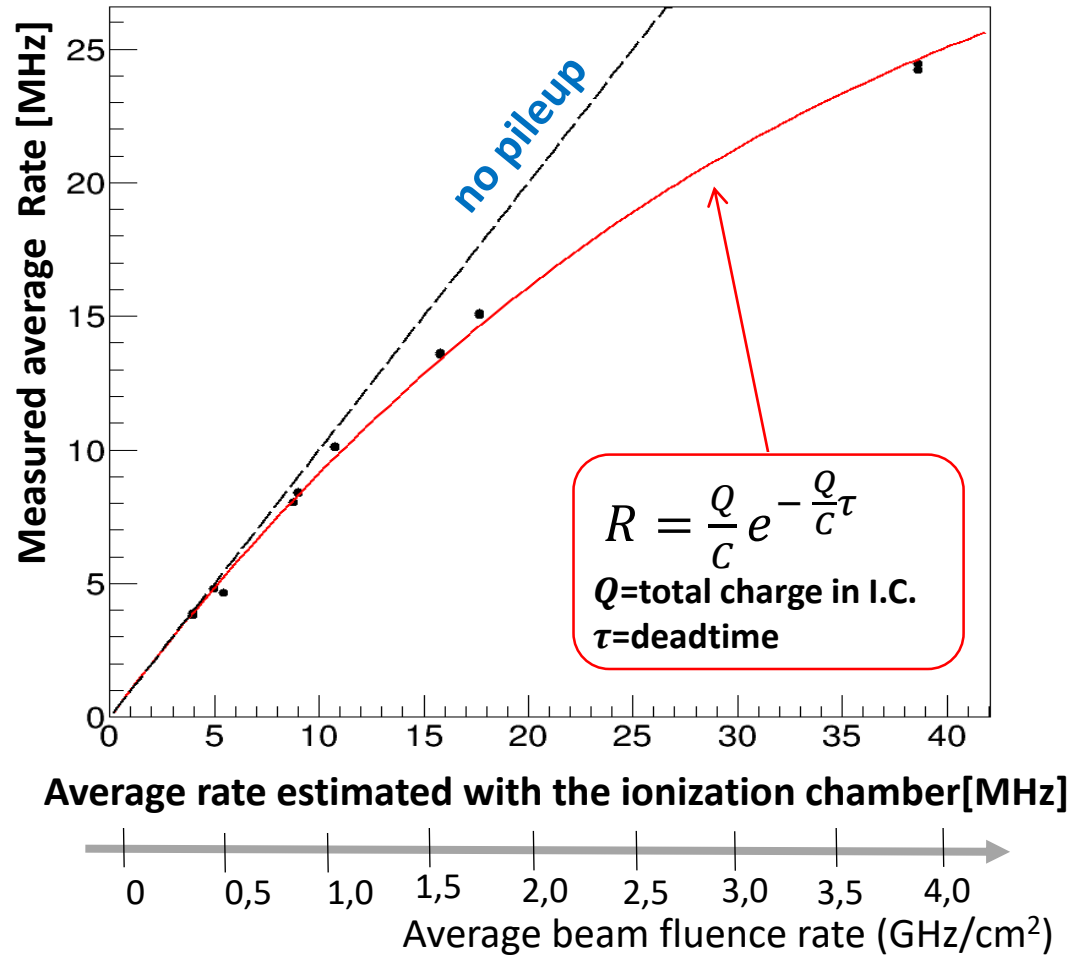


- Large inefficiency observed (up to 25% at largest clinical fluxes) → Correction required
- Data well described by paralyzable pileup model



Concern: pile-up inefficiency

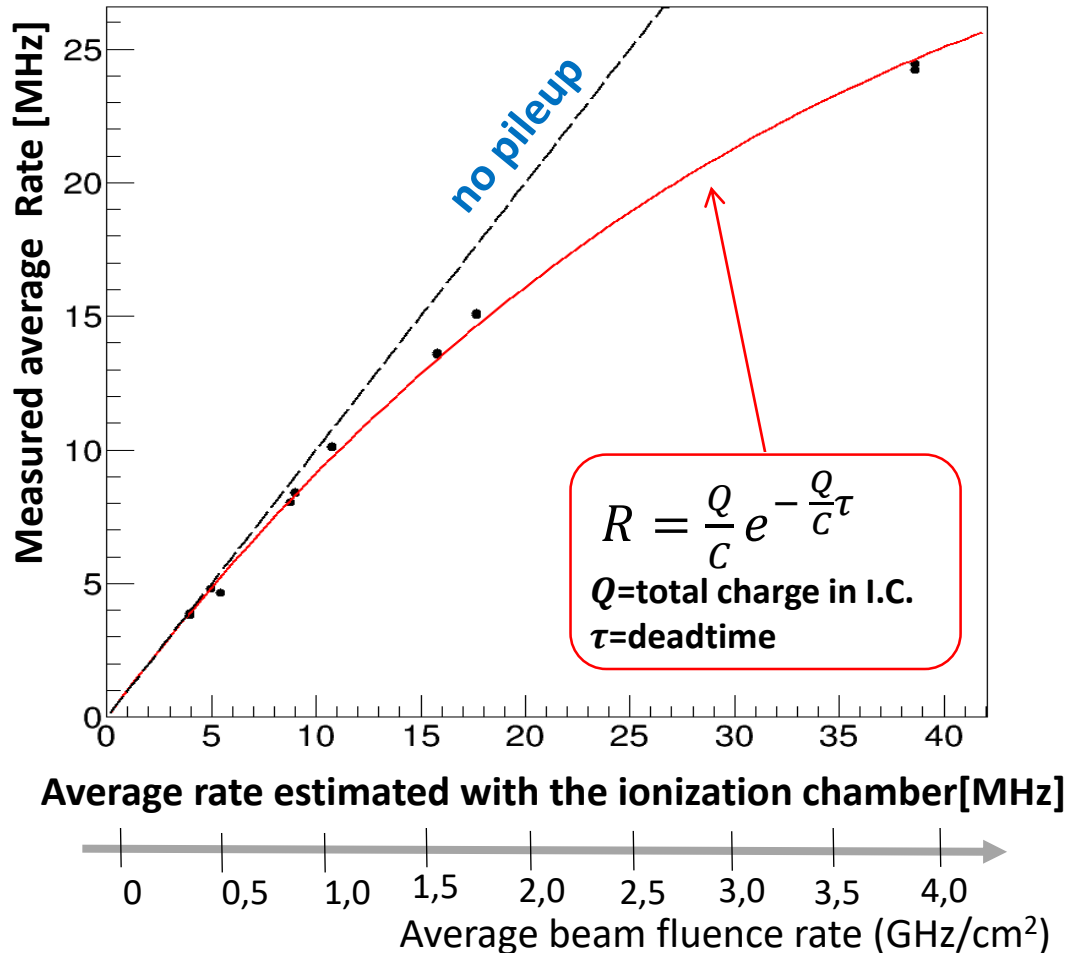
Measured vs. estimated rate, using a PTW pinpoint I.C. and a varied beam flux (20 – 50 – 100% of max)



- Large inefficiency observed (up to 25% at largest clinical fluxes) → Correction required
- Data well described by paralyzable pileup model → deadtime **much larger than expected**

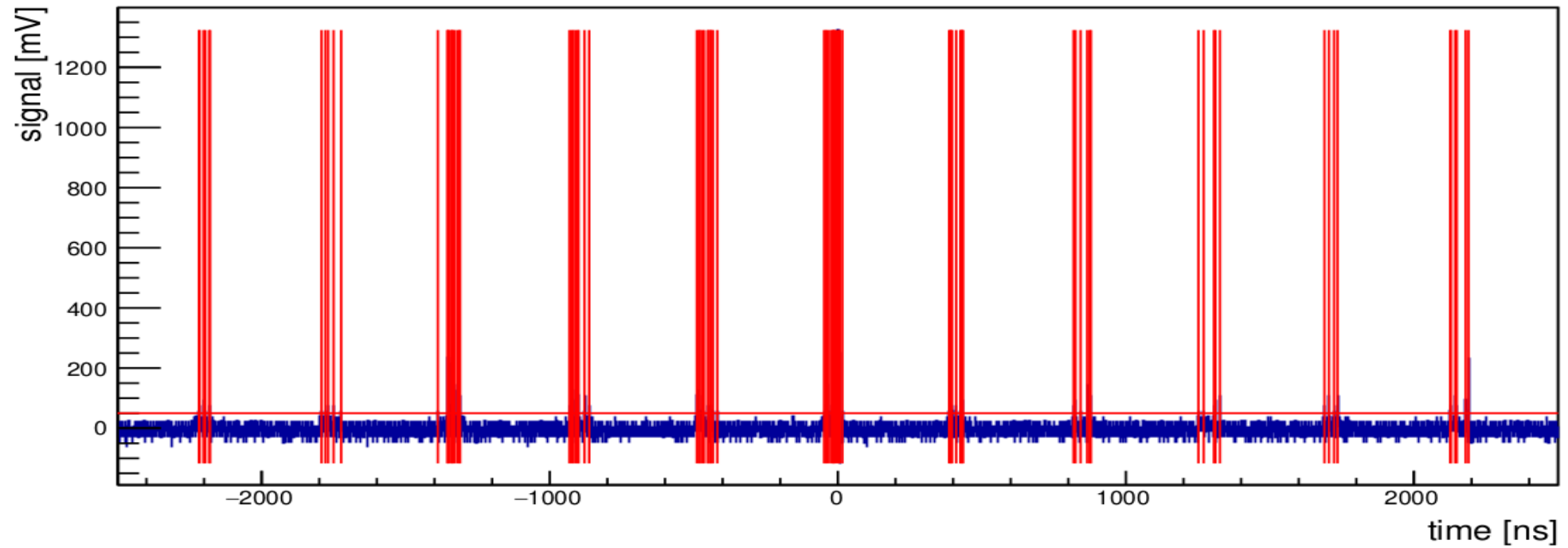
Concern: pile-up inefficiency

Measured vs. estimated rate, using a PTW pinpoint I.C. and a varied beam flux (20 – 50 – 100% of max)

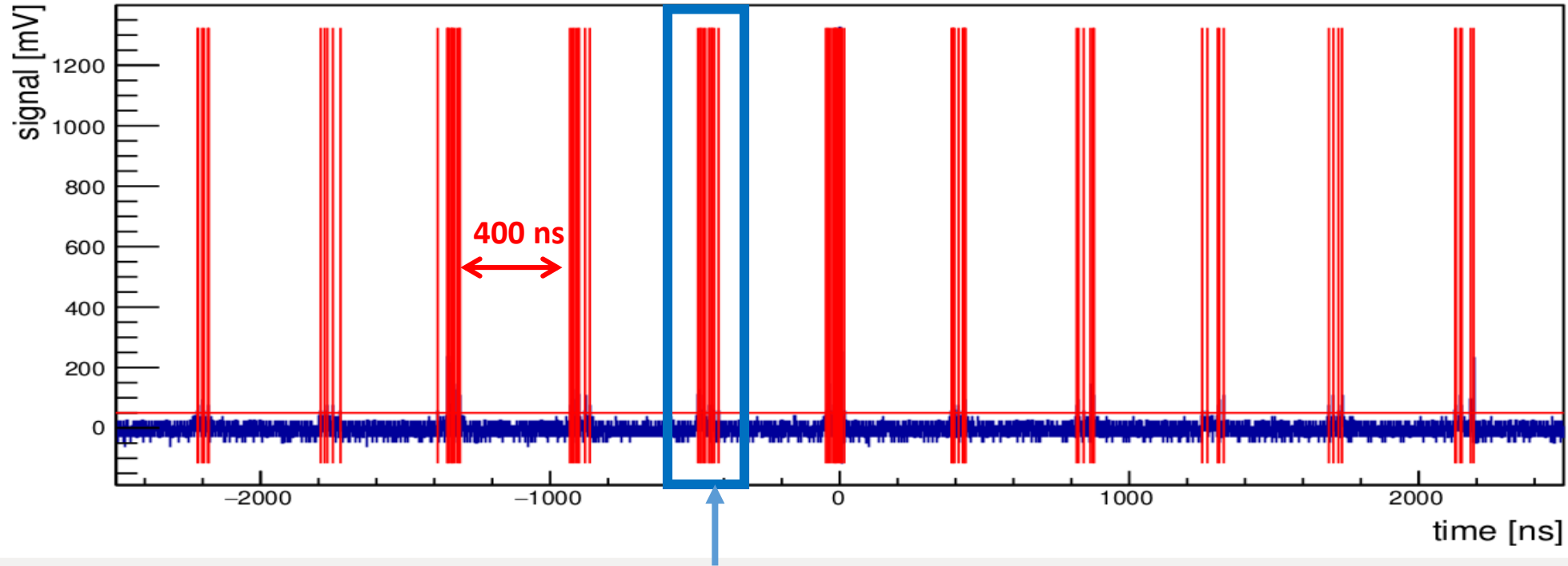


- Large inefficiency observed (up to 25% at largest clinical fluxes) → Correction required
- Data well described by paralyzable pileup model → deadtime **much larger than expected**
- Reason relies on the bunched structure of the CNAO beam (instantaneous flux ~ 10 X average)

Concern: pile-up inefficiency



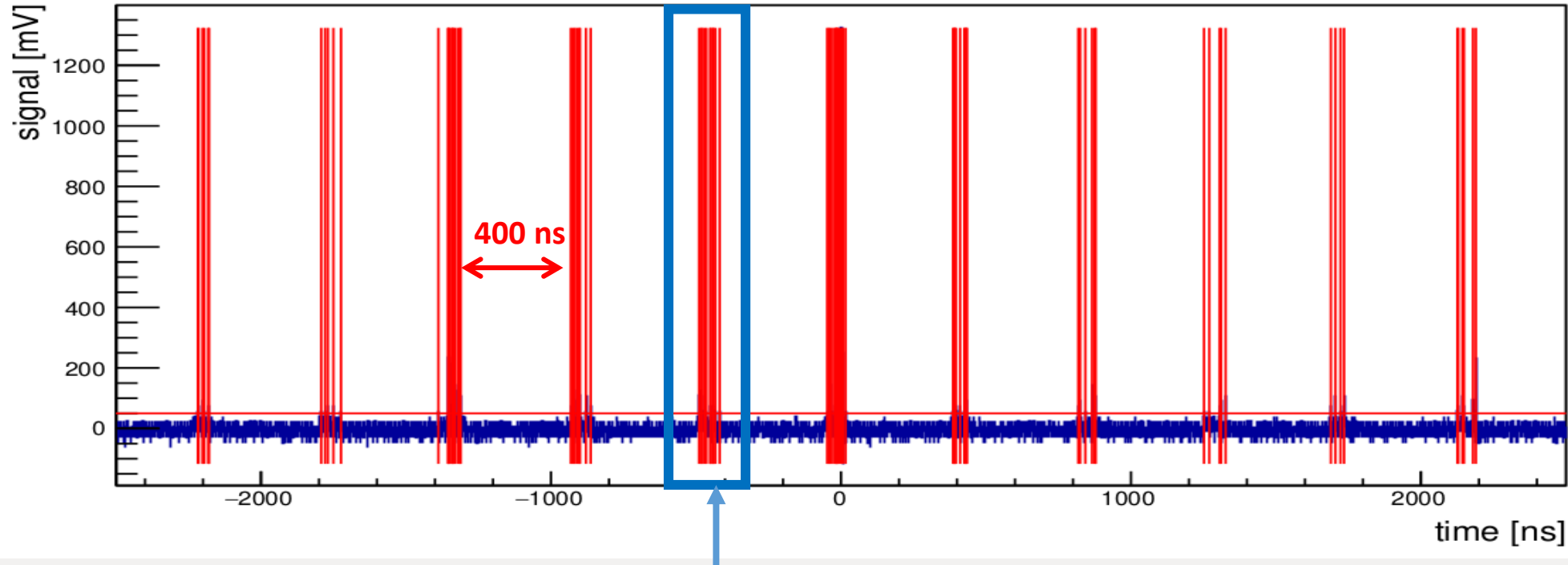
Concern: pile-up inefficiency



$\sim 10^{10}$ p/s cm² !!

➤ Measurement of CNAO proton beam structure.

Concern: pile-up inefficiency



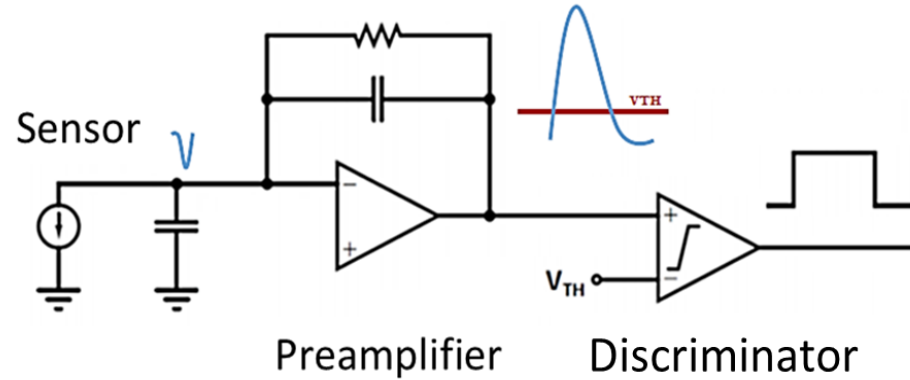
$\sim 10^{10}$ p/s cm² !!

- Measurement of CNAO proton beam structure.

Fast read-out electronics

Requirements

Input ch. range: **3 fC ÷ 140 fC**
Rate/channel: **up to 200 MHz**
Inefficiency **< 1 %**.

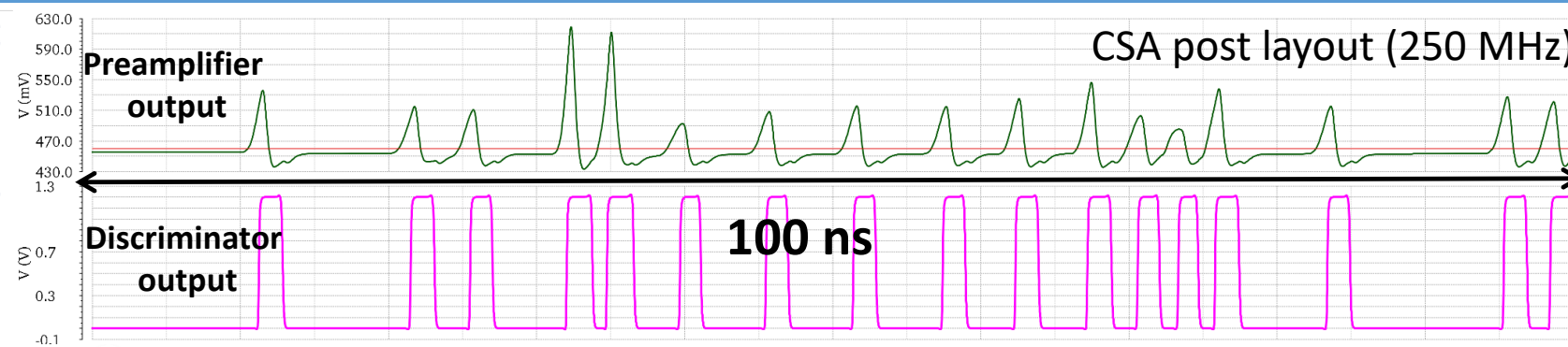


FPGA

- FE initialization
- Pulse counting
- Pileup correction

+ Additional functionalities
(threshold scan,)

2 alternative designs (CSA & TIA) of the amplifier developed and compared



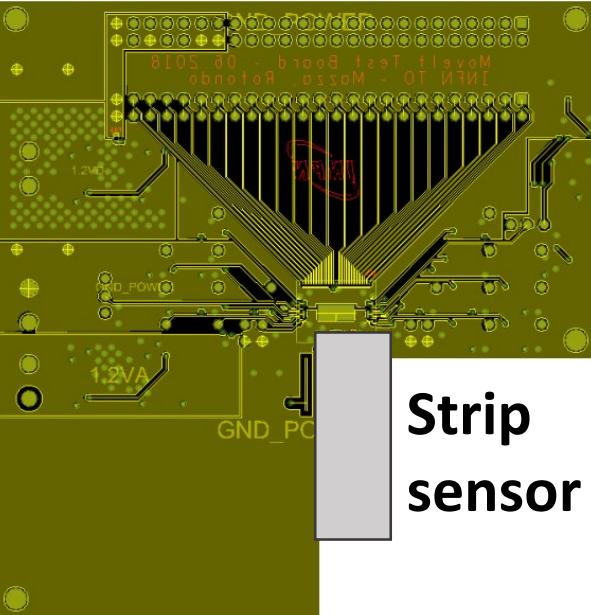
✓ Prototypes (24 ch) of the 2 architectures (UMC110 technology)

✓ Test Board

Counting - outlook

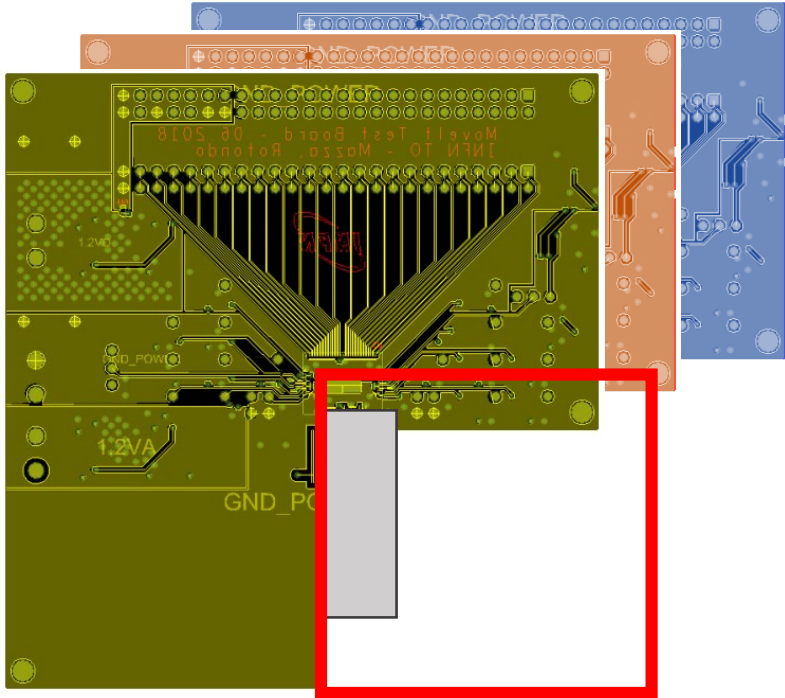


Test of complete chain...



Strip sensor

Test Board



3 x 3 cm²

FPGA

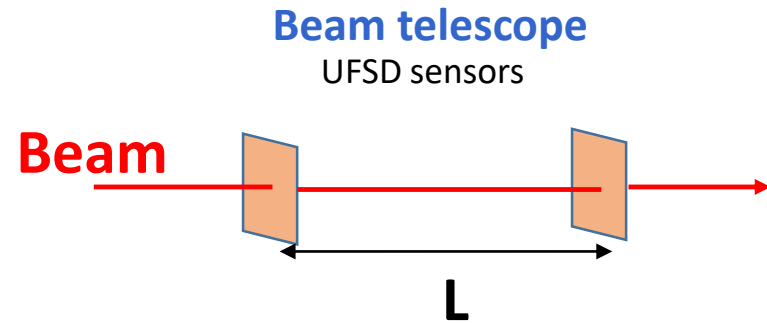


Energy Measurement



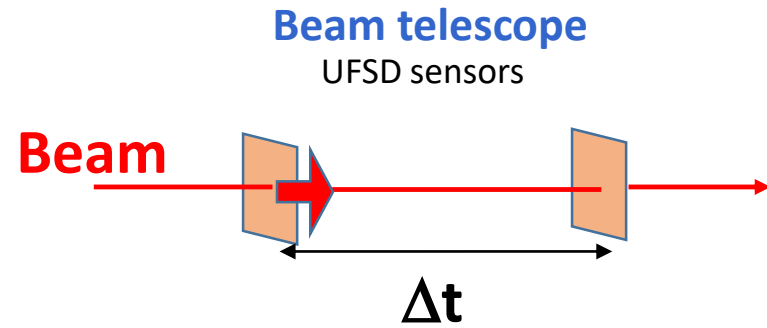
Energy measurement - coincidences

Beam energy measured from Time-of-Flight



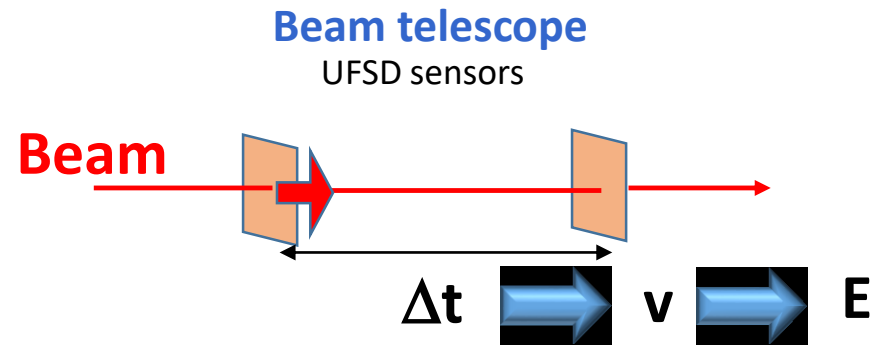
Energy measurement - coincidences

Beam energy measured from Time-of-Flight



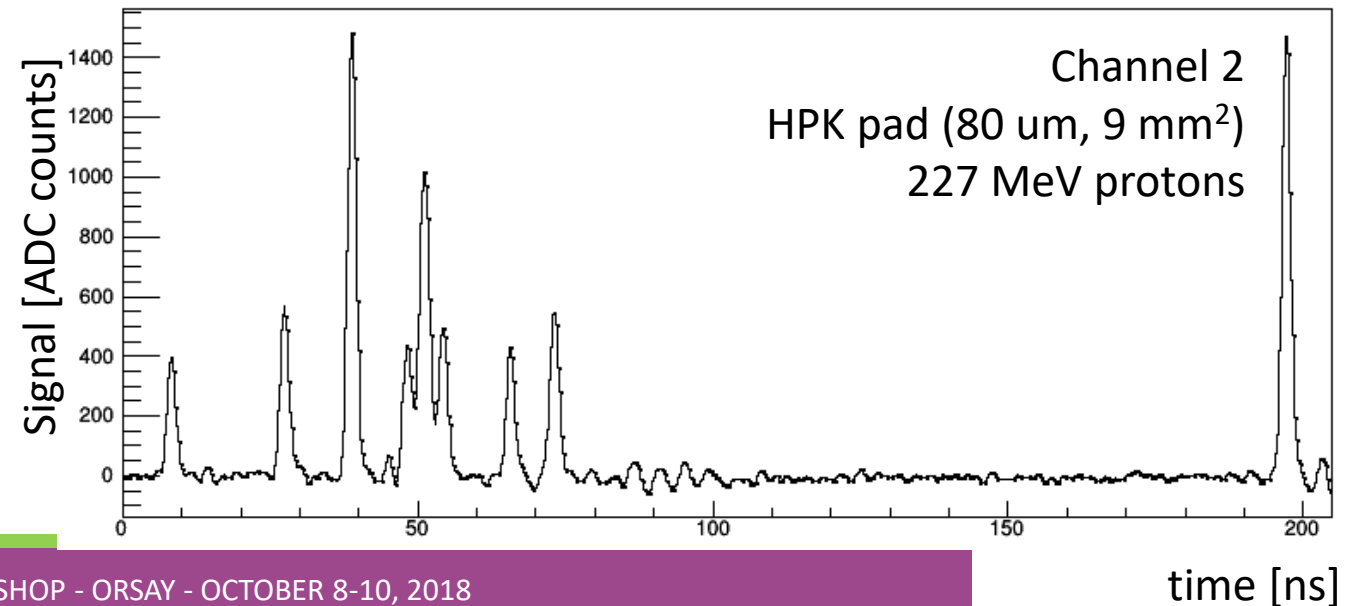
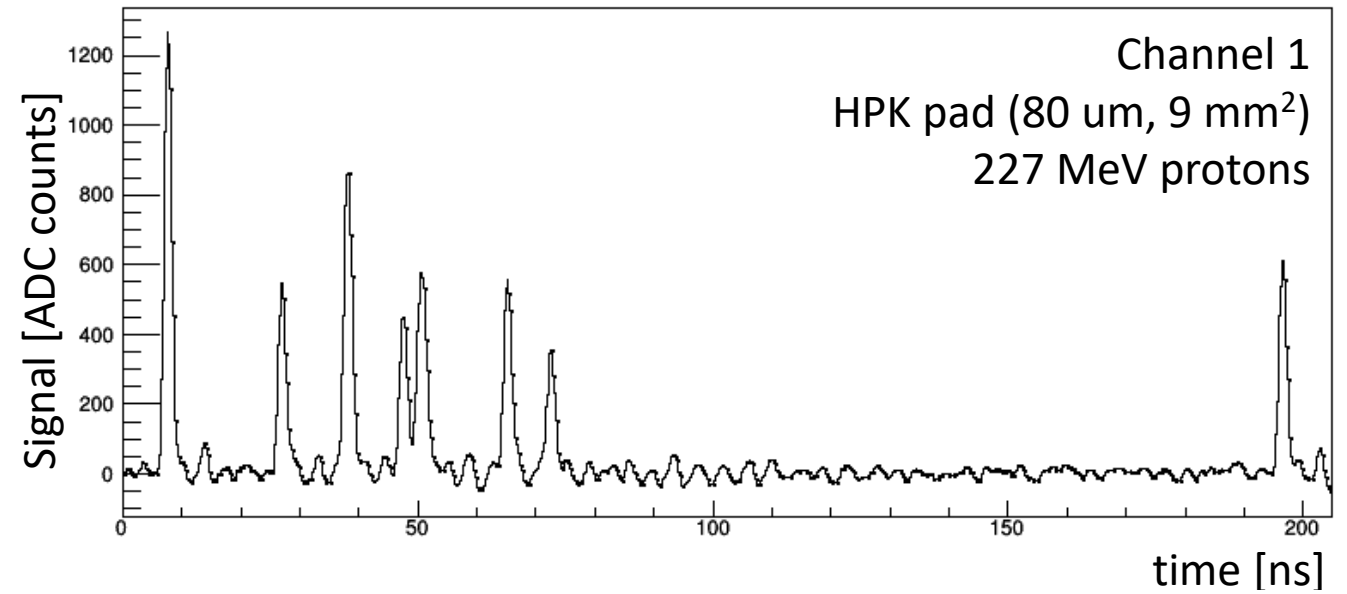
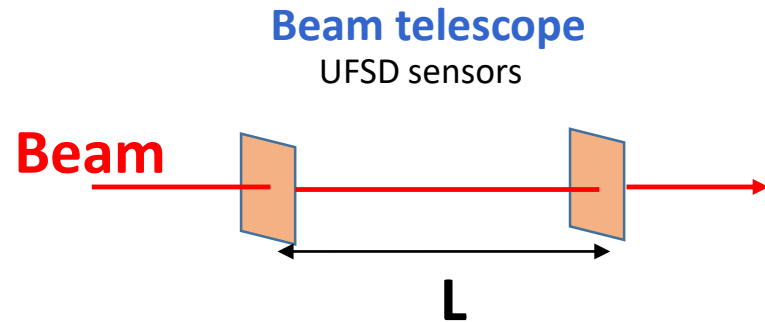
Energy measurement - coincidences

Beam energy measured from Time-of-Flight



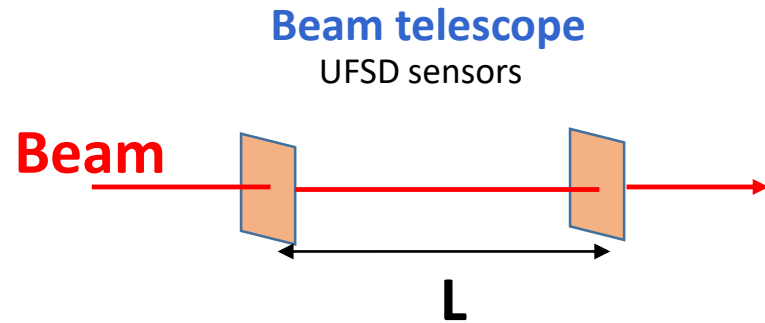
Energy measurement - coincidences

Beam energy measured from Time-of-Flight

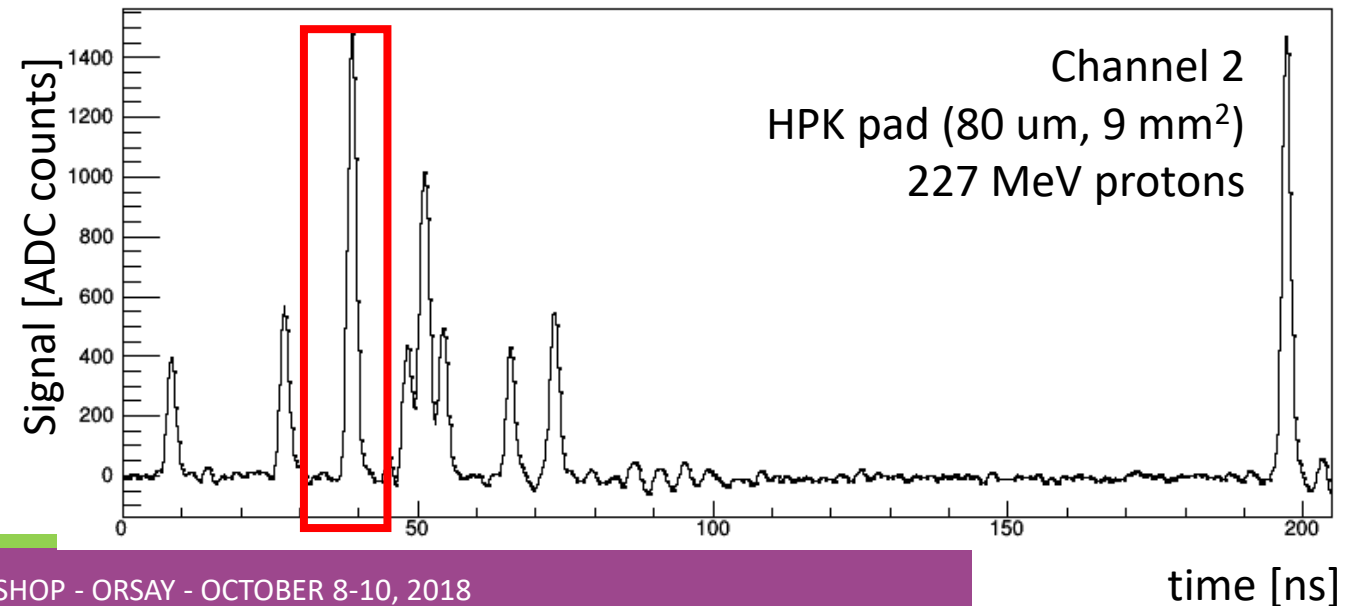
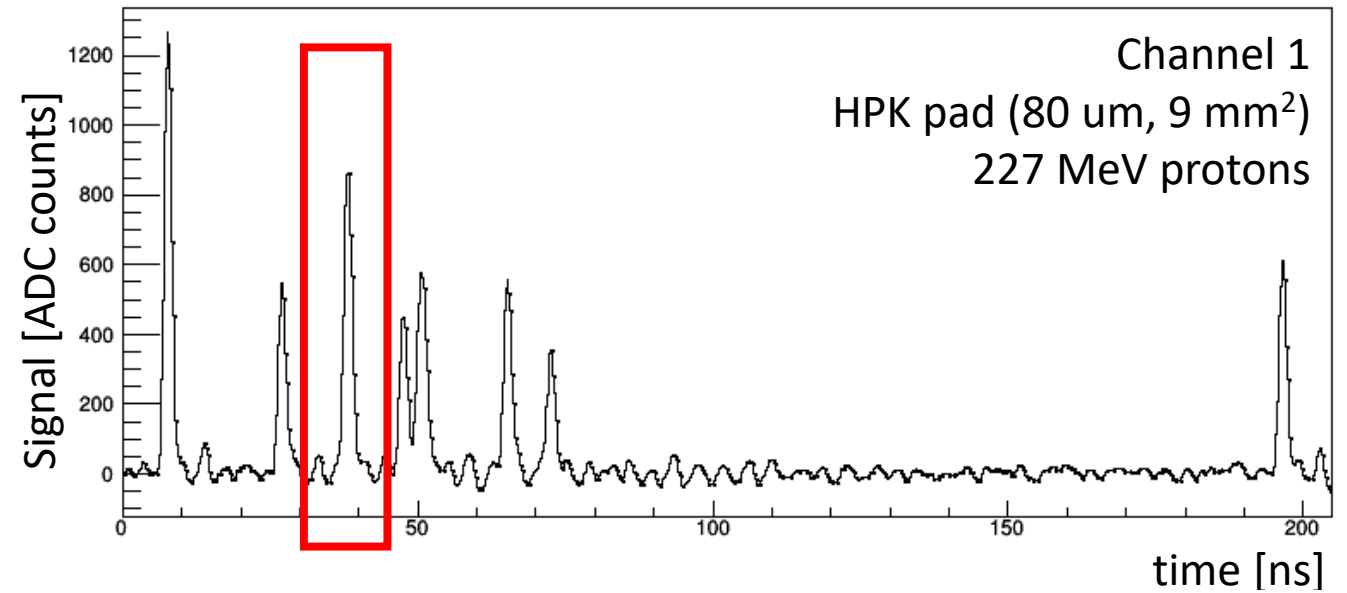


Energy measurement - coincidences

Beam energy measured from Time-of-Flight

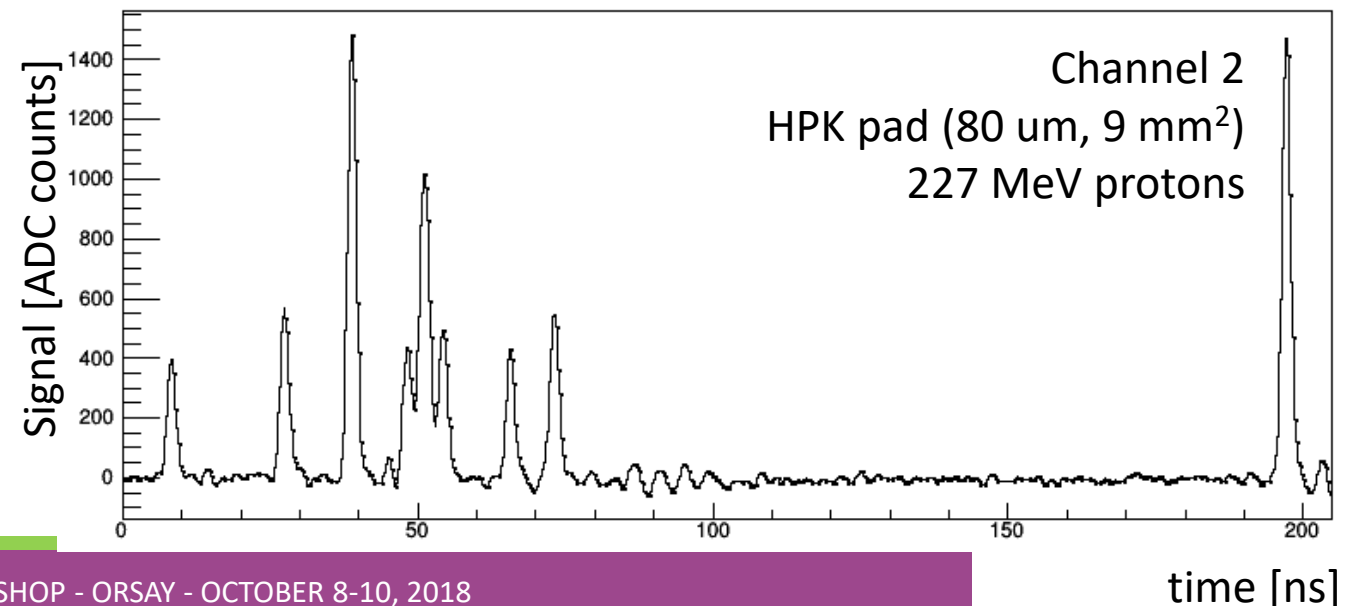
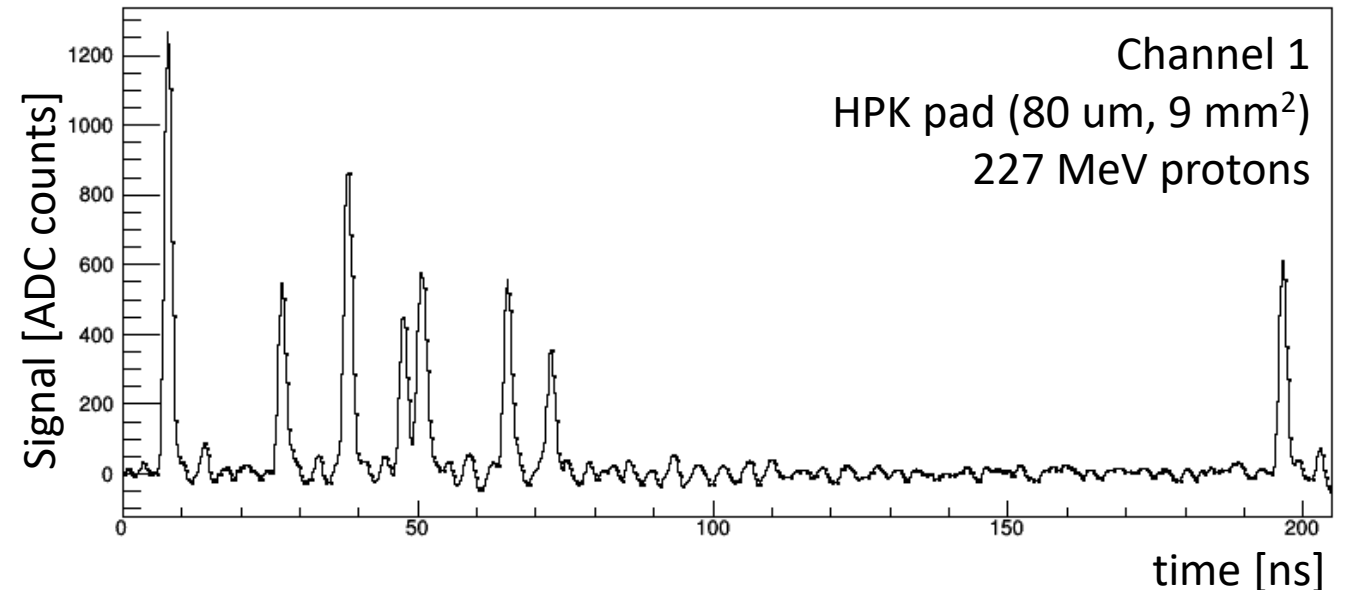
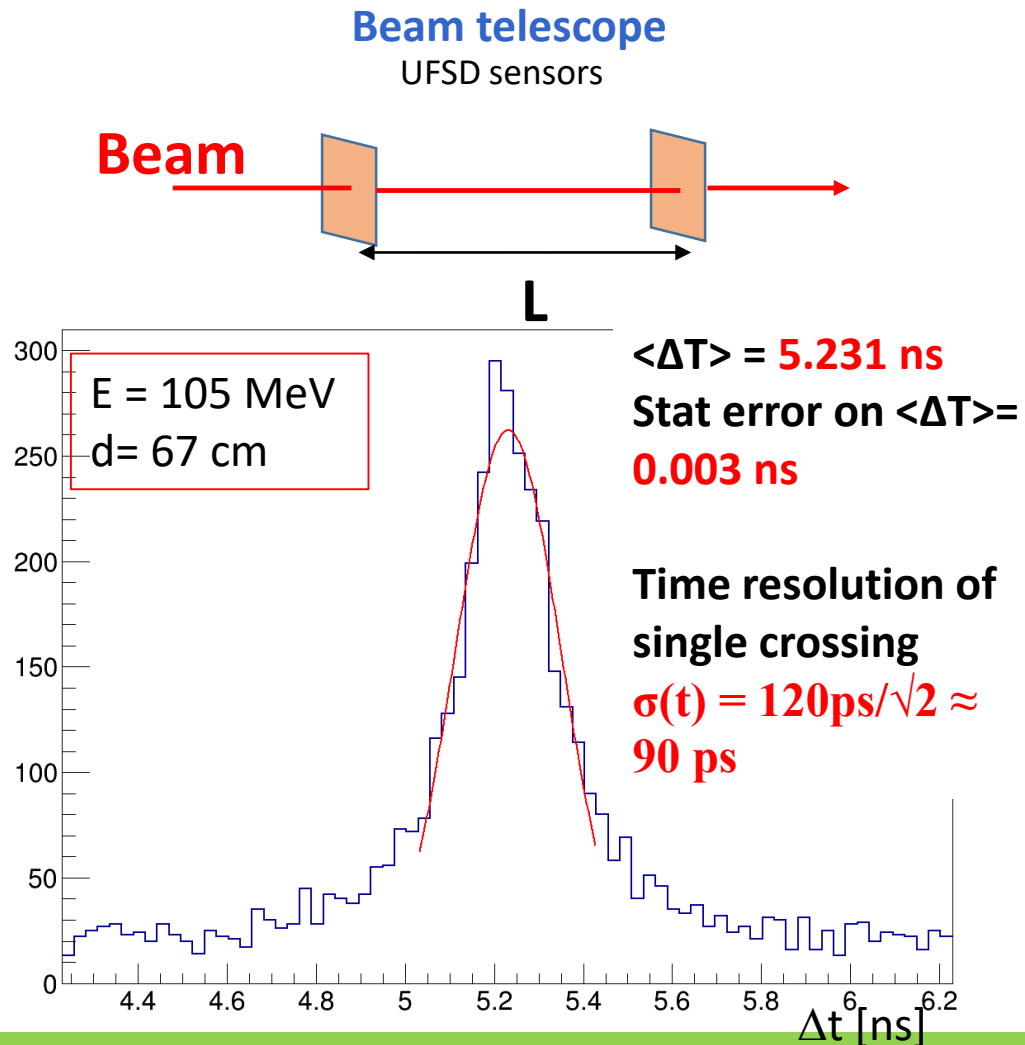


- Constant fraction discriminator algorithm applied on pulses signals

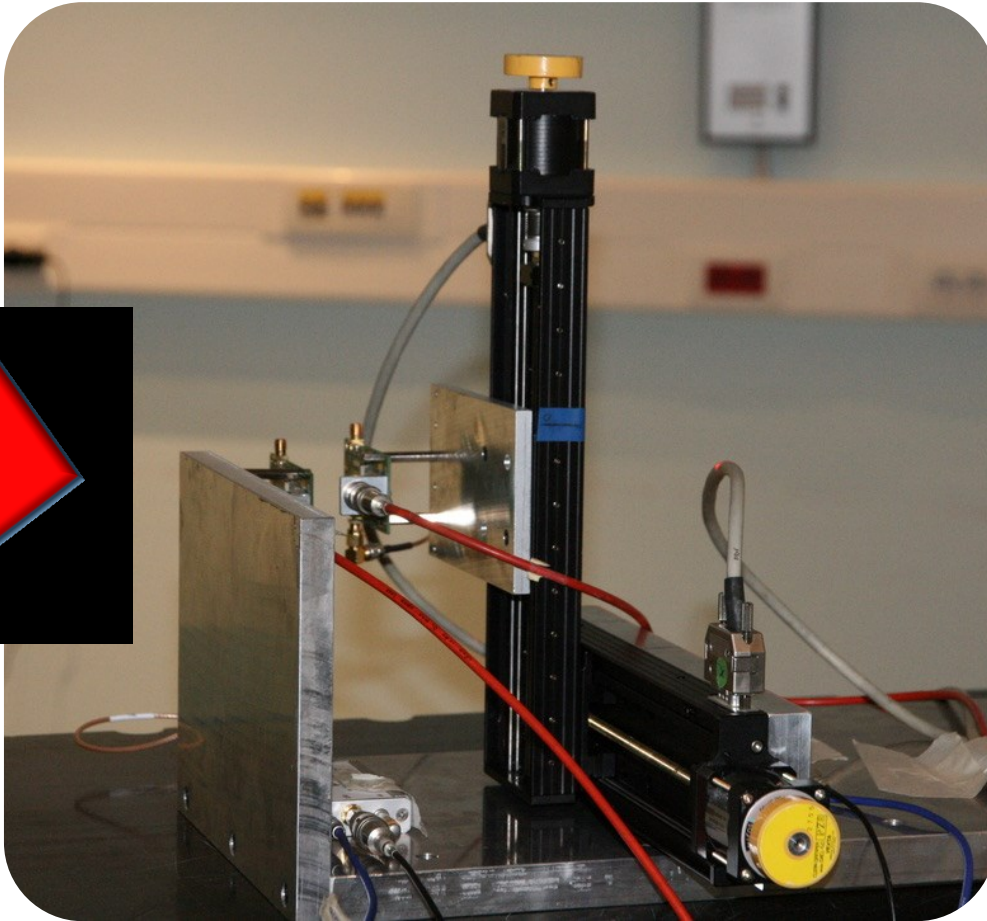


Energy measurement - coincidences

Beam energy measured from Time-of-Flight



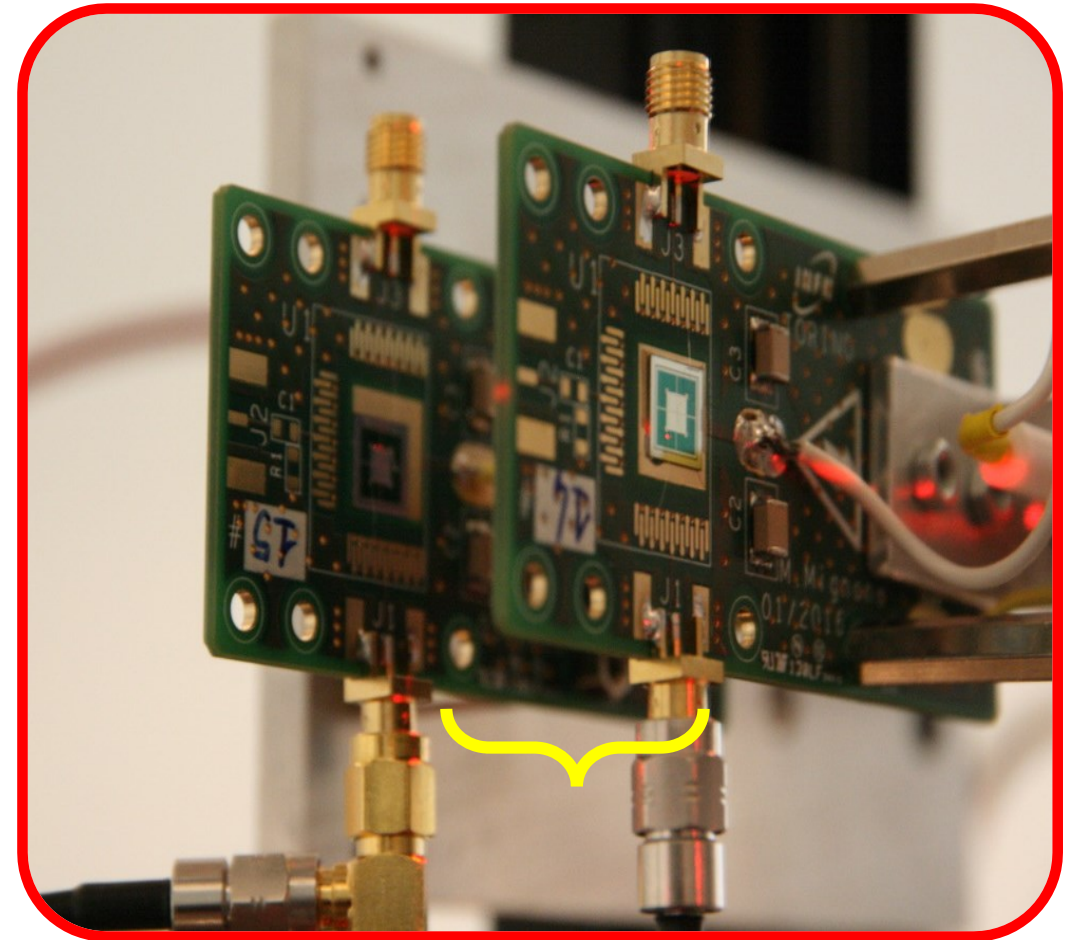
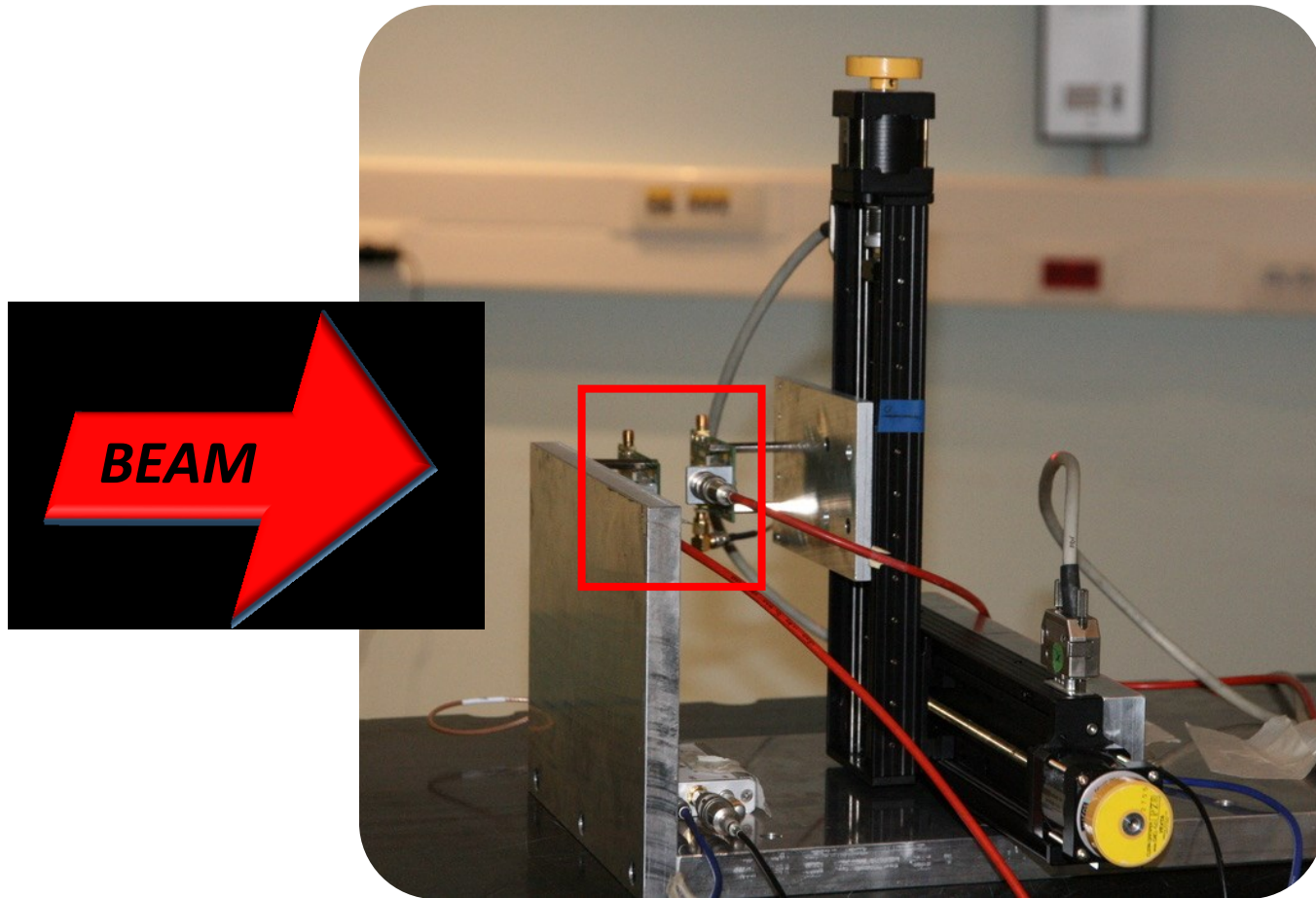
Energy measurement - test



4 distances= 7, 37, 67, 97 cm

5 energies= 62.73, 80.70, 106.24, 150.99, 228.56 MeV

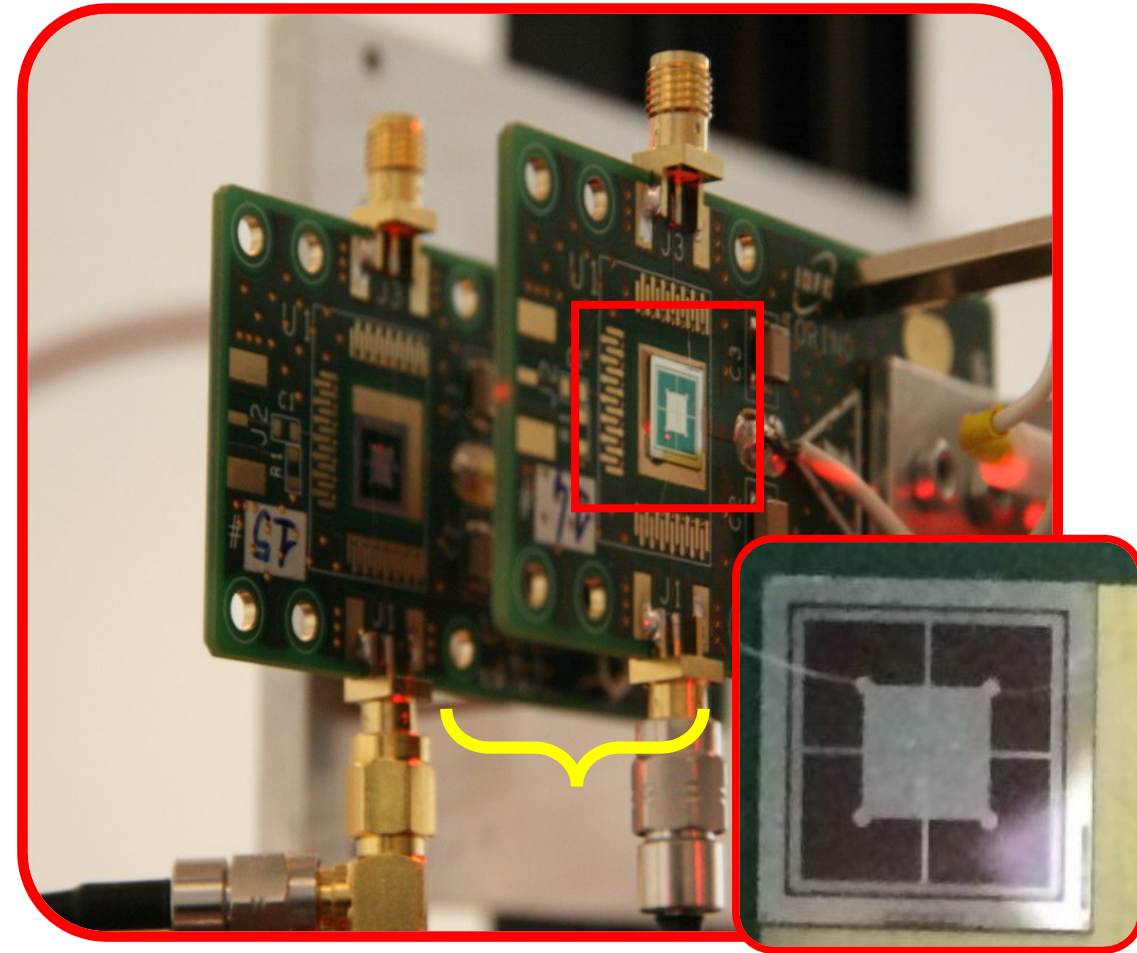
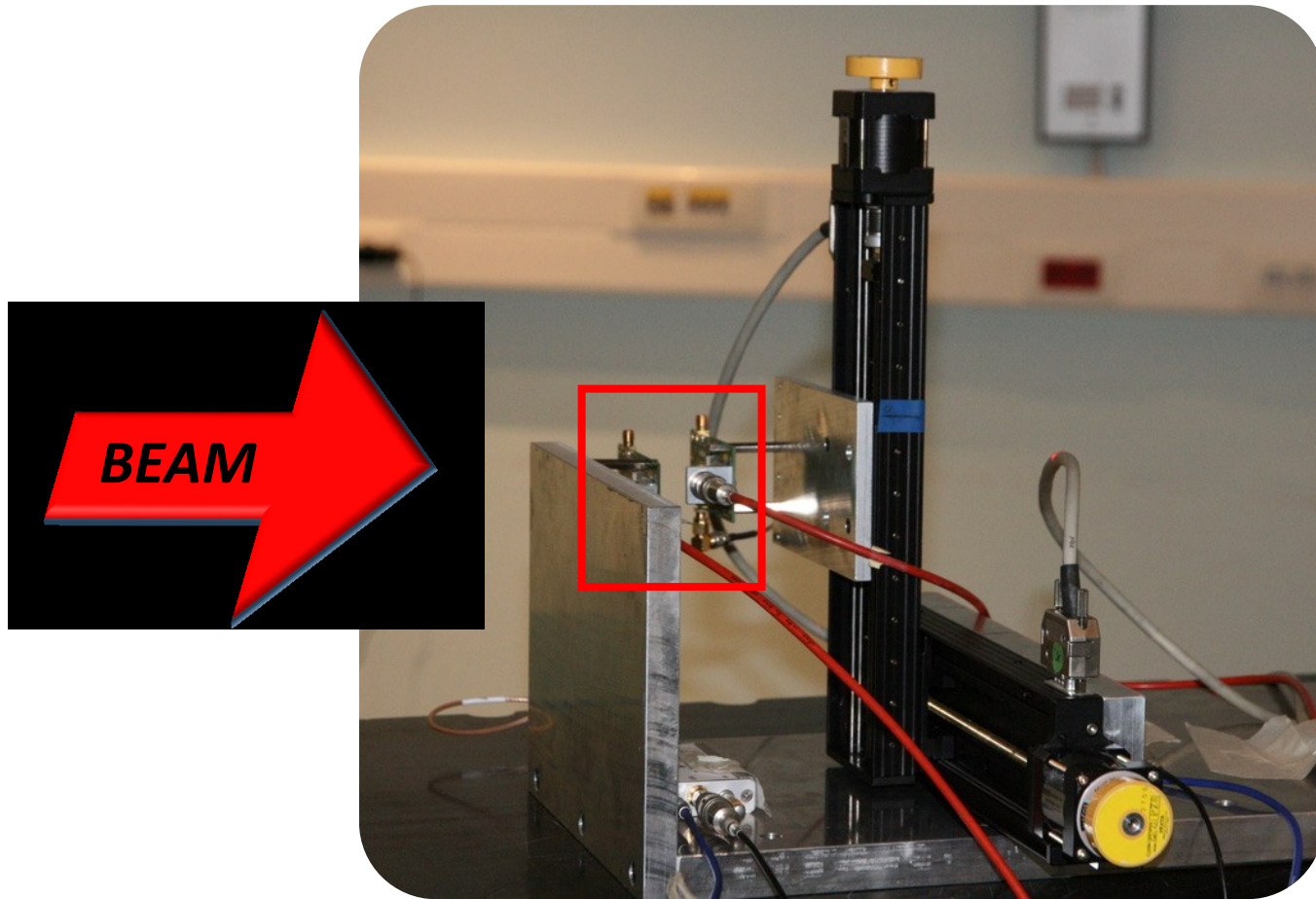
Energy measurement - test



4 distances= 7, 37, 67, 97 cm

5 energies= 62.73, 80.70, 106.24, 150.99, 228.56 MeV

Energy measurement - test

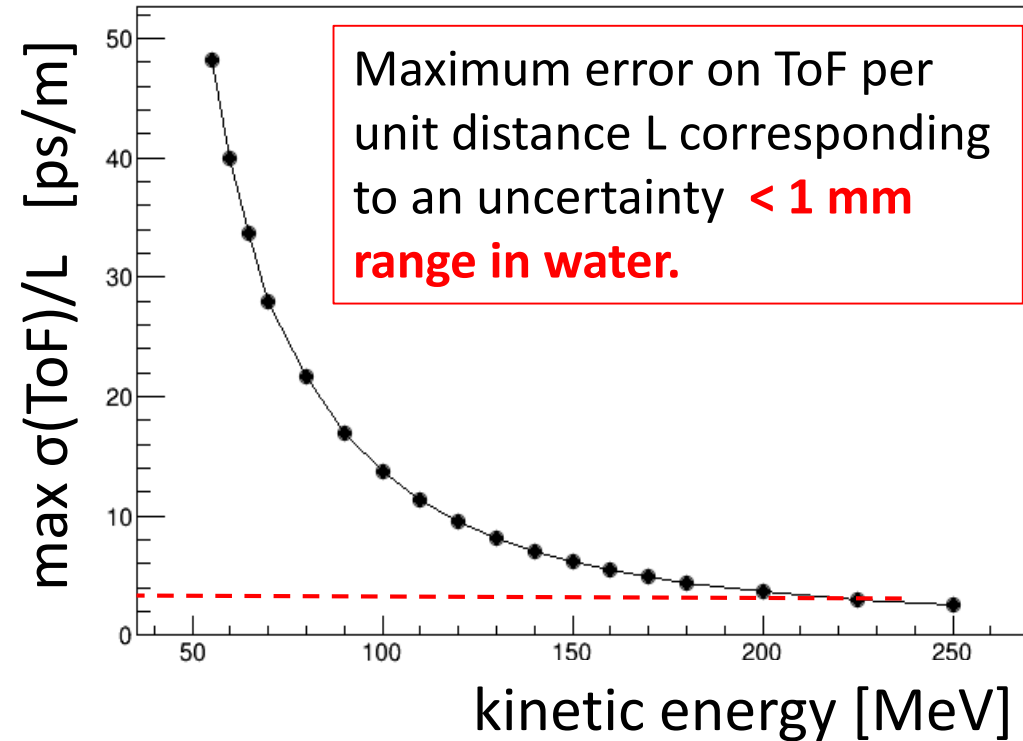


4 distances= 7, 37, 67, 97 cm

5 energies= 62.73, 80.70, 106.24, 150.99, 228.56 MeV

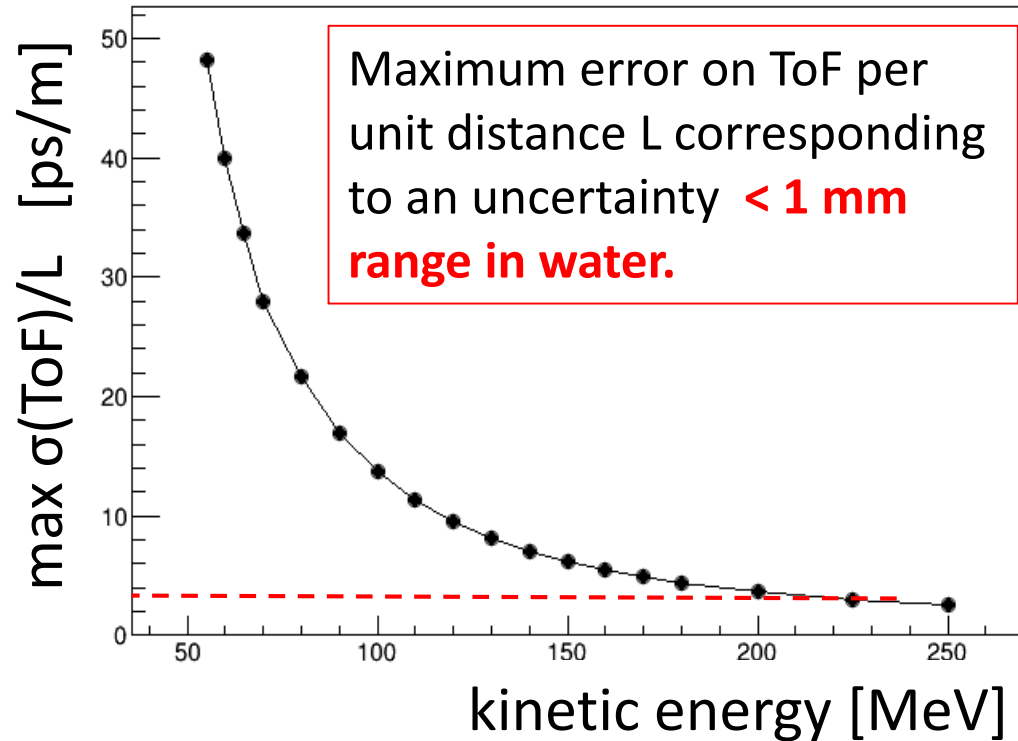
Hamamatsu 4* (3x3) mm² (80 μm)

Energy measurement – range requirements



For 1m distance the **max error on TOF = 4 ps**

Energy measurement – range requirements



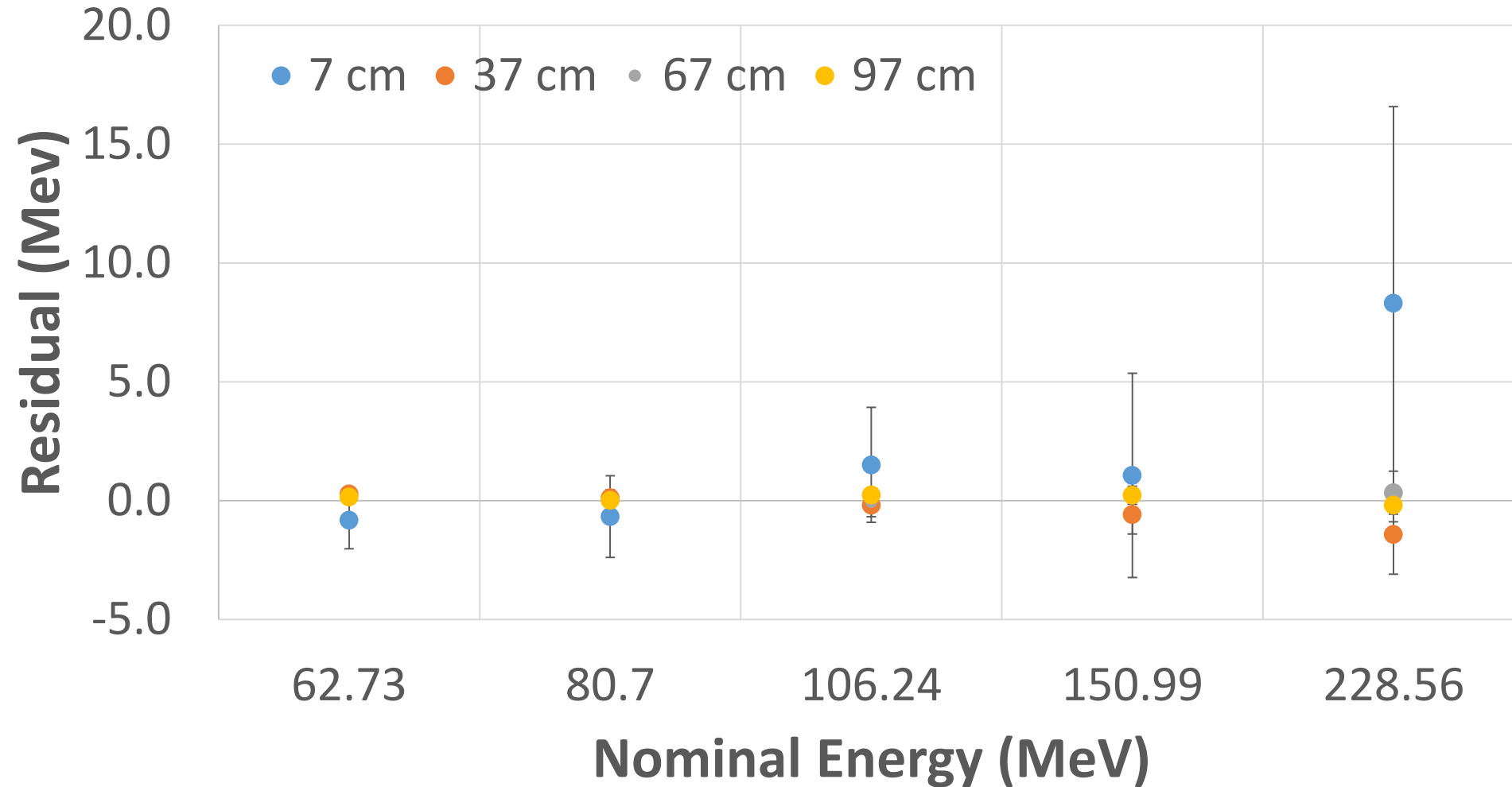
For 1m distance the **max error on TOF = 4 ps**

For 1m distance, 228 MeV, 10^{10} protons: **error on TOF = 4 ps**

Energy measurement – preliminary results

Residual vs Nominal Energy

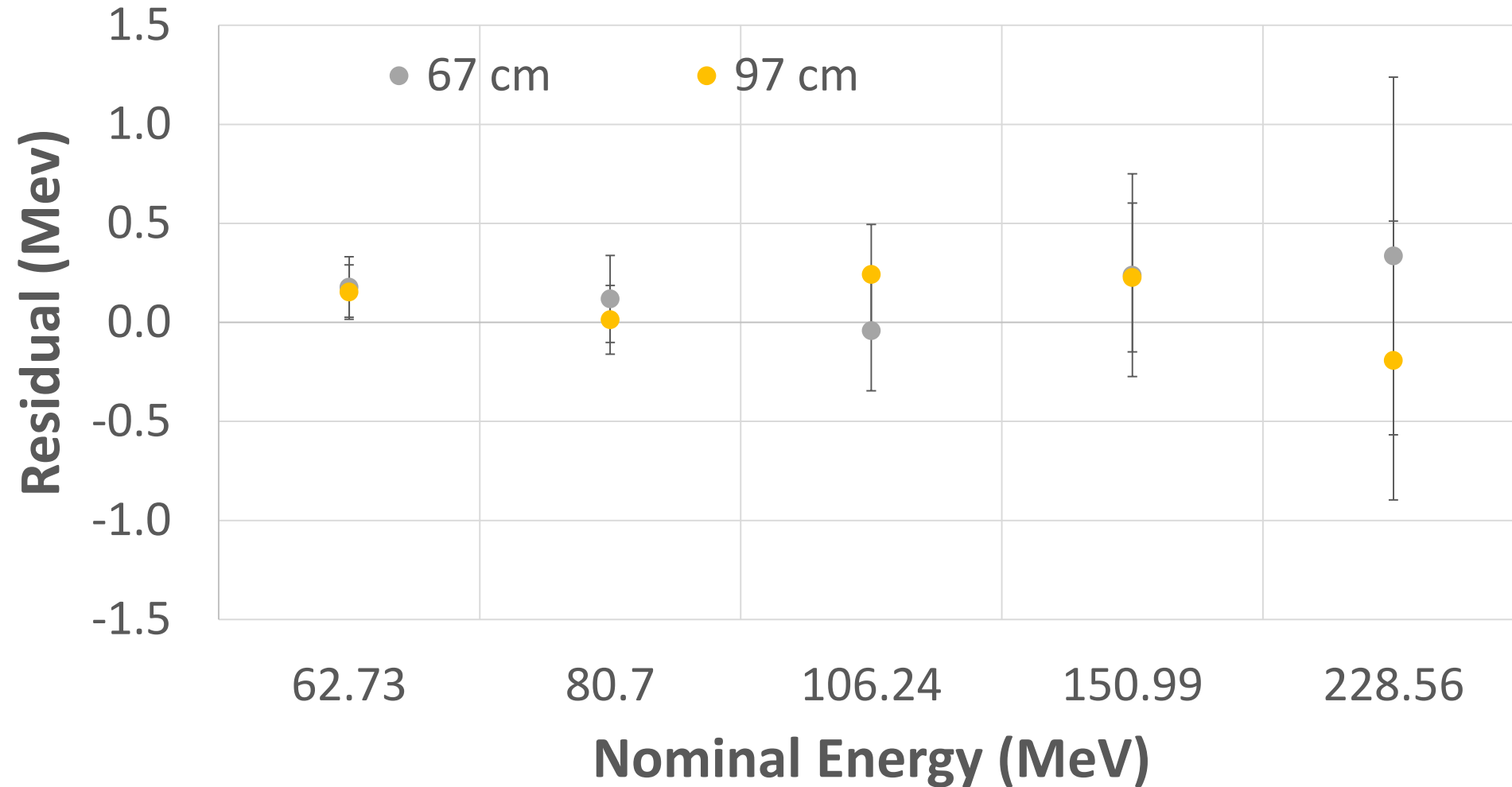
$$\text{Residual} = \text{Nominal E} - \text{Measured E}$$



Energy measurement – preliminary results

Residual vs Nominal Energy

$$\text{Residual} = \text{Nominal E} - \text{Measured E}$$

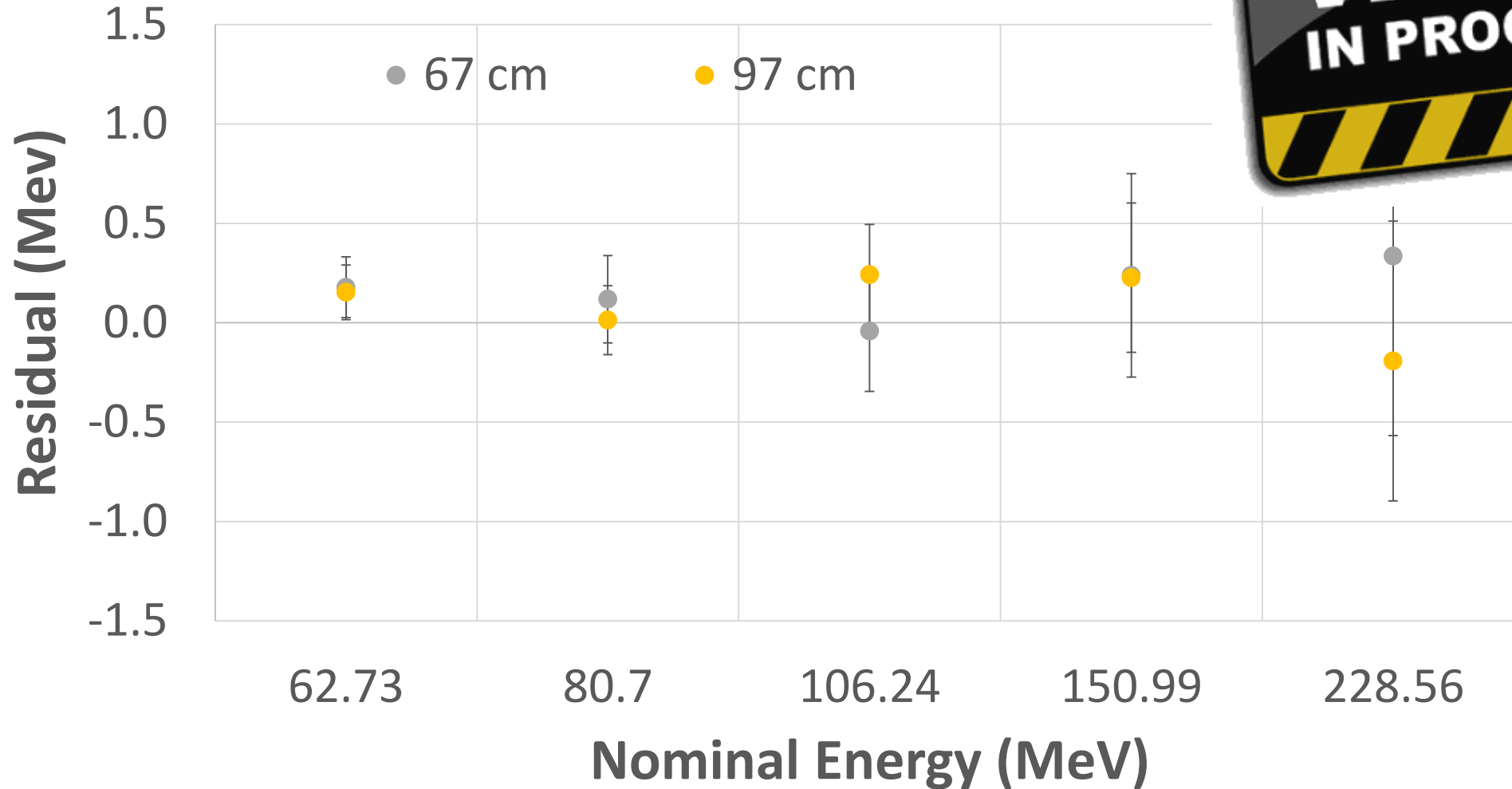


Energy measurement – preliminary results



Residual vs Nominal Energy

Residual =



Energy measurement – outlook

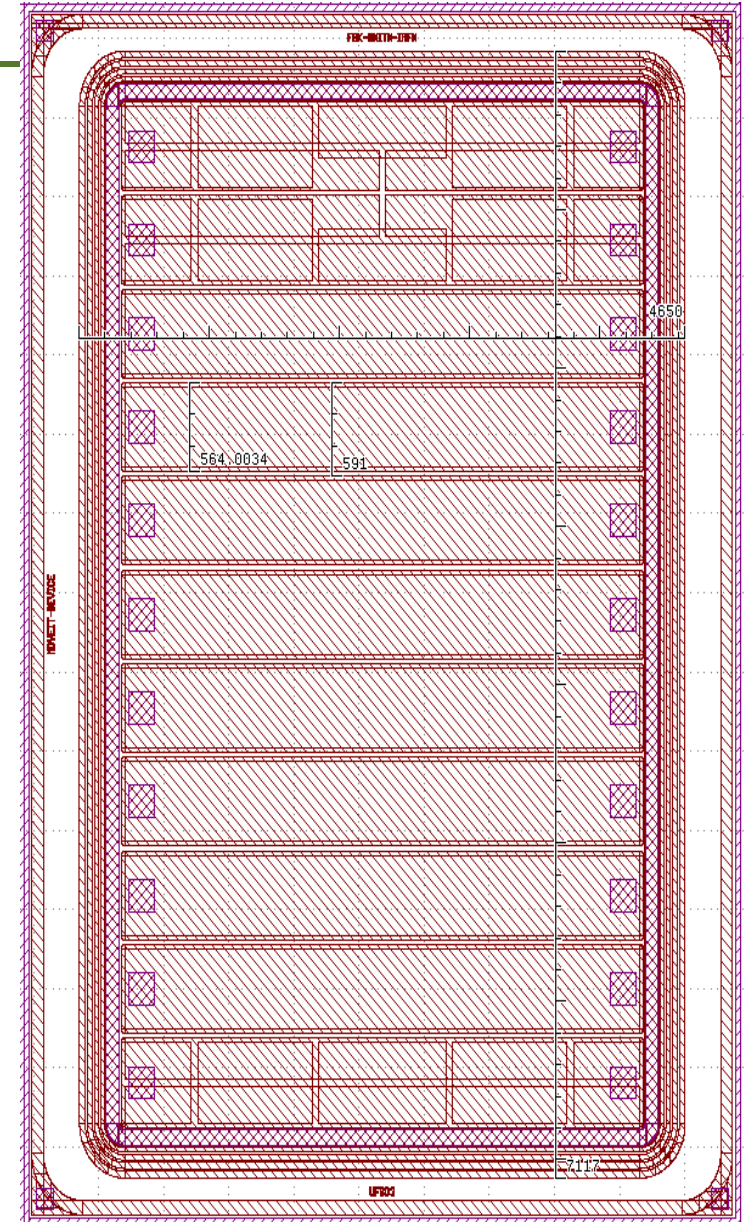
11 strips of 2.2 mm^2 ($3993 \text{ } \mu\text{m} \times 550 \text{ } \mu\text{m}$;
Pitch = $590 \text{ } \mu\text{m}$):

2 gain with optical windows;
8 gain (NO optical windows);
1 no gain with optical windows;

$50 \text{ } \mu\text{m}$ active thickness + $500 \text{ } \mu\text{m}$ handling wafer.



*Thinning of sensors;
Study and design of the read-out board;
Acquisition with DIGITIZER.*



Conclusions & Outlook

UFSD are a promising new technology for beam qualification and monitoring in Particle Therapy

Conclusions & Outlook

UFSD are a promising new technology for beam qualification and monitoring in Particle Therapy

2019

- ✓ Prototype for proton counting (3x3 cm² area, strip sensors).

➤ Fast collection time + Large S/N ratio

 **directly count number of beam ions**

Conclusions & Outlook

UFSD are a promising new technology for beam qualification and monitoring in Particle Therapy

2019

- ✓ Prototype for proton counting (3x3 cm² area, strip sensors).
- ✓ Prototype for real-time energy measurement (4x4 mm² area).

➤ Fast collection time + Large S/N ratio

 **directly count number of beam ions**

➤ Excellent time resolution

 **real-time measurement of the beam energy**

Conclusions & Outlook

UFSD are a promising new technology for beam qualification and monitoring in Particle Therapy

➤ Fast collection time + Large S/N ratio

 **directly count number of beam ions**

➤ Excellent time resolution

 **real-time measurement of the beam energy**

2019

- ✓ Prototype for proton counting (3x3 cm² area, strip sensors).
- ✓ Prototype for real-time energy measurement (4x4 mm² area).
- ✓ Dedicated Fast readout electronics (TERA10).

Conclusions & Outlook

UFSD are a promising new technology for beam qualification and monitoring in Particle Therapy

- Fast collection time + Large S/N ratio

 **directly count number of beam ions**

- Excellent time resolution

 **real-time measurement of the beam energy**

2019

- ✓ Prototype for proton counting (3x3 cm² area, strip sensors).
- ✓ Prototype for real-time energy measurement (4x4 mm² area).
- ✓ Dedicated Fast readout electronics (TERA10).



Radiobiological experiments

Conclusions & Outlook

UFSD are a promising new technology for beam qualification and monitoring in Particle Therapy

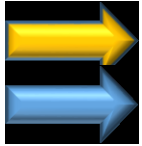
- Fast collection time + Large S/N ratio



directly count number of beam ions

OPEN ISSUE: pile-up inefficiency, radiation hardness

- Excellent time resolution



real-time measurement of the beam energy

OPEN ISSUE: systematic errors, radiation hardness

2019

- ✓ Prototype for proton counting (3x3 cm² area, strip sensors).
- ✓ Prototype for real-time energy measurement (4x4 mm² area).
- ✓ Dedicated Fast readout electronics (TERA10).



Radiobiological experiments

Conclusions & Outlook

UFSD are a promising new technology for beam qualification and monitoring in Particle Therapy

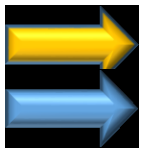
- Fast collection time + Large S/N ratio



directly count number of beam ions

OPEN ISSUE: pile-up inefficiency, radiation hardness

- Excellent time resolution



real-time measurement of the beam energy

OPEN ISSUE: systematic errors, radiation hardness

2019

- ✓ Prototype for proton counting (3x3 cm² area, strip sensors).
- ✓ Prototype for real-time energy measurement (4x4 mm² area).
- ✓ Dedicated Fast readout electronics (TERA10).



Radiobiological experiments



Clinics!



Acknowledgements

This work was supported by the INFN Gruppo V (MoVe-IT project) and by the European Union's Horizon 2020 Research and Innovation funding program (Grant Agreement no. 669529 - ERC UFSD669529).

We acknowledge the proactive collaboration of the Fondazione Bruno Kessler to this project.

We also thank the CNAO Foundation (Pavia) for the beam time accorded.



Thank you!

anna.vignati@to.infn.it

Spares

Energy measurement – Global Fit

$$\chi^2(\text{offset}, d_j) = \sum_{i,j} \left\{ \frac{(ToF_{ij} - \text{offset}) - ToF(E_i, d_j)}{\sigma_{ToF_{ij}}} \right\}^2$$

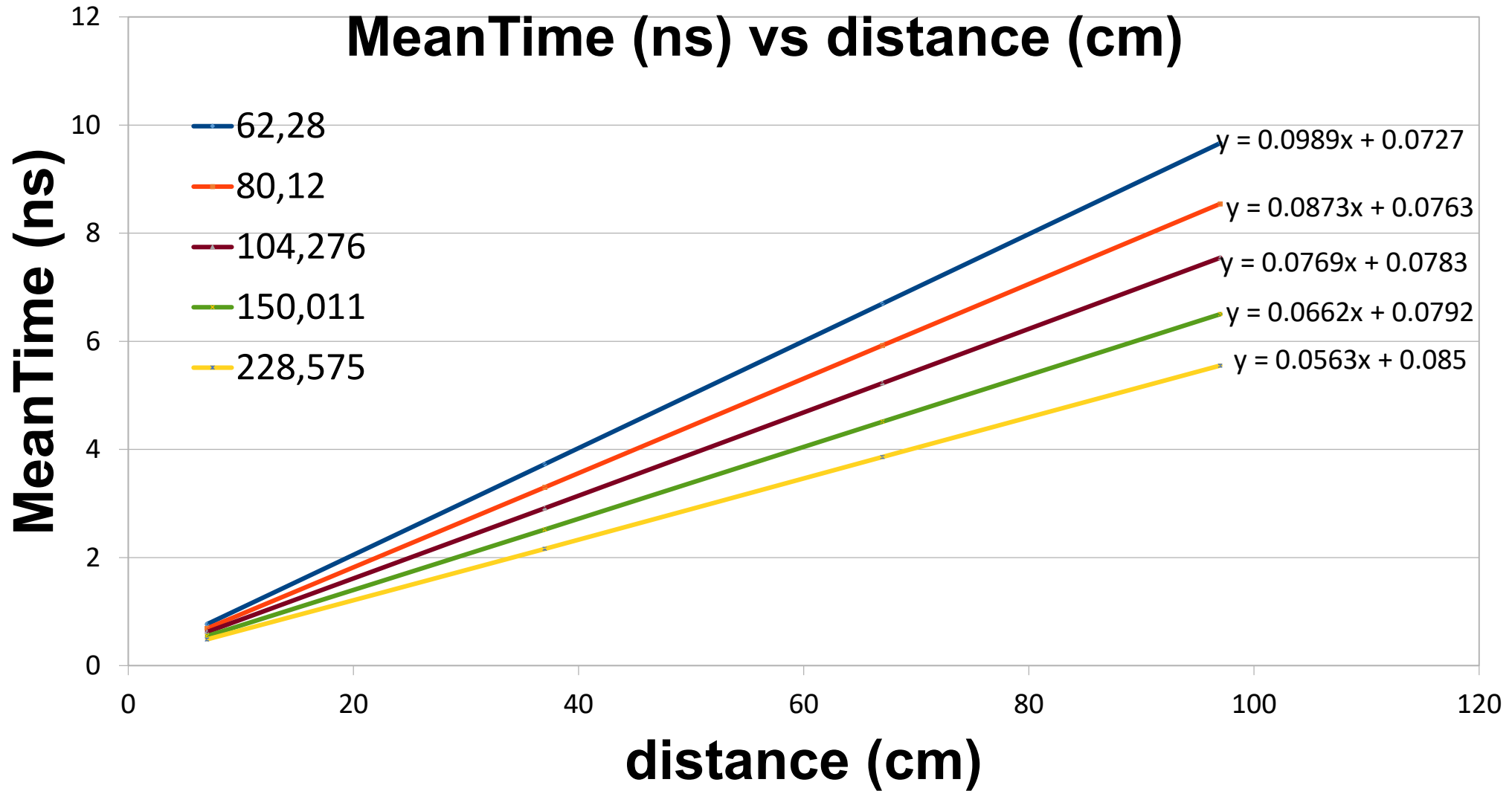
$$ToF(E, d) = \frac{Ed}{c\sqrt{E^2 - m^2c^4}}$$

Where

$i = 1 \rightarrow 5$ (E_i = energies of the beams)

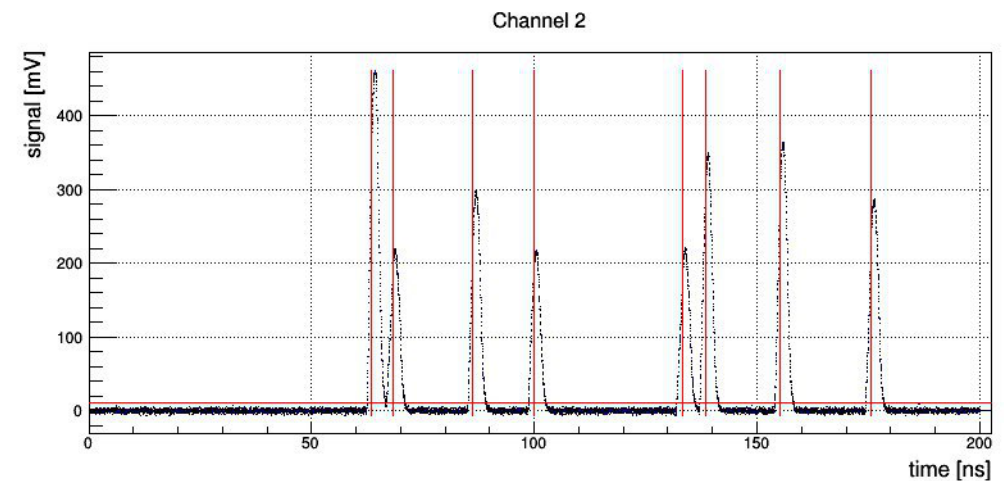
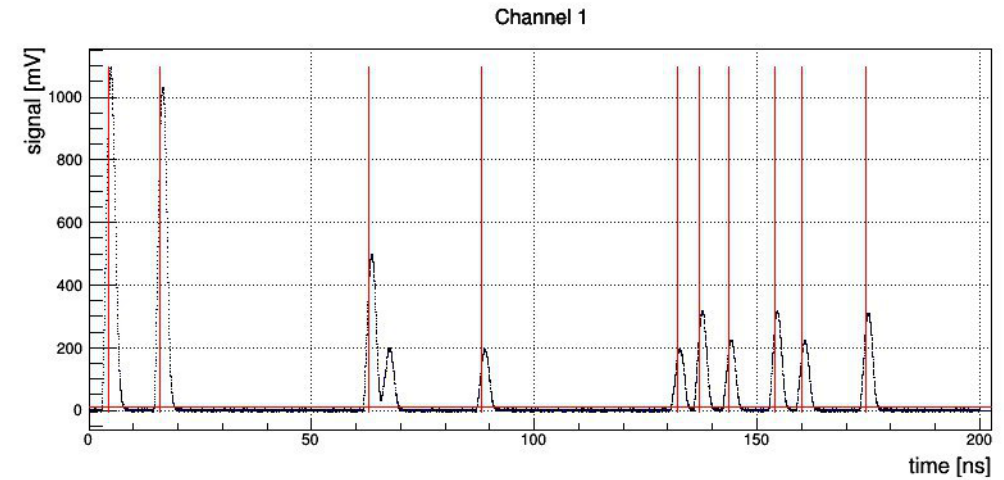
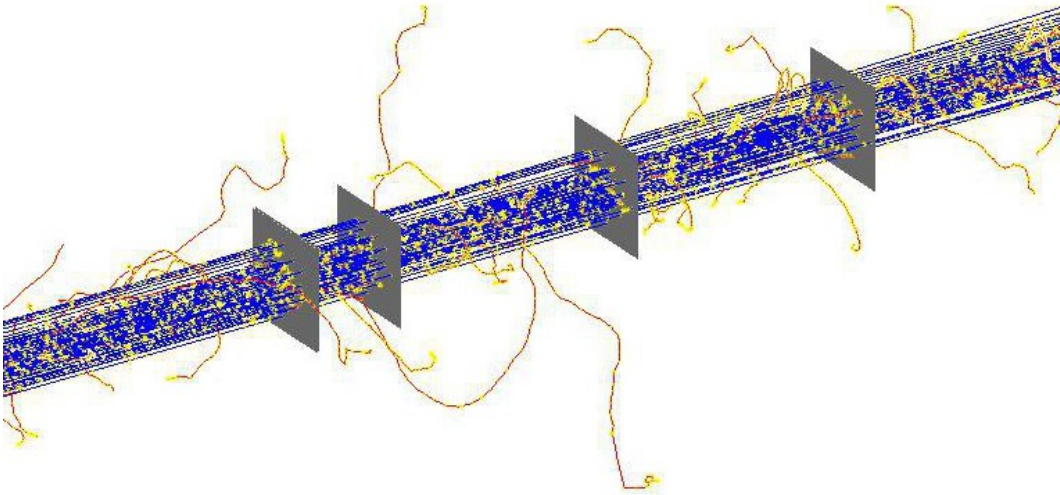
$j = 1, 2, 3, 4$ (d_j = distances between the two detectors).

Preliminary results (80 μm) – Δt vs distance



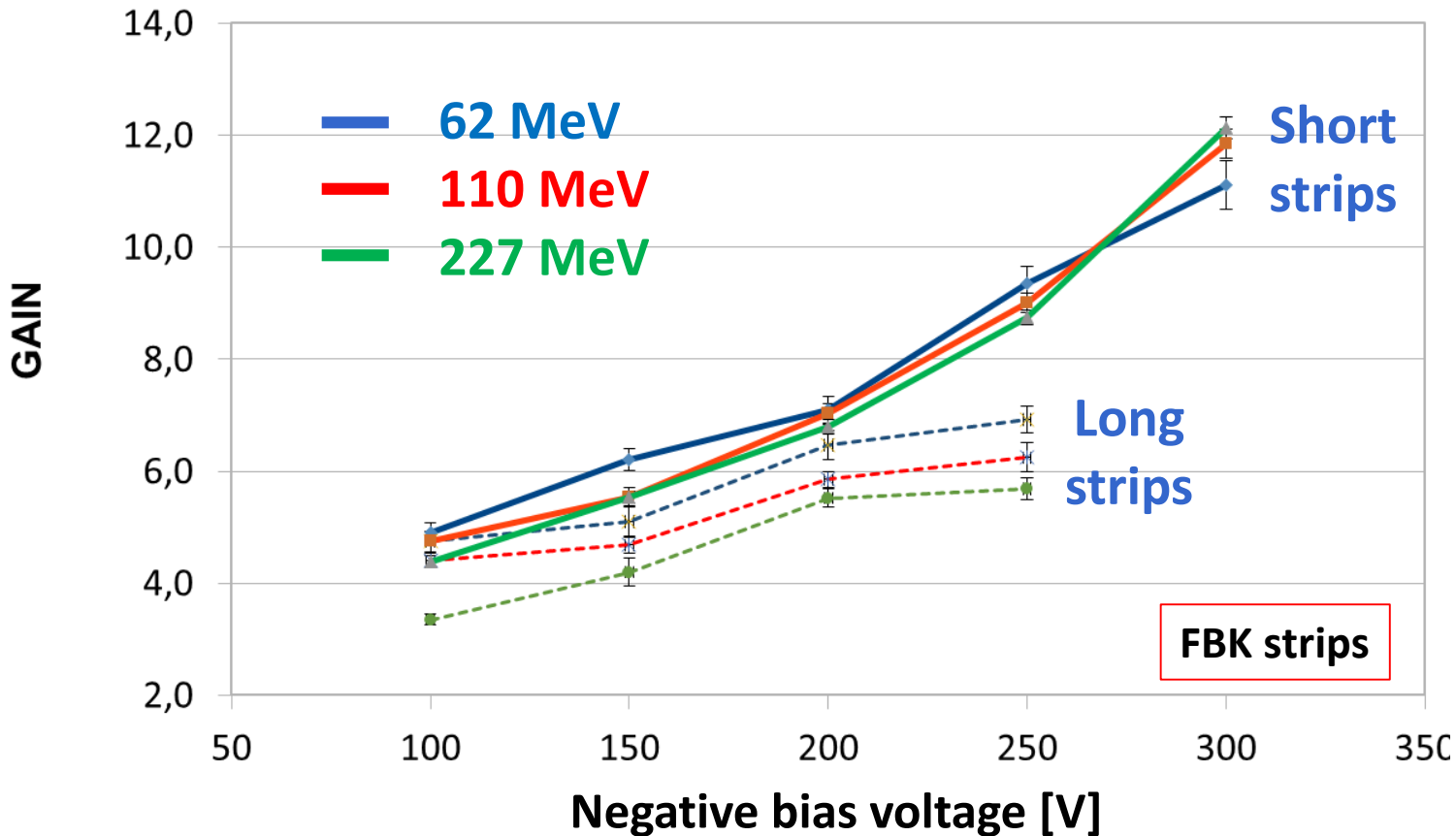
Simulation

GEANT4 simulation of material effects (energy loss and multiple scattering)
WEIGHTFIELD2 simulation of the UFSD response.

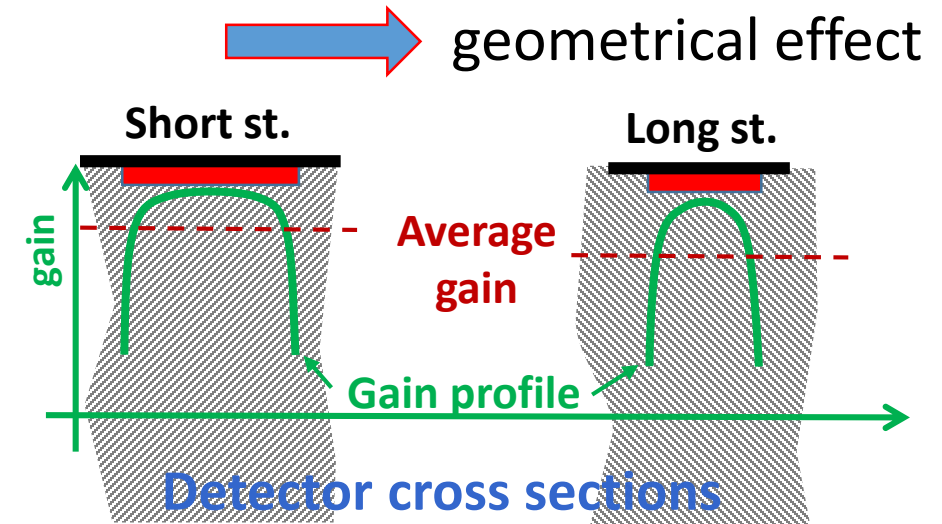


Gain of strips detectors

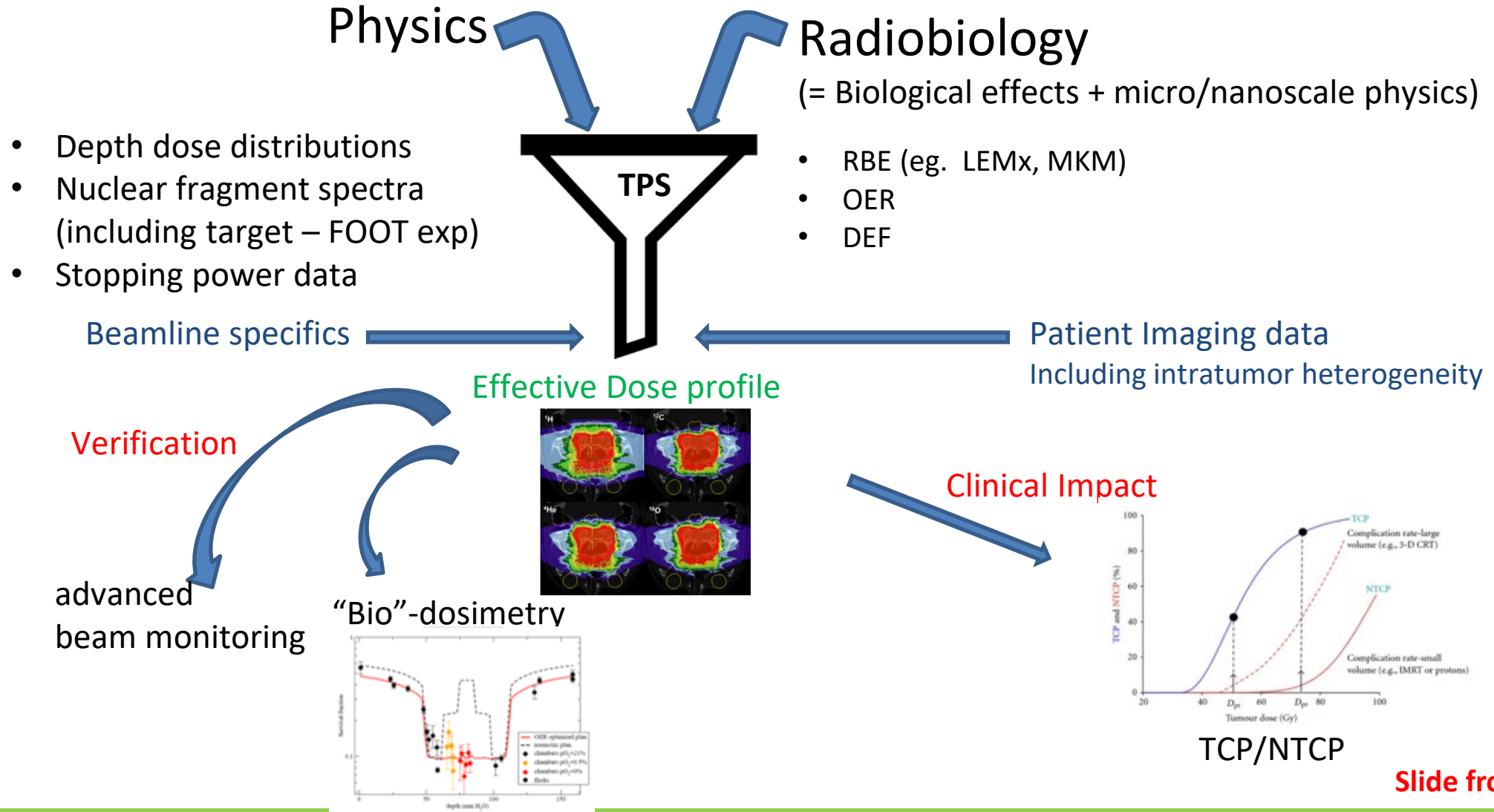
$$\text{Gain(V)} = \frac{\text{MPV}_{\text{gain}} \text{ (V)}}{\text{MPV}_{\text{no gain}} \text{ (V)}}$$



- Gain increase with V_{bias}
- Similar trend observed with laser source on test pads
- **Long strips** (thinner) show a **lower average gain** than short strips



A Graphical summary of MoVe IT



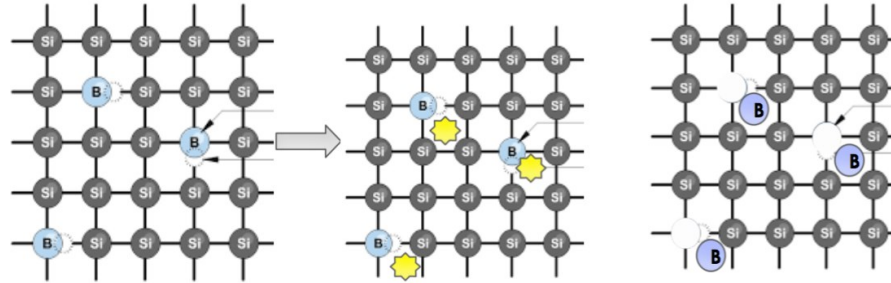
Motivation for the doping strategy of UFSD2 production

Main effect of the irradiation is the inactivation of the dopant in the gain layer

- Substitutional → interstitial (acceptor removal)
- Effect: reduction of gain

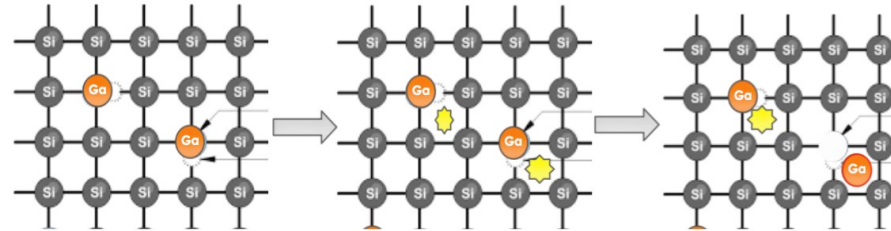
Boron

Radiation creates interstitial defects that inactivate the Boron



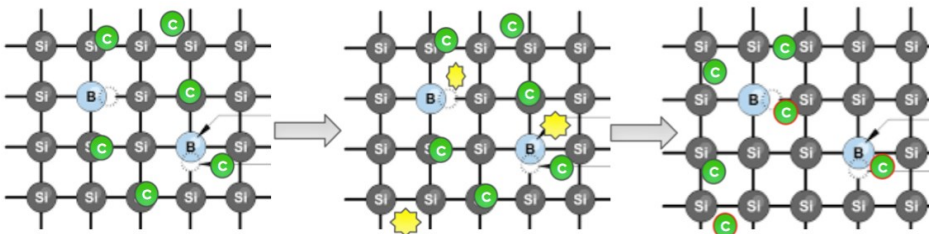
Gallium

From literature, Gallium has a lower possibility to become interstitial



Carbon

Interstitial defects filled with Carbon instead of with Boron and Gallium



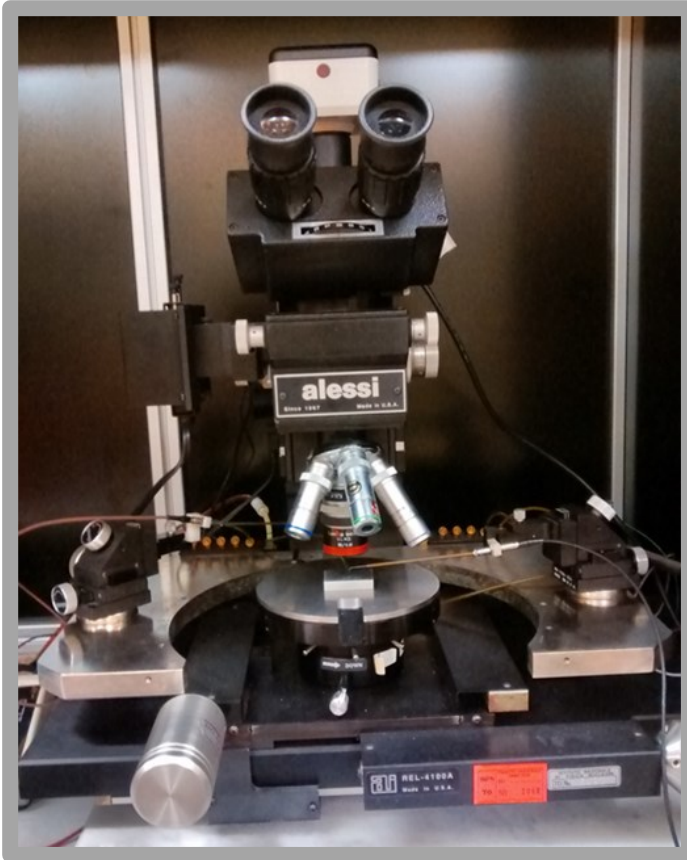
Slide from RD50 Collaboration

UFSD2 production @ FBK:

- 4 different gain layer strategies:
 - Boron (Low & High diffusion)
 - Carbonated Boron (High diffusion)
 - Gallium (Low diffusion)
 - Carbonated Gallium (Low diffusion)
- 4 (3) different doping concentration for Boron (Gallium) implants
- 2 different diffusion temperatures for Boron
- 2 carbon concentration (Low & High)

LAB setup for IV and CV curves

**MANUAL PROBE STATION
ALESSI**

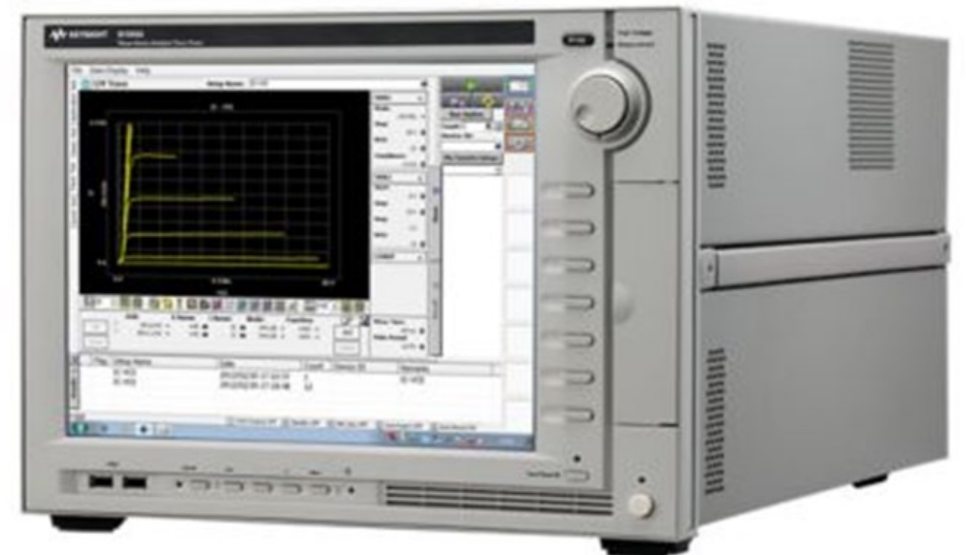


**CUSTOM PROBE CARD FOR
SIMULTANEOUS CONTACT
TO ALLSTRIPS + GUARD RING**

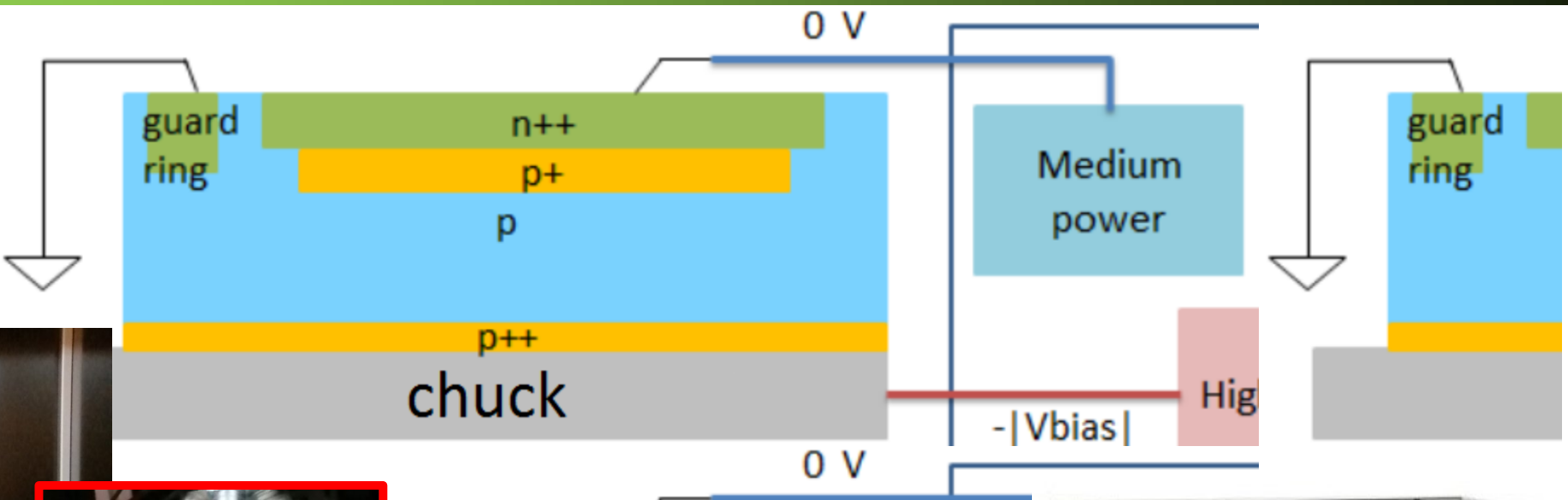


**POWER DEVICE
ANALYZER/CURVE TRACKER**

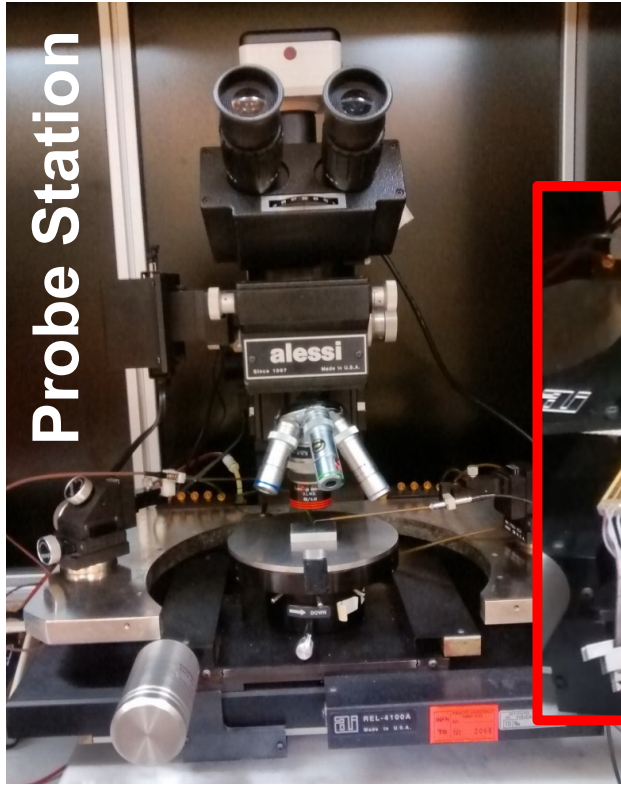
MODEL : KEYSIGHT B1505A



Strip Characterization



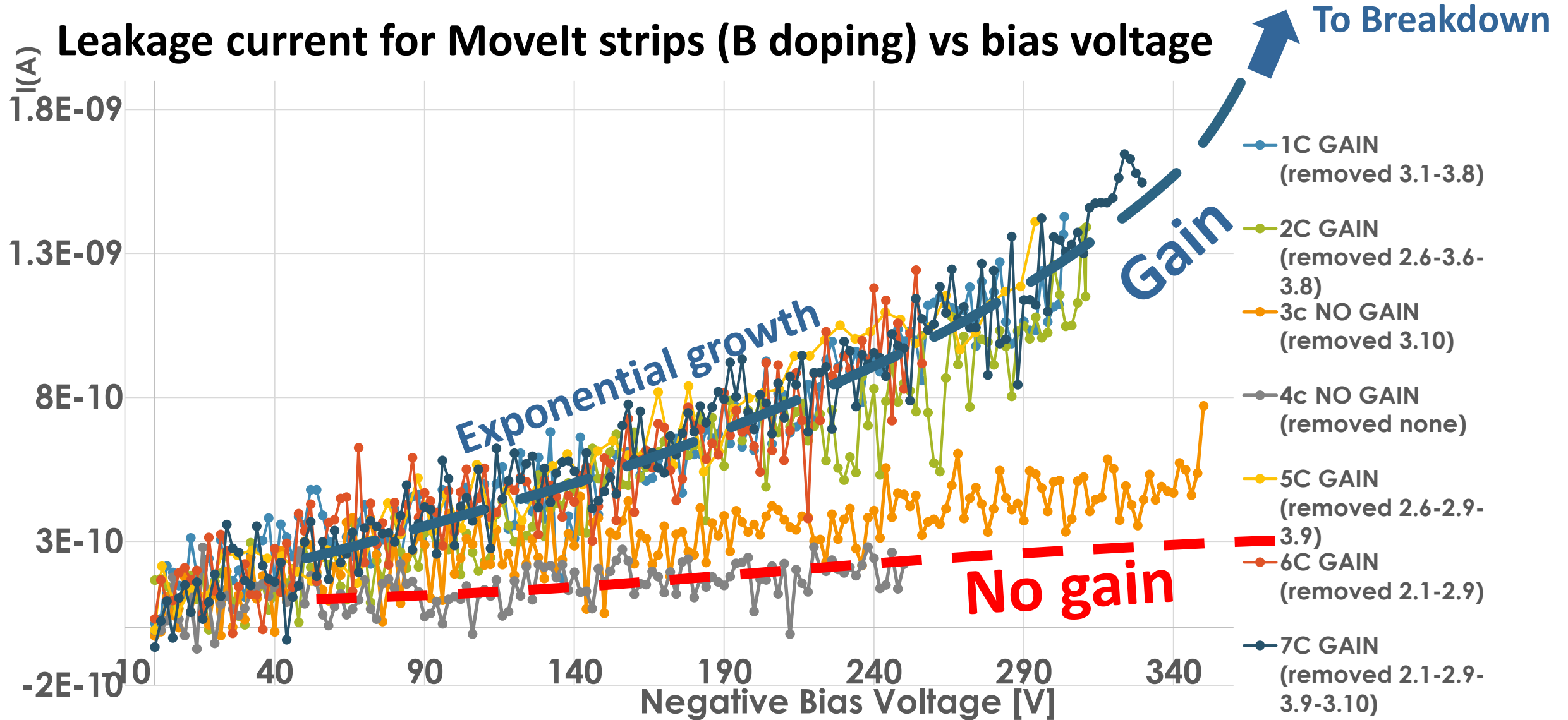
Probe Station



Probe Card

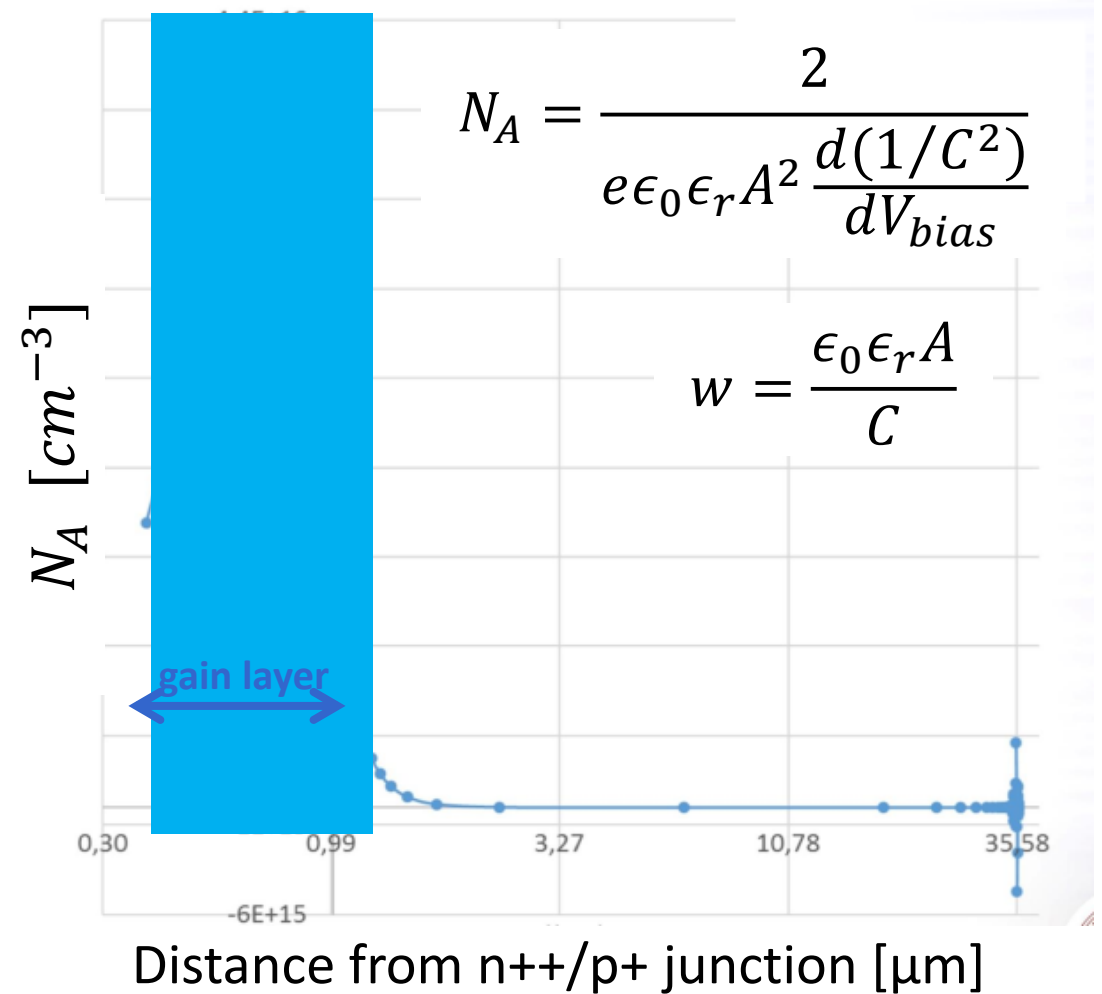
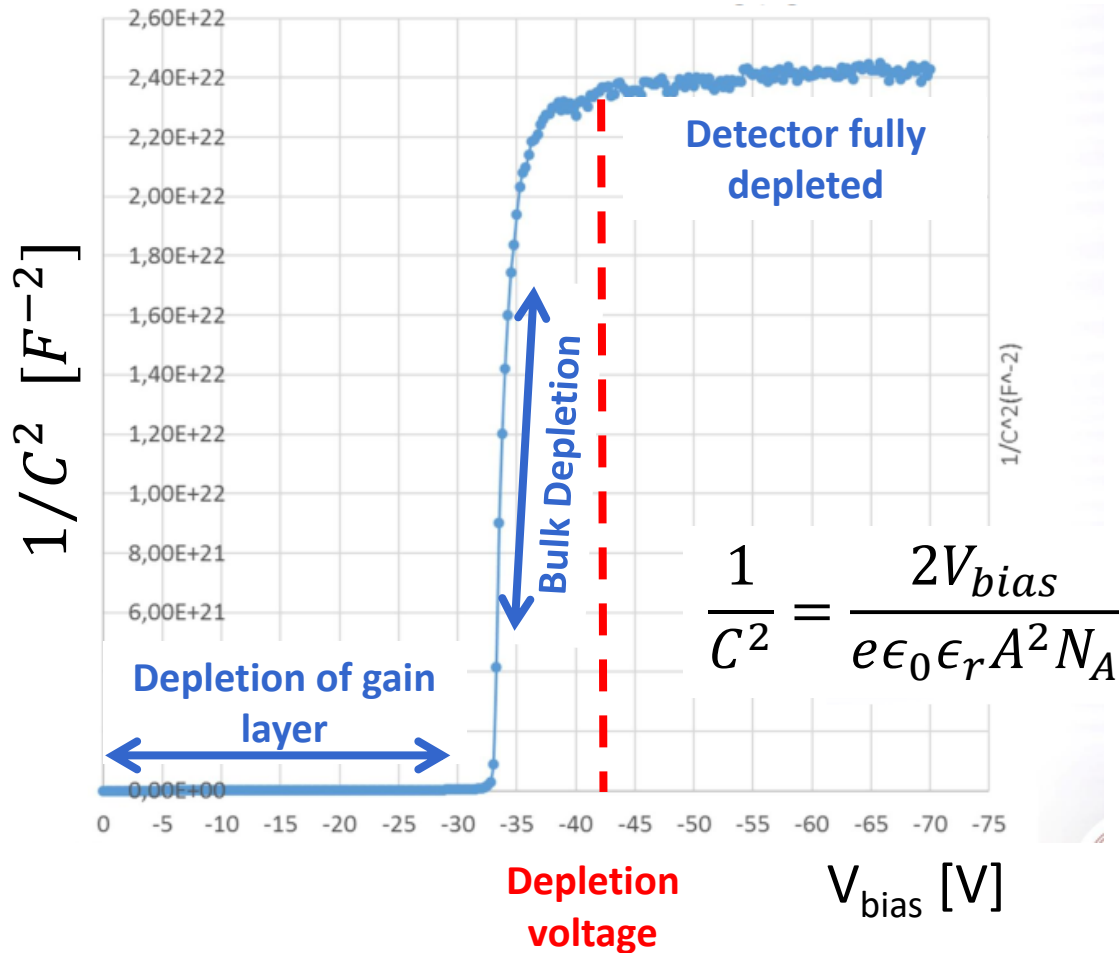


IV curves



CV curves

Allow to determine the doping profile: example a short Movelt strip (B doped)



Strip characterization with laser scan

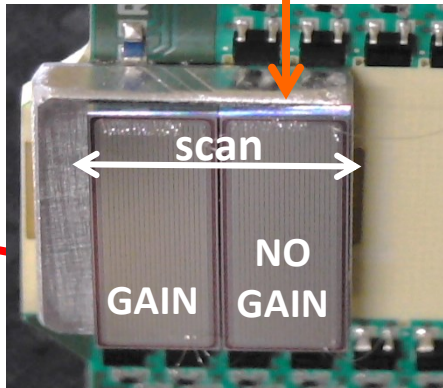
Picosecond Pulsed IR laser:

$\lambda = 1060 \text{ nm}$, Spot size $\sim 20 \mu\text{m}$

Multichannel Amplifier/Shaper board (CMS CT-PPS)

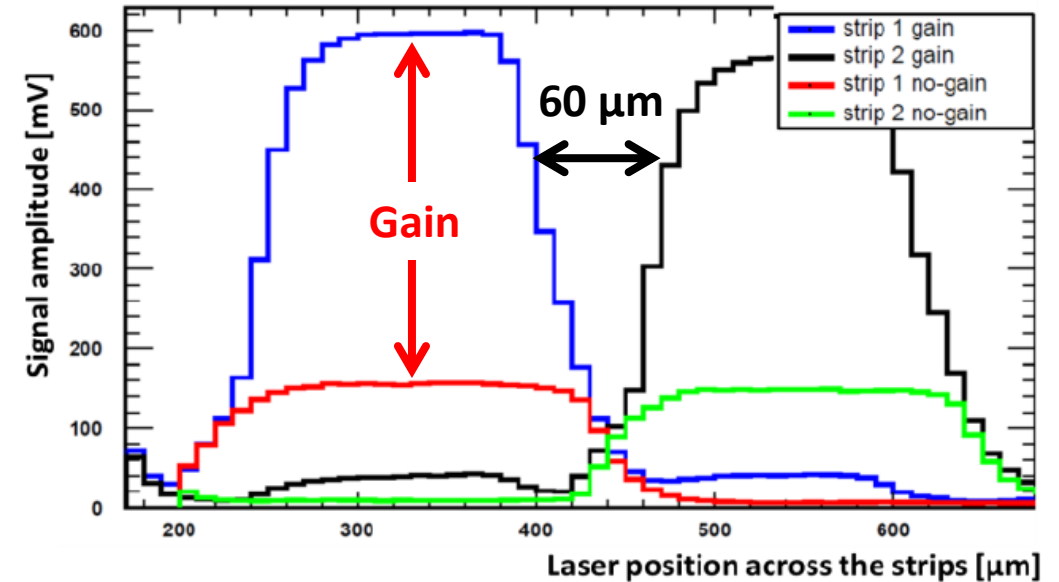
Front and back metallization: sensor mounted to allow laser scan along the strip edge

Laser beam



Short strips of (B doped)

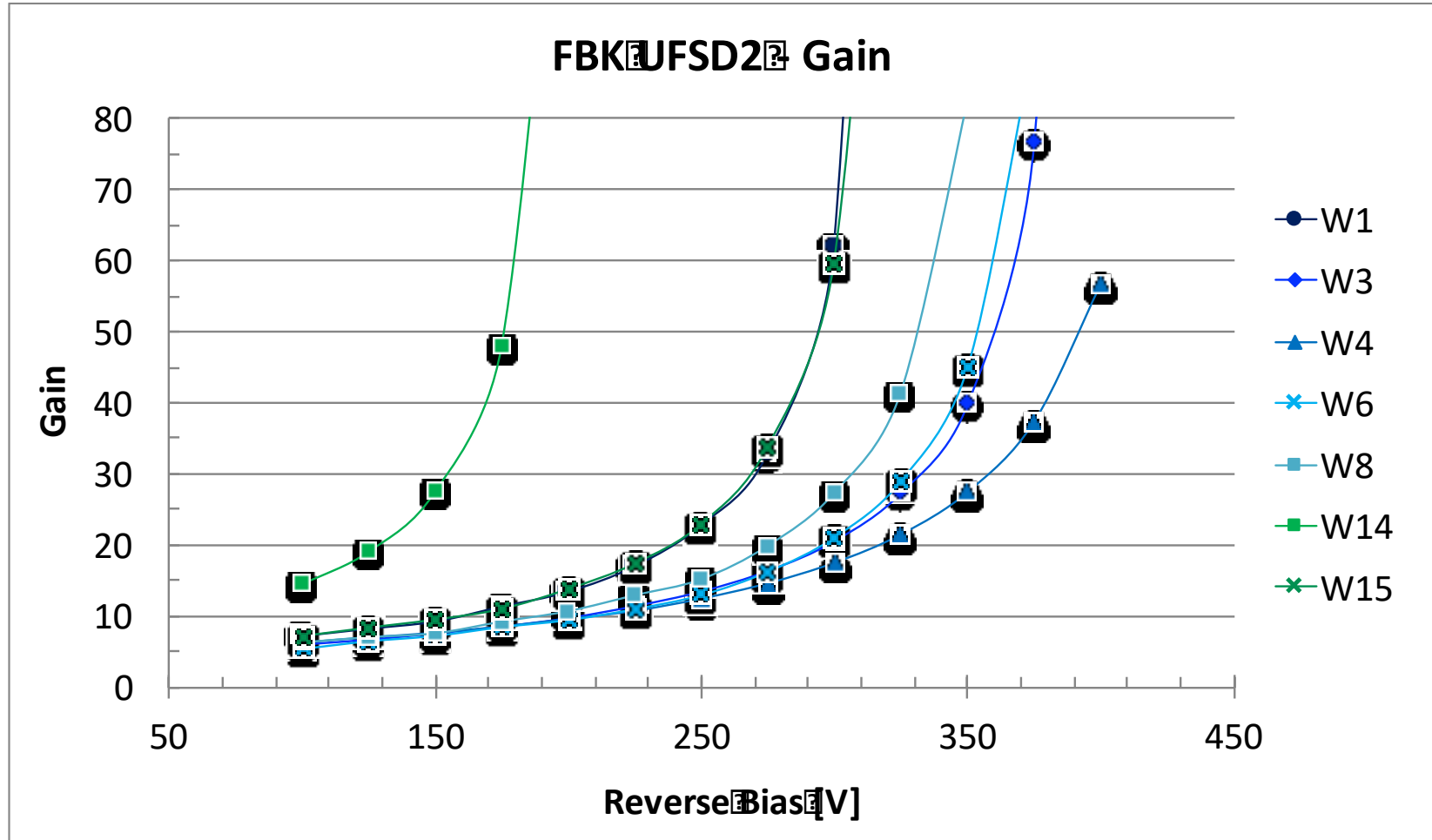
Signal amplitude scan between adjacent strips



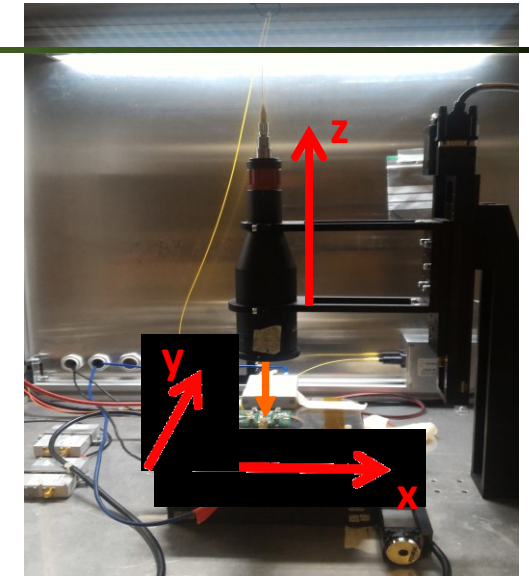
Results

- **Gain** ≈ 4 at $V_{\text{bias}} = -230 \text{ V}$
- **Dead area** $\sim 60 \mu\text{m}$
 - expected by sensor layout and by the production technology, in agreement with TCAD simulations
 - possibly reduced in next UFSD production

Gain Measurement with PS laser



$$GAIN = (Signal\ area\ LGAD) / (Signal\ area\ PiN)$$



TCT Setup from Particulars

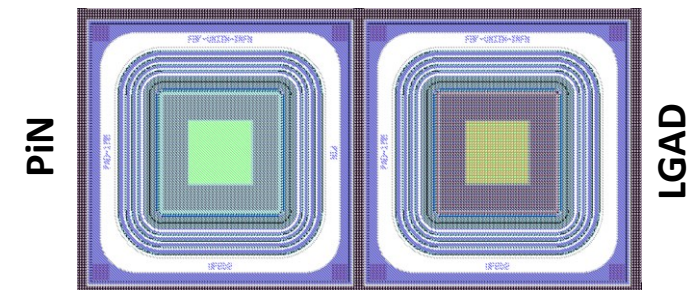
Pico-second IR laser at 1064 nm

Laser spot diameter $\sim 50\ \mu\text{m}$

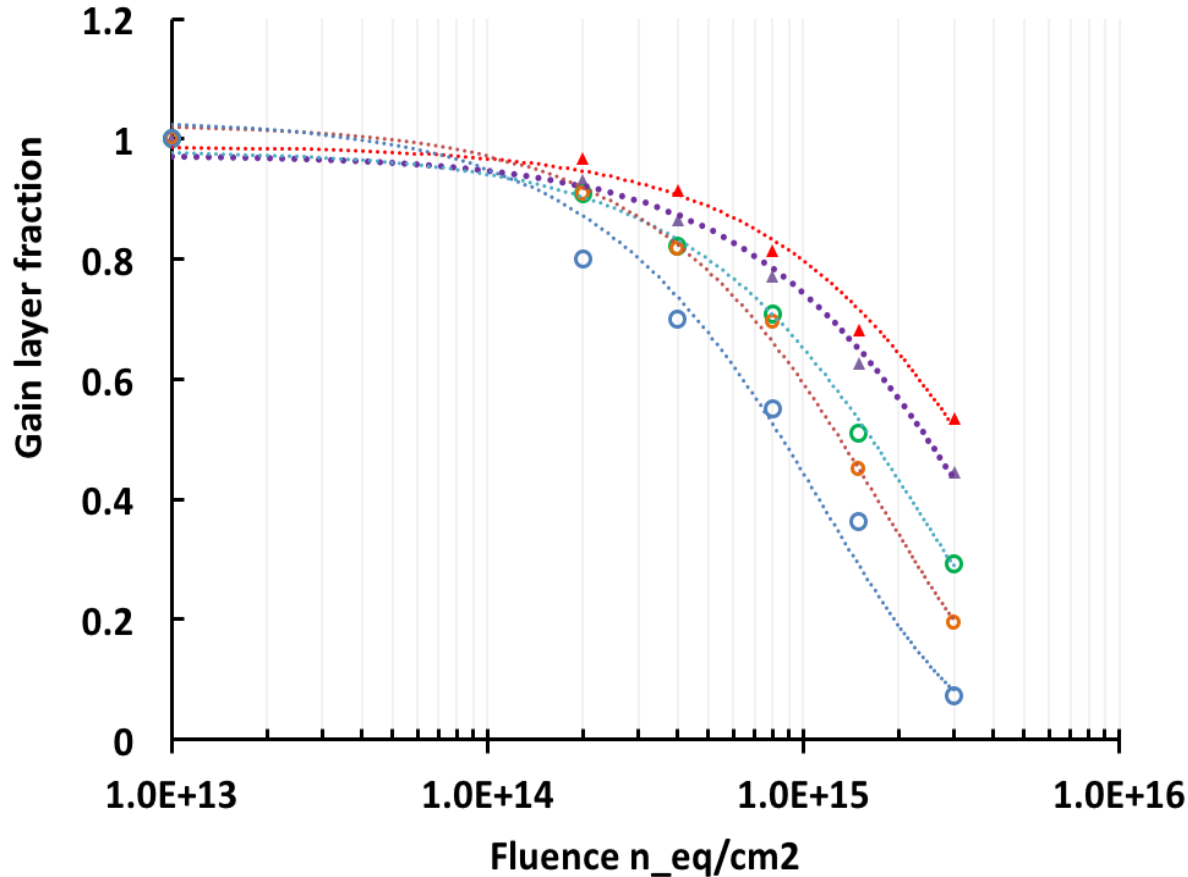
Cividec Broadband Amplifier (40dB)

Oscilloscope Lecroy 640Zi

Room temperature



Irradiation with neutrons



$$y = 9.9E-01e^{-2.1E-16x} \quad \blacktriangle \text{ W6 B+C - <CV>}$$

$$y = 9.7E-01e^{-2.7E-16x} \quad \blacktriangle \text{ W15 Ga+C <CV>}$$

$$y = 9.8E-01e^{-4.1E-16x} \quad \circ \text{ W1 LD <CV>}$$

$$y = 1.0E+00e^{-5.5E-16x} \quad \circ \text{ W8 B <CV>}$$

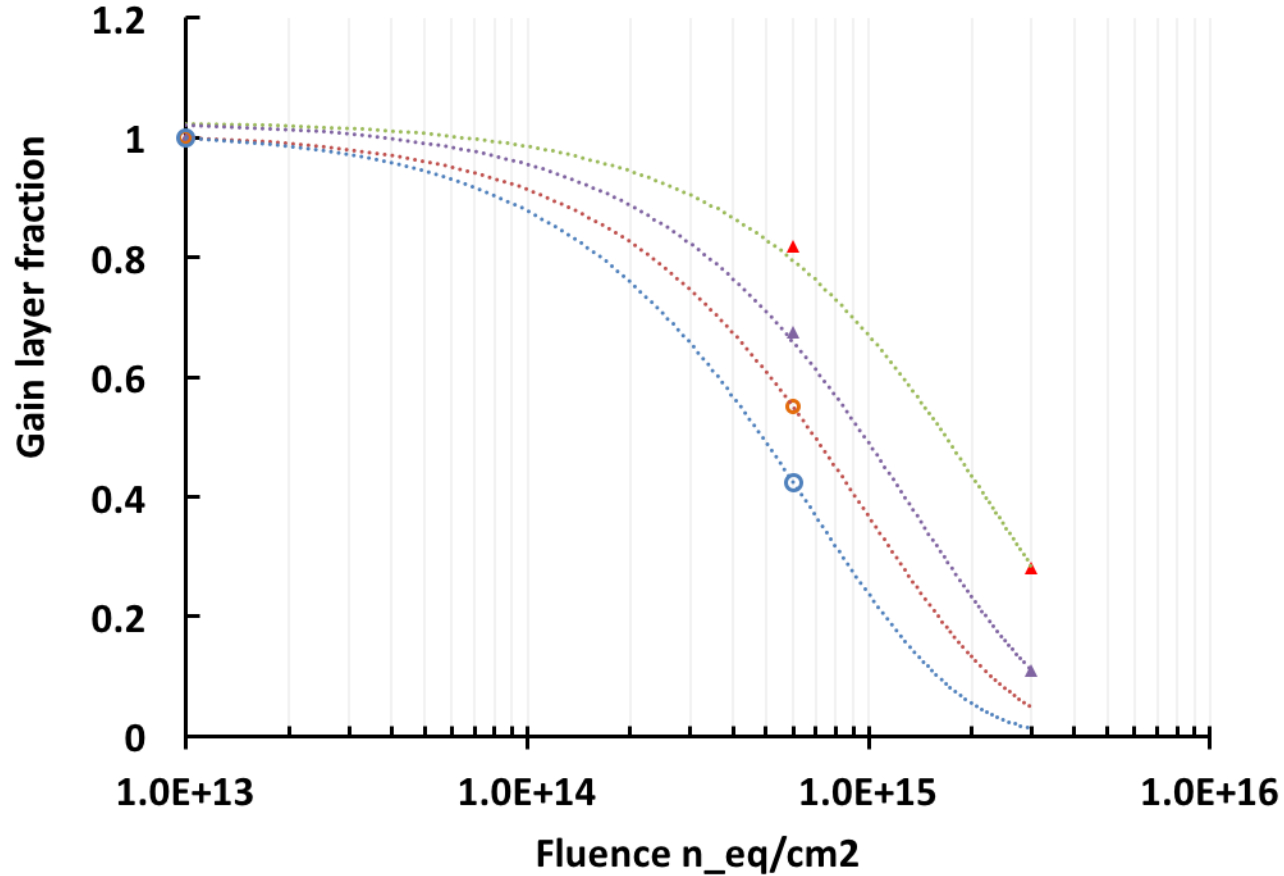
$$y = 1.0E+00e^{-8.5E-16x} \quad \circ \text{ W14 Ga <CV>}$$

Irradiation in Ljubljana

Fluence steps: 2 - 4 - $8 \cdot 10^{14} n_{eq}/cm^2$
1.5 - 3 - $6 \cdot 10^{15} n_{eq}/cm^2$
 $1 \cdot 10^{16} n_{eq}/cm^2$

- ▷ Carbonated sensors have a factor ~ 3 better acceptor removal coefficient
- ▷ Among not carbonated sensors, low diffusion Boron has the better response to irradiation

Irradiation with protons



$$y = 1.0E+00e^{-4.3E-16x} \quad \blacktriangle \text{ W6 B+C - <CV>}$$

$$y = 1.0E+00e^{-7.4E-16x} \quad \blacktriangle \text{ W15 Ga+C <CV>}$$

$$y = 1.0E+00e^{-1.0E-15x} \quad \circ \text{ W3 B <CV>}$$

$$y = 1.0E+00e^{-1.5E-15x} \quad \circ \text{ W14 Ga <CV>}$$

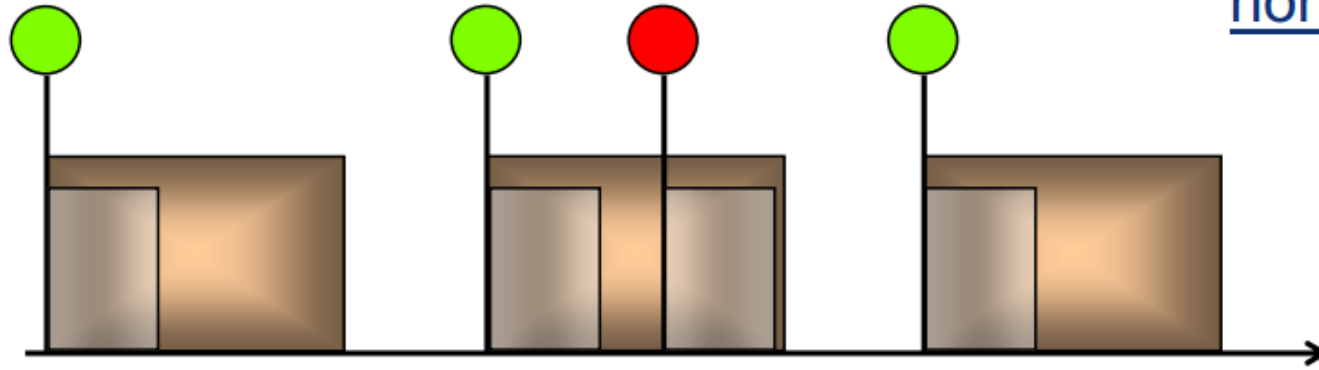
24 GeV/c Proton irradiation @ CERN PS

Fluence steps: 1 - $6 \cdot 10^{14} n_{eq}/cm^2$

1 - 3 - 6 - 9 $\cdot 10^{15} n/cm^2$

Pileup models

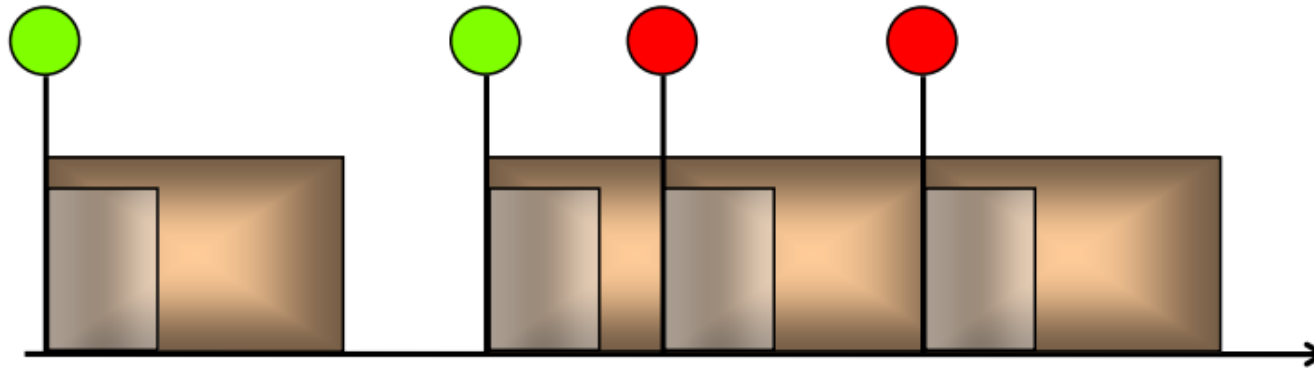
Non-paralyzable model



non-extending dead time

$$R = \frac{\rho}{1 + \rho\tau_{ne}}$$

Paralyzable model



extending dead time

$$R = \rho e^{-\rho\tau_e}$$